

DETERMINATION OF TOXIC MOLECULAR PRODUCTS AND HEAVY METALS FROM COMBUSTION OF UNPROCESSED AND PROCESSED COMMERCIAL CIGARETTES SOLD IN KENYA: COMPUTATIONAL MODELING AND EXPERIMENTAL STUDIES

By

Omare Micah Omari

A THESIS SUBMITTED IN PARTIAL FULFILLMENT OF THE REQUIREMENTS FOR THE DEGREE OF MASTER OF SCIENCE IN ANALYTICAL CHEMISTRY, MOI UNIVERSITY.

2015

DECLARATION

Declaration by the Candidate

This thesis is my original work and has not been presented for a degree in any other University. No part of this thesis may be reproduced without the prior written permission of the author and/ or Moi University.

Student Signature

Micah Omari Omare

Date

.....

.....

Declaration by Supervisors

This thesis has been submitted for examination with our approval as University supervisors

Dr. Jackson Cherutoi

Date

.....

.....

Department of Chemistry and Biochemistry

Moi University, Eldoret, Kenya

Dr. Joshua Kibet

Date

.....

.....

Department of Chemistry

Egerton University, Njoro, Kenya

DEDICATION

It is my genuine gratefulness and warmest regard that I dedicate this work to my parents Mr. Richard George Omare and Mrs. Rebecca Lavine Omare. Your continuous encouragement and moral support have given me strength to accomplish this task. May God bless you.

ABSTRACT

There is substantial evidence that inhaled toxicants such as cigarette smoke can cause irreparable damage to body cells, genetic material and the general respiratory landscape in smokers. Cigarette smoke contains organic and inorganic carcinogenic compounds that pose danger to human life. This study seeks to describe the toxic compound formation mechanism during cigarette smoking. Accordingly, this study computed the global energies and entropies, performed geometry optimization, estimated the toxicity indices of selected molecular products and investigated the heavy metal content in the solid and gas phase of cigarettes commonly sold in Kenya. Two cigarette brands with one unprocessed cigarette coded SM1, ES1 and Trd respectively, were selected for this study. To simulate actual cigarette smoking conditions, smoking apparatus were designed according to ISO 3402: 1999 standards. The heavy metals content was qualitatively and quantitatively determined using Atomic Absorption Spectrometry, AAS, (Shimadzu 6200) while Gas Chromatography-Mass Spectrometry (GC-MS), was used to analyze molecular by-products. Standard solutions for each of the heavy metals were prepared in the range 0.1 ppm to 8.0 ppm from which calibration curves were obtained with R^2 values of 0.995 ± 0.003 appropriately for quantification of each metal. Quantitative means for the three cigarette brands were compared using Analysis of variance (ANOVA) and significant levels measured at 95% confidence level with significant differences recorded at $p < 0.05$. Gaussian '03 computational program was used to perform thermochemical calculations at the Density Functional Theory (DFT) and Moller Plesset Perturbation (MP2) analytical gradient. The toxicity indices were determined using Quantitative Structural Activity Relationship (QSAR) technique incorporated in HyperChem computational platform. The results showed that lead (Pb) had the highest concentration in all cigarette brands; 6.776 ± 0.02 , 6.984 ± 0.03 and $7.119 \pm 0.05 \mu\text{g.g}^{-1}$ for Trd, SM1 and ES1 cigarettes respectively. Pb concentration was not significantly different in the three cigarette brands, $F(2, 15) = 2.555$, $p = 0.111$ while Cr was significantly higher in both Trd ($3.6254 \mu\text{g.g}^{-1}$) and SM1 ($3.5527 \mu\text{g.g}^{-1}$) compared to ES1 cigarette ($2.0882 \mu\text{g.g}^{-1}$) smoke. GC-MS results indicated that the yield of propanol and phenol at retention times of 4.04 and 8.88 minutes respectively reached a maximum of 7.2×10^8 and 2.2×10^8 at about 400°C before decreasing exponentially to about 1.2×10^8 and 9.0×10^7 GC area counts at 700°C respectively. The enthalpy data revealed that the exothermicity process for converting propanol and phenol to their respective deadly radicals decreased with increase in temperature. The estimated toxicity indices for propanol and phenol with their corresponding radicals were 0.55, 0.57, 2.31 and 1.99 respectively. The primary heavy metal component was Pb whereas propanoxy radical was estimated to be the most toxic by-product from cigarette smoking. There is a need for cigarette manufacturers to design cigarettes that can be smoked at lower temperatures to minimize the formation of lethal radicals and investigate sources of carcinogenic metals in cigarettes.

TABLE OF CONTENTS

DECLARATION	ii
DEDICATION	iii
ABSTRACT.....	iv
TABLE OF CONTENTS.....	v
LIST OF FIGURES	ix
LIST OF TABLES	xi
ACKNOWLEDGEMENT	xii
ACRONYMS.....	xiii
CHAPTER ONE	1
1.0 INTRODUCTION	1
1.1 Background to the Study.....	1
1.2 Statement of the Problem.....	3
1.3 Objectives of the Study	4
1.3.1 General Objective	4
1.3.2 Specific Objectives	4
1.4 Hypotheses.....	4
1.5 Justification of the Study	4
CHAPTER TWO	6
2.0. LITERATURE REVIEW	6
2.1 General Overview of Tobacco	6
2.2 Toxicological Impacts of Tobacco in Humans.	7

2.2.1 Phenol.....	8
2.2.2 Guaiacol	9
2.2.3 Butyrolactone	9
2.2.4 Propanol	9
2.3 Heavy Metals	11
2.3.1 Chromium.....	11
2.3.2 Copper	12
2.3.3 Cadmium	12
2.3.4 Lead.....	13
2.3.5 Zinc.....	13
2.3.6 Manganese.....	14
2.4 Computational Chemistry	15
2.4.1 Density Functional Theory (DFT).....	15
2.4.1.1 The Hohenberg-Kohn Theorem	16
2.4.1.2 The Kohn-Sham equations	18
2.4.2 Basis Sets	19
2.4.2.1 Polarized Basis Sets.....	20
2.4.2.2 Diffuse Basis Set	20
2.4.3 Møller-Plesset Perturbation Theory (MPn)	21
2.4.3.1 Second-Order Møller-Plesset Models (MP2).....	21
2.5 Geometry Optimization	23

CHAPTER THREE	25
3.0 METHODOLOGY	25
3.1 Sample Collection and Sample Preparation.....	25
3.1.1 Sample Collection for AAS Analysis.....	25
3.1.2 Sample Preparation for GC-MS Analysis	26
3.1.3 Experimental Investigation of Heavy Metals Using AAS	26
3.1.4 GC-MS Characterization of Molecular Products	27
3.1.5 Computational Methodology.....	28
3.1.6 Quantitative Structural Activity Relationship (QSAR).....	29
3.2 Data Analysis	29
CHAPTER FOUR.....	31
4.0 RESULTS AND DISCUSSION	31
4.1 Experimental Exploration of Toxic Molecular Products	31
4.1.1 Formation of Free Radicals.....	33
4.1.2 Computational Details	34
4.1.2.1 Calculation of Enthalpy Changes (ΔH)	34
4.1.2.2 Calculations of Change in Gibbs Energy (ΔG).....	38
4.1.2.3 Calculation of Entropy Changes (ΔS).....	41
4.1.3 Comparisons of MP2 and DFT Computational Results	43
4.1.4 Calculation of IR Data	47
4.1.5 Effects of a given Basis Set on Internal Energy	49

4.1.6 Toxicity Indices	50
4.1.7 Molecular Geometries.....	52
4.1.8 Molecular Orbitals	54
4.2 Heavy Metals Analysis	58
4.2.1 Heavy Metal Concentrations Partitioned in the Gas-Phase Cigarette Smoke	58
4.2.1.1 Mean Comparison For Heavy Metal Concentration in Cigarette Smoke	60
4.2.2 Heavy Metal Concentration Partitioned in Cigarette Solid-Phase.....	61
4.3 Rejection or Acceptance of Hypothesis	62
CHAPTER FIVE	63
5.0 CONCLUSION AND RECOMMENDATION.....	63
5.1 Conclusion	63
5.2 Recommendations.....	65
REFERENCES	66
APPENDICES	74

LIST OF FIGURES

Figure 1.1: The Anatomy Of Tobacco Cigarettes.....	2
Figure 2.1: Structures of Molecular Compounds for Computational Modeling.....	10
Figure 3.1: The Apparatus Set Up For Cigarette Smoking In The Laboratory	26
Figure 4.1: Experimental Release of Molecular Products from Cigarette.....	31
Figure 4.2: Propanol and Phenol yields from the combustion of SM1 cigarette brand.	32
Figure 4.3: Enthalpy Change for the Formation of Propanoxy Radical by DFT level Theory	36
Figure 4.4: Enthalpy Change for the Formation of Phenoxy Radical prediction by DFT Theory	37
Figure 4.5: Change in Gibbs Energy for the Formation of Propanoxy Radical	40
Figure 4.6: Change in Gibbs Energy for the Formation of Phenoxy Radical	40
Figure 4.7: Change in Entropy for the Formation of Propanoxy and Phenoxy Radicals	42
Figure 4.8: Enthalpy Change for the Formation of Propanoxy under DFT and MP2 Theories.....	44
Figure 4.9: Enthalpy Change for the Formation of Phenoxy under DFT and MP2 Theories.....	45
Figure 4.10: Change in Gibbs Free Energy for Formation of Propanoxy DFT and MP2	46
Figure 4.11: Change in Gibbs Energy for the Formation of Phenoxy in DFT and MP2 theories.....	46

Figure 4.12: IR Spectrum for Propanol.....	47
Figure 4.13: Variation in Internal Energy with Different Basis Sets.....	49
Figure 4.14: Optimized Geometries of Investigated Species.....	53
Figure 4.15: Molecular Orbitals for the Compounds under Study	57
Figure 4.16: Concentration of Heavy Metals Partitioned in the Gas-Phase Cigarette Smoke.....	57

LIST OF TABLES

Table 4.1: DFT Thermochemical Data for Molecular Compounds and Subsequent Radicals.....	35
Table 4.2: Gibbs Energy of Molecular Toxins and their respective Radicals	39
Table 4.3: MP2 Thermochemical Data for Molecular Compounds and their Subsequentradicals.....	43
Table 4.4: Vibrational Modes Displayed By Propanol.....	48
Table 4.5: QSAR Toxicity Indices for Organic Toxins and their Corresponding Free Radicals.....	51
Table 4.6: Mean Concentrations of Metals Partitioned in Cigarette Smoke	60
Table 4.7: Levels of Heavy Metal Concentrations Partitioned in Cigarette Ash.....	61

ACKNOWLEDGEMENT

I would like to express my sincere thanks to my supervisors Dr. Joshua Kibet of Egerton University and Dr. Jackson Cherutoi of Moi University for giving me the golden opportunity to do this special research project and ensuring that everything was done right. I am truly honoured to have been their student. My parents, brothers, sisters and friends are greatly acknowledged for their prayers, financial and moral support through this study. I thank Egerton University especially the department of chemistry whose facilities were used during sampling. The National Commission for Science, Technology and Innovation (NACOSTI) is highly acknowledged for funding this research.

ACRONYMS

B3LYP	Becke-3Parameter-Lee-Yang-Parr correlation function
DNA	Deoxyribose nucleic acid
ES1	Embassy cigarette
GTO	Gaussian type orbital
HOMO	Highest occupied molecular orbital
IARC	International agency for research on cancer
KS	Kohn-Sham
Log P	Logarithm of Octanol-Water partition coefficient
LUMO	Lowest Unoccupied Molecular Orbital
NIST	National institute of science and technology
PAHs	Polycyclic aromatic hydrocarbons
PM _{2.5}	Particulate matter (2.5 μm)
PM ₁₀	Particulate matter (10 μm)
QSAR	Quantitative structural activity relationship
STO	Slater type orbitals
SPSS	Statistical Package for Social Sciences
ZPVE	Zero point vibrational energy

CHAPTER ONE

1.0 INTRODUCTION

1.1 BACKGROUND TO THE STUDY

Tobacco biomass is of great interest because of its use in the form of cigarettes which generate various smoke compounds during pyrolysis reactions (Cho *et al.*, 2013). The thermolysis of complex plant materials such as tobacco gives rise to a variety of organic substances, most of which are produced by the process of pyrodegradation and pyrosynthesis. Tobacco is a complex plant material consisting of 6-15% cellulose, 10-15% pectin, approximately 2% lignin, and a variety of other components (Leffingwell, 1999), the exact composition being dependent on the tobacco variety and growing conditions (Leffingwell & Alford, 2005). Tobacco biomass consists of over 2500 chemical constituents, among them biopolymers, non-polymeric and inorganic compounds (Czégény *et al.*, 2009). For example, sugars (cellulose, pectin, alginates, laminarin and ethyl cellulose) are natural tobacco components which are also often added to tobacco during the manufacturing process (Cho *et al.*, 2013; Talhout *et al.*, 2011).

All over the world, there is a steady increase in the rate of consumption of tobacco products and in the number of smokers (Fuster *et al.*, 2011). This trend has aroused health concerns associated with its use. Tobacco burns at different combustion temperatures emitting potentially toxic by-products which are a major health concern due to the associated health disease like heart attack, stroke and cardiovascular death, mental illness and lung cancer (Ashraf, 2012). Tobacco is known to contain organic and inorganic carcinogenic compounds therefore making it one of the most harmful and toxic substance to human health (Prüss-Üstün *et al.*, 2004). The toxic substances contained in tobacco smoke include heavy metals such as arsenic, cadmium,

chromium, lead, nickel and zinc which find their way into the human body through inhalation during smoking and accumulate in body tissues. Figure 1.1 gives an illustration of how tobacco is packaged to produce a cigarette. The cigarette paper is made up of cellulosic material.



Figure 1.1: The Anatomy of Tobacco Cigarettes

The basis of computational chemistry is the Schrödinger wave equation expressed as follows:

$$H\psi = E\psi \quad \text{Equation 1.1}$$

where H is the Hamiltonian operator, ψ is the wave function (eigen function for the Hamiltonian) and E is the total energy of the system (eigen value in the equation).

The wave function describes the system and takes as variables the positions of electrons in the system leading to the equation:

$$H\psi(\vec{r}_1, \dots, \vec{r}_N) = E\psi(\vec{r}_1, \dots, \vec{r}_N) \quad \text{Equation 1.2}$$

Whereas \vec{r} describes the position of the electron in space, ψ allows the properties of the system to be deduced. The wave function can be orthogonal or orthonormal over all space depending on conditions of the wave function. Consider the expression given thus:

$$\langle \psi_i / \psi_j \rangle = \delta_{ij} \begin{cases} 1 \text{ if } i = j \\ 0 \text{ if } i \neq j \end{cases} \quad \text{Equation 1.3}$$

where δ_{ij} is called the Kronecker delta. Computational chemistry refers to a branch of chemistry utilizing computer simulation algorithms in solving chemical problems (Young, 2001). This is achieved by incorporating sufficiently well-developed methods of theoretical chemistry into effective computer programs, thereby allowing calculation of structures and properties of both molecules and solids. Whereas computational results are complementary to the information obtained by experimental methods, in some instances it has proved capable of predicting unobserved chemical phenomena (Ochterski, 2000).

1.2 Statement of the Problem

Whereas many efforts have been engaged towards understanding the pyrolytic behavior of tobacco, many complex and uncertain reaction processes are yet to be understood. The determination of molecular like components of tobacco using experimental methods such as Gas-Chromatography hyphenated to mass spectrometers has proved markedly difficult (Kulshreshtha & Moldoveanu, 2003; Lisko *et al.*, 2013). For this reason therefore, I have preferred computational methods that simulate the burning conditions in cigarette smoking in order to probe the thermodynamic, electronic, and mechanistic behavior of these compounds over the whole range of cigarette smoking. Additionally, the investigation of heavy metals and other elemental speciation formed from tobacco has not received a lot of attention in literature hence this study probed the quantity of these elements especially the heavy metals formed from combustion of tobacco.

1.3 Objectives of the Study

1.3.1 General Objective

The major objective of this study was to determine toxic molecular products and heavy metals from the combustion of processed and unprocessed cigarettes using experimental and computational methods.

1.3.2 Specific Objectives

1. To compute the global energies and entropies of selected molecular products from the burning of processed and unprocessed cigarette brands using Gaussian Computational platform.
2. To perform Geometry optimization of molecular products using Gaussian Computational program.
3. To calculate the toxicity indices of selected by-products of tobacco burning using HyperChem computational package
4. To determine the heavy metal content from the smoking of selected cigarette brands using Atomic Absorption Spectrometry (AAS).

1.4 Hypotheses

1. There are no heavy metals in the selected cigarette brands for this study
2. Unprocessed cigarette is not toxic compared to processed cigarettes

1.5 Justification of the Study

The concept of tobacco development, composition and toxicity is a very rich area of study (Zhou *et al.*, 2011). In recent years a lot of efforts have been devoted to the evaluation of the by-products of tobacco burning and the potency of cigarette smoking (WHO, 2006). However, the shortfalls in describing the toxic compound formation mechanism during tobacco burning and challenges of developing model compounds which can burn under conditions that simulate actual cigarette smoking with respect

to heating rate, temperature distribution, variation in oxygen concentration, and residence time, impede this undertaking (Schlotzhauer *et al.*, 1982). Cigarette smoke contains substances that pose danger to human life when inhaled and these have been classified as carcinogenic. Other diseases have been identified to occur as a result of biological effects of repeated inhalation of these toxic substances which are known to be produced by pyrosynthesis. Cigarette smoke has been identified to be one of the major causes of heart diseases, aneurysms, bronchitis, emphysema, strokes and cataracts. It has also been associated with high infertility rates, miscarriage, premature births and infant deaths. In the recent past, a lot of research has been devoted to the identification and quantification of the main sources of toxic metals into the human blood system and has created a lot of interest in research on the constituents of heavy metals in tobacco. Given that many of these complications and diseases have been associated with cigarette smoking, it will be inaccurate to conclude that a single component of tobacco is the causative agent. Therefore this study seeks to contribute more knowledge towards understanding tobacco composition and mechanisms of toxic compound formation during cigarette smoking.

CHAPTER TWO

2.0. LITERATURE REVIEW

2.1 General Overview of Tobacco

In the United States of America, it is estimated that about 440,000 premature deaths occur annually as a result of cigarette smoking (Centers for Disease Control Prevention, 2002). A total of about 6 million people died in 2011 as a result of tobacco use with 80% of the cases reported in developing countries. These deaths caused by tobacco use in both developed and developing countries is expected to increase. Cigarette smoking is regarded as one of the major preventable cause of premature death and tobacco consumption reduces the qualities of individuals' life. Cigarette smoking is a method through which nicotine that is predominantly present in tobacco is introduced into the human body (Nnorom *et al.*, 2005).

Cigarette smoke contains toxic, genotoxic and carcinogenic organic and inorganic compounds that cause adverse effects to human health (Massadeh *et al.*, 2003). About 4000 chemicals have been identified to be present in tobacco including nitrosamines, polyaromatic hydrocarbons and heavy metals such as cadmium, lead and thallium which cause disease in human beings (Pappas *et al.*, 2007). About 5000 chemicals are generated upon burning the tobacco ingredients (Chalouhi *et al.*, 2012). When one smokes, the organic and inorganic compound in tobacco form part of the mainstream smoke, sidestream smoke, and ash and cigarette butt, finding their way into the smokers' body system through the oral cavity to the lungs from where they are further transferred to the peripheral circulation and other body organs (Pappas *et al.*, 2007).

Borgerding and Klus (2005) describe tobacco smoke as the aerosol made of solid-liquid droplets in the gaseous state that is produced by complex and overlapping burning, pyrolysis, pyrosynthesis, distillation, sublimation and condensation

processes. Individuals who are smokers can inhale the cigarette smoke directly while those that are non-smokers can inhale it from cigarette contaminated environments through passive smoking posing harm to both individuals (Nnorom *et al.*, 2005).

During smoking, temperatures of about 800 °C occur in the center of the burning cigar. When the smoker makes a puff, the temperatures rise up to 910-920 °C at the burning zone edge and temperature then decreases rapidly from these high temperatures of more than 800 °C to the temperatures of ambient air. This decrease in temperature occurs as a result of endothermic, energy-consumption processes such as distillation and sublimation that occur behind the glowing cone (Borgerding & Klus, 2005).

2.2 Toxicological Impacts of Tobacco in Humans.

Different researchers have carried out research and studies about cigarette smoking and cigarette smoke including the trace and heavy metal constituents and their impacts on human health. Dumatar and Chauhan (2011) conducted a study on the effects of cigarette smoking in human and in their research, they found out that smoking increases the heart beat rate and hence blood pressure as a result of nicotine intake. Maternal smoking has been correlated with decreased performance on tests of intelligence, academic achievement, short-term and verbal working memory, long-term and immediate memory for auditory and verbal material, executive function, increased incidence of behavioral indices during childhood and adolescence, hyperactivity, and attention deficit (Cho *et al.*, 2013; Duncan *et al.*, 2009).

Cigarette smoking exposes the developing foetus to nicotine and this may pose significant environmental risk factor for variability in reading skills (Duncan *et al.*, 2009). Borgerding and Klus (2005), conducted a research where they analyzed complex mixtures of cigarette smoke. In their work, they addressed the physical

nature and chemical composition of tobacco. Hoffmann *et al.* (2001), found out that more than 70 of the thousands of chemicals in cigarette have been proved to be carcinogenic and only nicotine causes addiction in tobacco products. Genotoxic carcinogens that are present in cigarette smoke cause disastrous mutagenic effects once they attack the lung cells (Duncan *et al.*, 2009). Human exposure to these mixtures of chemical carcinogens in cigarette smoke has horrendous consequences in terms of lung cancer mortality (Hecht, 2012).

Chiba and Masironi (1992), documented the biochemical effects of toxic and heavy metals in tobacco smoke. Cigarette smoke is highly toxic due to the generation of toxic pyrolysis products (Dempsey *et al.*, 2011). [ENREF 83](#) classified tobacco smoke as harmful and toxic to human health. An understanding of the mechanism of lung cancer initiation by cigarette smoke can provide new insights on how lung cancer can be prevented in smokers (Hecht, 2012). Based on the compounds which have been found to be ubiquitous in cigarette smoke, four have been selected for the experimental and computational studies to be carried out in this research. These compounds include phenol, propanol, guaiacol and Butyrolactone. The molecular structures of tobacco toxins investigated in this work are presented in Figure 2.1.

2.2.1 Phenol

Phenol is produced as a result of pyrolysis of aromatic acids and aliphatic acids above temperatures of 200 °C (Senneca *et al.*, 2007). Cigarette smoke contains a number of structurally diverse substituted phenols. Substituted phenols that have electron releasing groups form phenoxy free radicals which are toxic while substituted phenols that have electron withdrawing groups do not form these phenoxy radicals but they are known to exert their toxicity through lipophilicity (Smith *et al.*, 2002). Cigarette smokers get exposed to these free radicals either through vapor or

particulate phase of cigarette smoke aerosol which display free radicals activity (Blakley *et al.*, 2001). Researchers have reported a total of 380 substituted phenols in cigarette smoke but many of these have not been characterized in order to allow their exact identification (Smith *et al.*, 2002).

2.2.2 Guaiacol

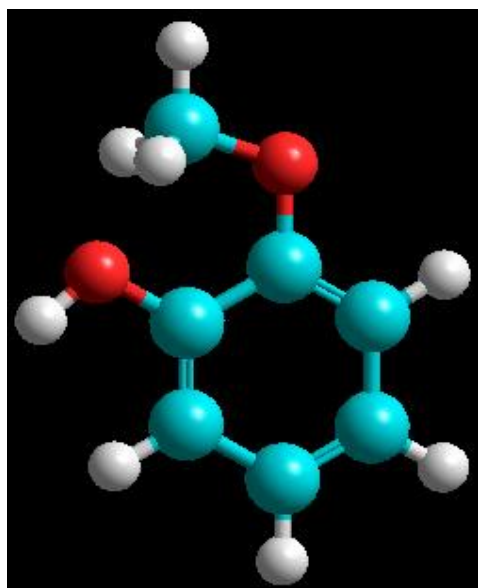
Guaiacol is found in tobacco leaf oil (Burdock, 2009), distillation waters of orange leaves, coffee, and butter oil. Guaiacol finds application in flavor composition like tobacco, rum and fruit and spice complexes. It has been identified in domestic tobacco and in tobacco smoke at levels ranging from 6-13 $\mu\text{g}/\text{cigarette}$ (mainstream) and 8-21 $\mu\text{g}/\text{cigarette}$ (sidestream), and in the gaseous and semi volatile phases of tobacco smoke (Carmines, 2002).

2.2.3 Butyrolactone

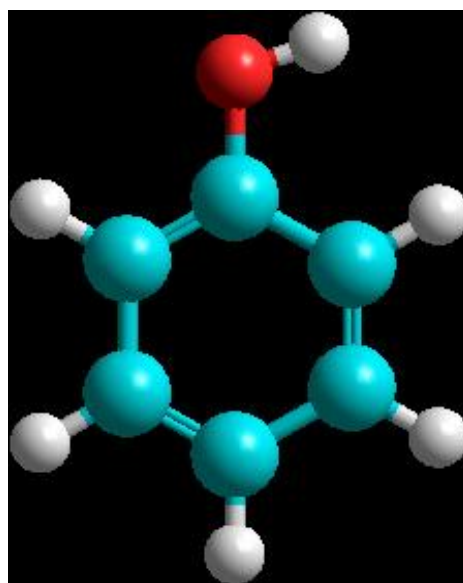
Butyrolactone has been detected in alcoholic beverages, tobacco smoke, coffee and several foodstuffs. It is used in cigarettes as a flavoring agent to modify the taste and flavor of tobacco smoke (Sivilotti *et al.*, 2001). Butyrolactone is one of the lactones that have been identified in cigarette smoke with alkylating potential and has been reported to be carcinogenic (Lou *et al.*, 2010).

2.2.4 Propanol

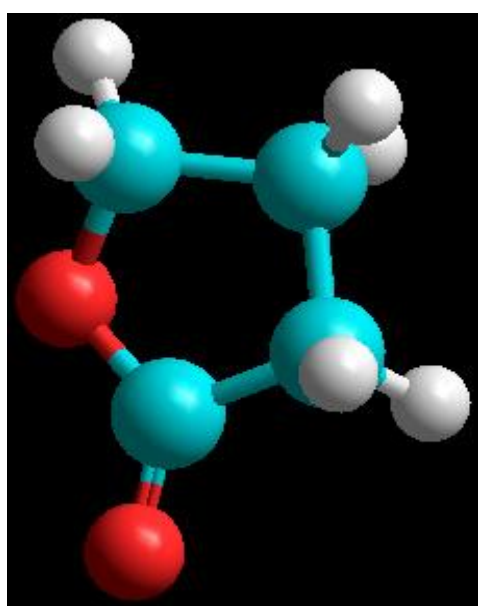
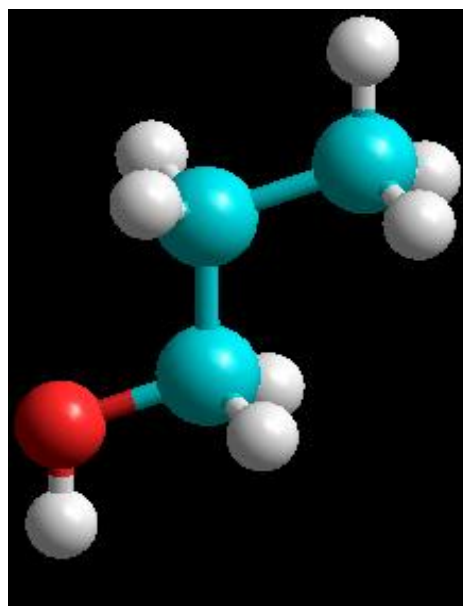
Limited information is available in literature concerning the production of propanol during the pyrolysis of tobacco thus making this research one of its kind to investigate and perform computational modeling of propanol in conditions that imitates the actual cigarette smoking.



guaiacol



phenol

 γ -butyrolactone

1-propanol

Figure 2.1: Structures of Molecular Compounds for Computational Modeling

2.3 Heavy Metals

Heavy metals in cigarette tobacco have been reported to cause serious damages to human health (Zhang *et al.*, 2005). Different researchers have clarified that the amount of toxic heavy metals such as cadmium in fat (Rauhamaa *et al.*, 1986), blood (Erzen & Kragelj, 2006), and liver (Bernhard *et al.*, 2005) of tobacco smokers is much higher than in those of non-smokers (Zhang *et al.*, 2005). Heavy metals such as Cd, Cr, Pb, Hg, and Ni are known to accumulate in body tissues and fluids as a result of cigarette smoking (Galażyn-Sidorczuk *et al.*, 2008). Accordingly, the heavy metals that were investigated in this study include chromium, copper, cadmium, lead, zinc and manganese. These metals are known to have a potential toxic effect on human life and they have known toxic properties (Çifçi & Ölcücu, 2007)

2.3.1 Chromium

Chromium is one of the metals that researchers have reported to be present in cigarette smoke and known to be carcinogenic (Miller, 2013). Although chromium is a vital element in the human body, it can quickly become toxic at high concentrations (Ryan & Clark, 2010). Ryan and Clark (2010), conducted a research on trace metals in tobacco and cigarette, and they found out that chromium is detectable in tobacco smoke as well as tobacco ash. Among the many environmental sources of chromium to human, the Agency for Toxic Substances and Disease Registry (2008) identifies tobacco smoke as one of the sources. Tobacco smoke is known to contain chromium (VI) and researchers have identified chromium (VI) compounds as carcinogenic to humans (IARC. International Agency for Research on Cancer, 2004). Bernhard *et al.* (2005), in their work on metals in cigarette have classified chromium as hazardous to human beings because of its accumulation in the blood circulation system.

2.3.2 Copper

Copper is one of the trace metals which plays a vital role in the functioning of different enzymes and other cell proteins in the human body but too much accumulation of copper within the cells is known to be toxic given that only small amounts are required for the wellbeing (Ashish *et al.*, 2013; Pourhabbaz & Pourhabbaz, 2012). High levels of copper concentrations within the cell initiate detoxification of reactive oxygen species and it becomes toxic. According to Ashish *et al.* (2013), copper metal in its pure uncombined metallic state is not toxic but its common salts like sulphates and sub-acetate renders the metal poisonous. Jung *et al.* (1998), conducted research comparing the concentrations of heavy metals in different cigarettes and realized that copper metal was present in significant amounts. This could be an entry means through which the metal is taken into human blood system.

2.3.3 Cadmium

Cigarette smoking has been linked as the most significant source of Cd exposure to the human population (Ashraf, 2012). Al-Bader *et al.* (1999), argue that smoking and food are the major sources of Cd into humans. Cadmium gets into the body system by smoking tobacco, diet, water drinking and inhalation from air and cigarette smoke has been proven to contain substantial amount of cadmium (Ashraf, 2012). High levels of cadmium in lungs, Liver, and kidney tissues blood have been associated with smoking (Gairola & Wagner, 1991; Hoffmann *et al.*, 2001). Cadmium accumulation in the body over years causes kidney damage and fragile bones (Kjellström, 1979). It is also known to cause stomach irritation, vomiting and diarrhea in human (Ashraf, 2012). Cd present in tobacco smoke contributes substantially to cancer risk hence it is classified as a group 1 carcinogen (Fowles & Dybing, 2003; Galażyn-Sidorczuk *et al.*, 2008; IARC International Agency for Research on Cancer, 2012).

2.3.4 Lead

Lead metal is known to be one of the most toxic metals capable of causing serious effects in human brains, nervous system and red blood cells (Hammond & Dietrich, 1990; Harrison & Laxen, 1981). Researchers in Britain carried out a study on middle-aged men and they found out that there exists a strong relationship between blood lead concentrations and alcohol, and cigarette smoking (Shaper *et al.*, 1982). The (Fewtrell *et al.*, 2004) estimates that smokers inhale about 2-6% of lead in cigarettes. Lead metal is efficiently extracted from the soil by tobacco plants (Pappas *et al.*, 2007). Lead is known to be one of the most toxic metals that have caused extensive environmental pollution and health problems (Tangahu *et al.*, 2011). Consequently, levels of heavy metals such as lead in tobacco are higher when grown in soil having high ambient heavy metal concentrations (Pappas *et al.*, 2007). Human exposure to lead is known to cause mild mental retardation which basically translates to IQ points loss, increased blood pressure, anemia and gastrointestinal effects (Fewtrell *et al.*, 2004; Nevin, 2000; Prüss-Üstün *et al.*, 2004). Inhalation transports heavy metals such as lead in mainstream cigarette smoke through the oral cavity to the lungs where they are further transferred to the peripheral circulation and other body organs along with other smoke constituents including addictive nicotine (Pappas *et al.*, 2007).

2.3.5 Zinc

Zinc is one of the essential trace metals required in the body for proper functioning of the cells and some other enzymes (Pourhabbaz & Pourhabbaz, 2012). However, when zinc concentrations increases beyond the required levels; it is rendered toxic since it induces pathological conditions that are associated with oxidative stress. Although zinc is presumed to be nontoxic and an essential nutrient to human beings, studies show that the free ionic zinc (Zn^{2+}) poses danger to the body cells. This is because

zinc is capable of destroying neurons, glia and other types of body cells (Nriagu, 2007). These free Zn^{2+} ions could be very toxic since they can cause apoptosis. Ingestion of too much zinc by human beings has been proven to cause lethargy, light headedness, staggering, difficulty in writing clearly, anxiety, depression, somnolence and comatose (Nriagu, 2007). The entry path of zinc into human body is either by inhalation, entry via the skin or by ingestion with each exposure type allowing different concentrations of the metals in the blood (Plum *et al.*, 2010).

2.3.6 Manganese

Manganese is an essential element that is required by the human body for normal functioning and development. Its entry into human blood system is known to cause an impact on the homeostatic balance leading into poisonousness (Crossgrove & Zheng, 2004). According to Crossgrove and Zheng (2004), manganese poisoning occurs as a result of overexposure affecting the central nervous system and at times the lungs, liver and cardiac system. Too much accumulation of Manganese in the brain is known to cause neurotoxicity (Lee, 2000). Therefore, when individuals are frequently exposed to Mn they are likely to suffer from progressive, permanent, neurodegenerative damage causing symptoms closely likened to those of idiopathic Parkinson's disease (Inoue & Makita, 1996). Smoking of cigarette has not been classified as the leading route through which manganese enters the human blood system. Chiba and Masironi (1992) conducted a research on toxic and trace elements in tobacco and tobacco smoke and they didn't find any significant relationship between Mn levels in blood and smoking habits but the small level concentrations of Mn in cigarette when inhaled can cause significant effects to the homeostatic balance in the human body system.

2.4 Computational Chemistry

The expression computational chemistry can largely be used when a mathematical technique is sufficiently well developed and automated for operation on a computer in order to calculate the structures and properties of molecules and solids (Young, 2001). It is one of the most valuable and essential tools that chemists use in molecular design and it describes the generation, manipulation and representation of 3-dimensional structures (Nadendla, 2004). Computational chemistry has been developed from quantum mechanics which gives a mathematical account of the behavior of electrons that has never been found to be wrong (Young, 2001).

The entire field of computational chemistry has been constructed around approximate solutions, some of which are more accurate than any known experimental data (Taylor, 2011). Quantum chemical calculations of thermodynamic data have been developed beyond the level of simply reproducing experimental values, and can now make accurate predictions for molecules whose experimental data are unknown and the target is usually set as ± 2 kcal/mol for global energies and entropies (Ramachandran *et al.*, 2008).

2.4.1 Density Functional Theory (DFT)

This is a ground state method that is used to calculate the properties of many electron systems from first principles calculations (Capelle, 2006). DFT is successfully used in describing structural and electronic properties in many materials ranging from atoms to molecules making it a first tool in first principles calculation that describe and predict the properties of molecular systems (De Silva & Wesolowski, 2012).

DFT focuses on describing interacting systems of fermions through its density and not through wave function (Harrison, 2003). Given a number of N electrons in a solid, that obey the Pauli principle and repulse one another through the Coulomb potential,

it will imply that the basic variable of the system depends only on three spatial coordinates x , y , and z – rather than $3N$ degrees of freedom (Aydin *et al.*, 2011). The knowledge of DFT is important in determining the properties of a molecule in its ground state (Furche & Rappoport, 2005). If one knows the exact electron density, $\rho(r)$, then the cusps of this density would occur at the positions of the nuclei (De Silva & Wesolowski, 2012). Knowledge of the nuclei would therefore give the nuclear charge.

2.4.1.1 The Hohenberg-Kohn Theorem

The Hohenberg-Kohn theory consists of two theorems; the first Hohenberg-Kohn theorem and the second Hohenberg-Kohn theorem (De Silva & Wesolowski, 2012). The first Hohenberg-Kohn theorem states that the density of any system determines all ground state properties of the system (Harrison, 2003).

$$E = E[\rho] \quad \text{Equation 2.1}$$

where, ρ is the ground state density of the system?

According to Harrison (2003), the second Hohenberg-Kohn theorem shows that there is a variational principle for the above energy density functional ρ . If ρ' is not the ground state density function of the above system, then;

$$E[\rho'] > E[\rho] \quad \text{Equation 2.2}$$

Considering a system of N interacting electrons under an external potential $V(r)$ (Coulomb potential) the system having a non-degenerate ground state shall have only one ground state charge density $n(r)$ which responds to a given $V(r)$. Since the system has many interacting electrons, we obtain a Hamiltonian, $H = T + U + V$

with a ground state wave function ψ ; where T is the kinetic energy, U the electron-electron interaction, V the external potential; the charge density $n(r)$ is defined as;

$$n(r) = N \int |\psi(r, r_2, r_3, \dots, r_N)|^2 dr_2 \dots dr_N \quad \text{Equation 2.3}$$

Considering a different Hamiltonian $H' = T + U + V'$ (V and V' do not differ by a constant) with ground state wave function, ψ , and assuming that the ground state charge densities, $n(r)$, are the same, then the inequality below holds:

$$E' = \langle \psi' | H' | \psi' \rangle < \langle \psi | H' | \psi \rangle = \langle \psi | H + V' - V | \psi \rangle \quad \text{Equation 2.4}$$

that is,

$$E' < E + \int (V(r) - V'(r)) n(r) dr \quad \text{Equation 2.5}$$

ψ , and ψ' are different because they are Eigen states of different Hamiltonians and thus the inequality is strictly suggesting that no two different potentials can have the same charge density. According to the first Hohenberg-Kohn theorem, the ground state E energy is uniquely calculated by the ground-state charge density (Dreizler & Gross, 2012). In mathematical terms, E is a function, $E[n(r)]$ of $n(r)$.

$$E[n(r)] = \langle \psi | T + U + V | \psi \rangle = \langle \psi | T + U | \psi \rangle + \langle \psi | V | \psi \rangle = F[n(r)] + \int n(r) V(r) dr$$

$$\text{Equation 2.6}$$

where $F[n(r)]$ is a universal functional of the charge density $n(r)$ and not of, $V(r)$.

For this functional, Harrison (2003) explains that a variational principle holds and the ground state energy is minimized by the ground state charge density and the DFT

reduces the N -body problem to the determination of a 3-dimensional function $n(r)$ which minimizes a functional $E[n(r)]$.

2.4.1.2 The Kohn-Sham equations

These equations map systems of interacting electrons to an auxiliary system of non-interacting electrons with the same ground state charge density, $n(r)$. In a system of non-interacting electrons, according to (Harrison, 2003) the ground state charge density is represented as a sum over one-electron orbitals (the KS orbitals), $\psi_i(r)$:

$$n(r) = 2 \sum_i |\psi_i(r)|^2 \quad \text{Equation 2.7}$$

where i , runs from 1 to $\frac{N}{2}$, if double occupancy of all physical states are assumed and

the KS orbitals are given as the solution of the Schrödinger equation.

$$\left(-\frac{\hbar^2}{2m} \nabla^2 + V_{KS}(r) \right) \psi_i(r) = \varepsilon_i \psi_i(r) \quad \text{Equation 2.8}$$

m , is the electron mass obeying orthogonal constraints:

$$\int \psi_i^*(r) \psi_j(r) dr = \delta_{ij} \quad \text{Equation 2.9}$$

According to Capelle (2006) the existence of a unique potential, $V_{KS}(r)$ having $n(r)$ as its ground state charge density is a consequence of the Hohenberg and Kohn second theorem which holds irrespective of the form of the electron-electron interaction U .

2.4.2 Basis Sets

A basis set is a statistical model that describes the orbitals inside a system, which estimates the total electronic wave function, used to perform theoretical calculations (Foresman & Frisch, 1996). In quantum chemistry, a basis set is a set of one particle function used to build molecular orbitals (Leach, 2001). Orbitals are one electron functions and are of two types; Slater-type orbitals (STO) and Gaussian-type orbitals (GTO). Slater-type orbitals are represented by the equation;

$$\phi_{abc}^{STO}(x, y, z) = Nx^a y^b z^c e^{-\xi r} \quad \text{Equation 2.10}$$

where;

N is a normalization constant

a, b, c controls angular momentum, $L = a + b + c$

ξ (xi) control the width of the orbital. Large values of ξ give tight functions and small values of ξ give diffuse functions (Weigend *et al.*, 2003) especially in cases involving H- like atoms with at least 1s orbitals that are known to be lacking radial nodes and are not pure spherical harmonics. Gaussian Type Orbitals (GTO) are represented by the following equation;

$$\phi_{abc}^{GTO}(x, y, z) = Nx^a y^b z^c e^{-\xi r^2} \quad \text{Equation 2.11}$$

Just like in STO a, b, c control angular momentum while $L = a + b + c$ and ξ control the width of the orbital for cases atoms that are no longer H-like atoms.

GTOs are much easier to compute and are universally used by quantum chemists. Electronic structure basis sets calculation makes use of Gaussian functions to

construct the orbitals (Petruzielo *et al.*, 2011). Gaussian computer program provides a wide range of pre-defined basis sets that are classified by the number and types of basis functions they contain (Foresman & Frisch, 1996).

2.4.2.1 Polarized Basis Sets

A polarized basis set removes the limitation of orbitals changing size without changing shape. These polarized basis sets add orbitals with angular momentum beyond what is required for the ground state in the description of all the atoms in the ground state thereby allowing these atoms to change shape (Binkley *et al.*, 1980; Gianturco & Huo, 2013). Polarized basis sets are represented as shown,

$6-31G(d)$, $6-31G^*$, $6-31G(d,p)$ and $6-31G^{**}$. The signs (d) and $*$ are functions added to atoms with $Z > 2$ (atoms with large atoms). The symbols (d,p) and $**$ represent p -type functions added to H atoms. During the molecule formation processes, atomic orbitals become distorted bipolarization (Gianturco & Huo, 2013).

2.4.2.2 Diffuse Basis Set

Diffuse basis set can be used to describe anions, molecules with lone pairs, excited states and transition states (loosely held electrons) (Langhoff & Kern, 1977). Diffuse functions are large size s-type and p-type functions which allow orbitals to occupy large space (Langhoff & Kern, 1977; Petersson *et al.*, 1988). They are represented as shown.

$6-31+G(d)$ or $6-31++G(d)$

$6-31+G(d)$ represents a basis set with an additional larger p-function for atoms with $Z > 2$ while $6-31++G(d)$ describes a basis set with additional larger s-function for H-like atoms.

2.4.3 Møller-Plesset Perturbation Theory (MPn)

2.4.3.1 Second-Order Møller-Plesset Models (MP2)

This is a practical correlation energy scheme that is based on the recognition that the Hartree-Fock wave function, ψ and the ground state energy, E are approximate solutions to the Schrödinger equation. They are the exact solution to an analogous problem involving the Hartree Fock Hamiltonian, \hat{H}_0 , in the place of the ‘exact’ Hamiltonian, \hat{H} (Hehre, 2003). If the Hartree-Fock wave function ψ and energy are very close to the exact wave function and the ground state energy E , according to Hehre (2003), the exact Hamiltonian is written as;

$$\hat{H} = \hat{H}_0 + \lambda \hat{V} \quad \text{Equation 2.12}$$

where;

\hat{V} is a small perturbation

λ is a dimensionless parameter

Expanding the exact wave function and energy in form of the Hartree-Fock wave function, we get

$$E = E^{(0)} + \lambda E^{(1)} + \lambda^2 E^{(2)} + \lambda^3 E^{(3)} + \dots \quad \text{Equation 2.13}$$

$$\psi = \psi_0 + \lambda \psi^{(1)} + \lambda^2 \psi^{(2)} + \lambda^3 \psi^{(3)} + \dots \quad \text{Equation 2.14}$$

Substituting equation 2.13 to 2.14, into the Schrödinger equation and gathering terms in λ^n yields,

$$\hat{H}_0 \psi_0 - E^{(0)} \psi_0 \quad \text{Equation 2.15a}$$

$$\hat{H}_0 \psi^{(1)} + \hat{V} \psi_0 - E^{(0)} \psi^{(1)} + E^{(1)} \psi_0 \quad \text{Equation 2.15b}$$

$$\hat{H}_0 \psi^{(2)} + \hat{V} \psi^{(1)} - E^{(0)} \psi^{(2)} + E^{(2)} \psi_0 \quad \text{Equation 2.15c}$$

Multiplying each of the equations 2.15 by ψ_0 and integrating over all space yields the following expression for the n^{th} order (MPn) energy (Hehre, 2003).

$$E^{(0)} - \int \dots \int \psi_0 \hat{H}_0 \psi_0 d\tau_1 d\tau_2 \dots d\tau_n \quad \text{Equation 2.16a}$$

$$E^{(1)} - \int \dots \int \psi_0 \hat{V} \psi_0 d\tau_1 d\tau_2 \dots d\tau_n \quad \text{Equation 2.16b}$$

$$E^{(2)} - \int \dots \int \psi_0 \hat{V} \psi^{(1)} d\tau_1 d\tau_2 \dots d\tau_n \quad \text{Equation 2.16c}$$

In this case the Hartree-Fock energy is the sum of the zero and first order Møller-Plesset energies (Hehre, 2003).

$$E^{(0)} - \int \dots \int \psi_0 \left(\hat{H} + \hat{V} \right) \psi_0 d\tau_1 d\tau_2 \dots d\tau_n E^{(0)} + E^{(1)} \quad \text{Equation 2.17}$$

The correlation energy is written as;

$$E_{corr} - E_0^{(2)} + E_0^{(3)} + E_0^{(4)} + \dots \quad \text{Equation 2.18}$$

The first term in equation (2.17) can be expanded as follows

$$E^{(2)} - \sum_{i < j}^{\text{molecular}} \sum_{a < b}^{\text{orbitals}} \sum_{\text{unocc}} (\varepsilon_a + \varepsilon_b + \varepsilon_i + \varepsilon_j)^{-1} [(ij||ab)]^2$$

Equation 2.19

where ε_i and ε_j are energies of the occupied molecular orbitals, ε_a , and ε_b are energies of unoccupied molecular orbitals. Integrals $ij||ab$ are over filled (i and j) and (a and b) empty molecular orbitals and they account for changes in electron-electron interactions due to electron promotion,

$$(ij || ab) - (ia | jb) - (ib | ja)$$

Equation 2.20

where;

$ia | jb$, involve molecular orbitals and not basis functions (Hehre, 2003; Kong *et al.*, 2000).

2.5 Geometry Optimization

This is a procedure that is used to find the arrangement of nuclei whose potential energy is a minimum (Bargholz *et al.*, 2013). In order for atoms to be brought together, a lot of energy is needed. Geometry optimization in Gaussian involves making an initial guess for the geometry and then calculating the derivative of the potential energy with respect to each of the nuclear coordinates (Ochterski, 2000). The gradient represents forces acting on each atom and can be used to obtain new geometry that is closer to the equilibrium geometry (Schlegel, 2011). In order to ascertain that equilibrium geometry has been obtained, the process is repeated until the gradient approaches zero (Stewart, 1989). Starting with the input structure, the

search for equilibrium follows the potential energy surface such that it is continuously traveling toward a minimum energy (Schlegel, 2011). The calculation is said to converge once it has reached a minimum energy point on the potential energy surface (Pesch *et al.*, 1992). Because the objective is to find the global minimum on the molecular compounds, it is imperative that the input structure is well chosen (Schlegel, 2011).

CHAPTER THREE

3.0 METHODOLOGY

3.1 Sample Collection and Sample Preparation

Two brands of processed cigarettes smoked in Kenya were purchased from vendors and used without further treatment. Unprocessed tobacco dried leaves of about 10 grams were bought from the market and the place of origin identified.

3.1.1 Sample Collection for AAS Analysis

The composite sample of each brand was prepared by smoking five cigarettes picked randomly from a pack of 20 cigarettes implying that the heavy metal contents reported in this study is an average of 5 cigarettes. That is, the result of 5 cigarettes according to ISO (1999:3402) standards were averaged to enhance the reproducibility of data. The experimental set up is presented in Figure 3.1. A cigarette stick was placed at the tip of tubing connected to a vacuum and lit with a match stick. To sustain the burning of the cigarette, a syringe was used to draw in air to the burning cigarette. The cigarettes were smoked by creating a low pressure using a syringe at a rate of 35 mL/s according to ISO 3402:1999 standards and cigarette smoke collected in 50 mL analytical grade methanol containing 2 drops of 1M nitric acid in a conical flask as shown in Figure 3.1. Unprocessed tobacco leaves of mass equivalent to that of five cigarettes were accurately weighed and then smoked using a smoking pipe. The samples were labeled and stored in dark crimp top vials for AAS analysis.

The ash from the two processed cigarettes, SM1 and ES1, and unprocessed cigarette were carefully collected and mixed with 50 mL methanol and 2 drops of 1M nitric acid, stirred vigorously and filtered through Whatman No.4 filter paper into 250 mL volumetric flask. The filtrate was then stored for AAS analysis.



Figure 3.1: The Apparatus Set Up for Cigarette Smoking in the Laboratory

3.1.2 Sample Preparation for GC-MS Analysis

50 mg of tobacco from processed cigarette brand SM1 were weighed accurately to the nearest mg and packed in a quartz reactor of volume 1.6 cm^3 . The sample in the quartz reactor was placed in an electrical heater (muffle furnace) whose temperature can be varied between $20 \text{ }^\circ\text{C}$ and $1000 \text{ }^\circ\text{C}$. The muffle furnace was purchased from Thermo Scientific Inc., USA. The SM1 cigarette samples were then burned in flowing nitrogen inside the quartz reactor and the smoke effluent was allowed through a transfer column. The study employed conventional pyrolysis techniques in which new tobacco samples were used at every pyrolysis temperature as described by (Kibet *et al.*, 2013). The pyrolisate was then collected in 10mL of methanol in crimp top vials waiting for GC-MS analysis.

3.1.3 Experimental Investigation of Heavy Metals Using AAS

Flame Atomic Absorption Spectrometer (AAS) with computer aided systems was employed in these experiments to detect the presence of heavy metals. The AAS used

in this work was Shimadzu 6200 (Japan) with a graphite furnace. The machine was operated with wavelength and the slit width set at 357.9 and 0.2 nm, respectively. The flame type used was air-acetylene, and the oxidant flow rate was set to run at 1.5 L/min. The sensitivity of the instrument was 0.055 ppm, and the detection limit was 0.001 ppm. The lamp current was 5 mA and the optimum working range of the instrument was 0.001-20.0 ppm. The chemical reagents used were of analytical gradient. The working solutions of the metals to be examined (Pb, Cd, Zn, Cu, Mn and Cr) were prepared by dilution of standard solutions in concentrations ranging from 0.1 - 8 µg/L in 1 % v/v nitric acid. The AAS determination of all cations was performed under the recommended conditions for each metal. The various metal concentrations from the sample solution were determined from the calibration curves based on the absorbance obtained from the unknown samples.

3.1.4 GC-MS Characterization of Molecular Products

The organic by-products from the smoking of tobacco were investigated using a GC-MS machine. The pyrolysate was collected in 1mL methanol in crimp top vials for 5 minutes and then analyzed using Agilent 6890 Gas Chromatography hyphenated to a Mass Selective Detector (MSD) to quantitatively determine the yields of molecular compounds. 1µL of sample dissolved in methanol was injected into a GC column (HP-5MS, 30m x 250 µm x 0.5 µm). The temperature of the injection port was set at 200 °C. Temperature programming was applied at a heating rate of 25°C for 10 minutes, holding for 2 minute at 250° C, followed by a heating rate of 10 °C for 5 minutes, and holding for 5 minutes at 300 °C. The Mass Selective Detector (MSD) was operated on the Total Ion Current Mode (TIC) and the ion source was set at 70 eV. The molecular compounds were identified using National Institute of Science and Technology software (NIST, USA). To ensure the correct compound was positively

identified, the retention times of pure compounds (standards) were determined and matched with those of the analytes.

3.1.5 Computational Methodology

All theoretical calculations of the molecules investigated were performed with the Gaussian 03 computational program package. *Ab initio* calculations including correlation effects were made by using the Density Functional Theory (DFT) and MP2 level of theories with the 6-31++ G (d, p) basis set. The frequency calculations provided thermodynamic quantities such as Zero-Point Vibrational Energy (ZPVE), temperature corrections, and absolute entropies (Truhlar *et al.*, 2004).

The optimized geometries and Molecular Orbitals (MOs) of molecular components were used in frequency calculations in order to determine their global energies and subsequently establish their global minima. The averaged vibrational nuclear positions of the molecules were used for harmonic frequency calculations which resulted in Infrared (IR) intensities. The ¹³C nuclear magnetic resonance chemical shifts of the compounds were calculated by invoking the keyword NMR at the DFT level with Becke's three parameter hybrid method using the Lee-Yang-Parr correlation function (B3LYP) method and the 6-31++ G(d,p) polarized and diffuse basis set (Stewart, 1989). Enthalpy changes were computed between the enthalpies of formation of the reactant (neutral compound) and its corresponding free radical using the following thermo chemical equation (Kibet *et al.*, 2014).

$$\Delta H^0 = \sum (\varepsilon_0 - H_{corr})_{products} - \sum (\varepsilon_0 - H_{corr})_{reactants} \quad \text{Equation 3.1}$$

where ΔH^0 is change in enthalpy, H_{corr} is a correction to thermal enthalpy and ε_0 is the sum of electronic and thermal enthalpies.

3.1.6 Quantitative Structural Activity Relationship (QSAR)

The computational software HyperChem® (2002) was employed in the determination of the bioactivity of the molecular by products and radicals and perform geometry optimizations (energy minimizations) in order to determine the lowest energy conformation of the molecules. The HyperChem computational software contains a collection of computational tools including Quantitative Structural Activity Relationship (QSAR) which were used to determine the relative toxicities of the compounds under study (Karelson *et al.*, 1999). In predicting the relative toxicities, the logarithm of octanol-water partition coefficient (K_{ow}) parameter was calculated (Lessigiarska *et al.*, 2005). Log P is an important parameter that measures the lipophilicity of a compound which correlates with biological activities including mutagenicity and carcinogenicity (Smith *et al.*, 2002). The K_{ow} values of these compounds were estimated and checked whether they were too high (exceeding 2.0) or low. If the K_{ow} value of a compound is too high, it implies that the compound can bio-accumulate in the body system leading to occurrence of long term and extensive destruction of the body cells (Lobo *et al.*, 2010; WHO, 2006).

3.2 Data Analysis

The data obtained from AAS were carefully interpreted and presented in graphs and tables which showed how the heavy metals were distributed in the different cigarette brands and tobacco leaves under investigation. All statistical tests were performed with the aid of SPSS statistical package, version 18. Significant levels were measured at 95% confidence level with significant differences recorded at $p < 0.05$. Means for the three cigarette brands in the study were compared using analysis of variance (ANOVA). Thus, with more than two categories of the independent variable (for example, Trd, SM1 and ES1 cigarettes), post hoc tests were conducted to establish the

specific pairs of means which were different from each other. When the variance of the metal concentration means was equal, Tukey's honestly significant difference test (HSD) was used to conduct the post hoc tests, and when it was unequal, the Games – Howell test was used. The computed enthalpies were analyzed and data interpreted using graphs of various parameters (enthalpy, internal energy, entropy, and temperature) plotted. This information was presented using graphs and charts.

CHAPTER FOUR

4.0 RESULTS AND DISCUSSION

The aim of this work was to experimentally determine selected toxic molecular products (propanol, phenol, butyrolactone and guaiacol) and heavy metals (Pb, Cd, Cr, Cu, Mn and Zn) in mainstream smoke of unprocessed and processed commercial cigarettes smoked in Kenya and perform computational modeling on the selected toxic molecular products.

4.1 Experimental Exploration of Toxic Molecular Products

The results showed that cigarette smoke yielded numerous organic compounds but those of interest in this study are presented in the chromatogram shown in figure 4.1.

Propanol, butyrolactone, phenol and guaiacol had retention times 4.04, 8.14, 8.88, and 12.18 minutes respectively.

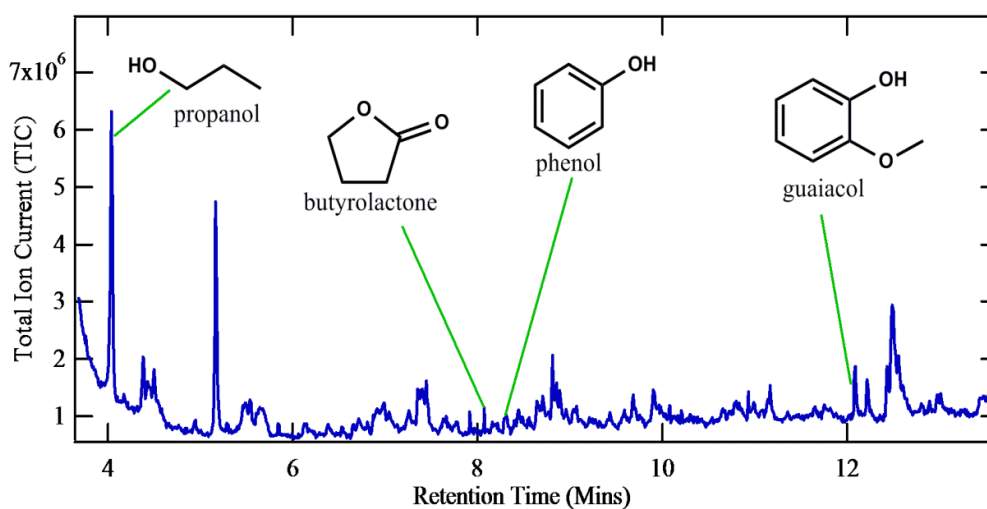


Figure 4.1: Experimental Release of Molecular Products from Cigarette

Experimental release of propanol and phenol from cigarette was explored and theoretical enthalpy and electronic calculation was performed using Gaussian 03 computational code. The evolution of propanol and phenol was monitored using GC-MS and the results presented in Figure 4.2. Figure 4.2 shows that propanol and phenol

yields peaked at about 400 °C before decreasing significantly to a yield intensity of approximately 1.2×10^8 and 9.2×10^7 GC area counts, respectively at 700 °C. Notably, high amounts of propanol were produced throughout the whole pyrolysis temperature compared to that of phenol. For instance, at 400 °C, propanol was approximately three times higher than phenol.

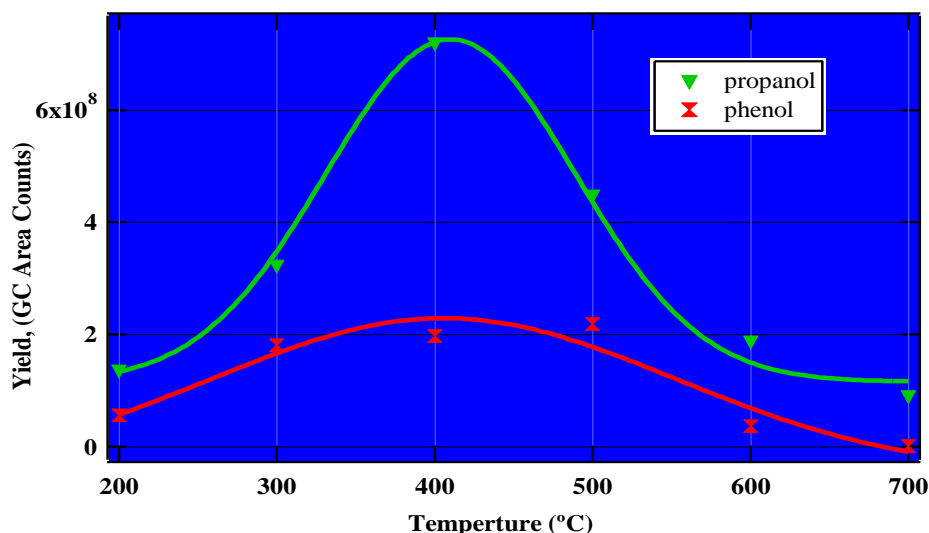


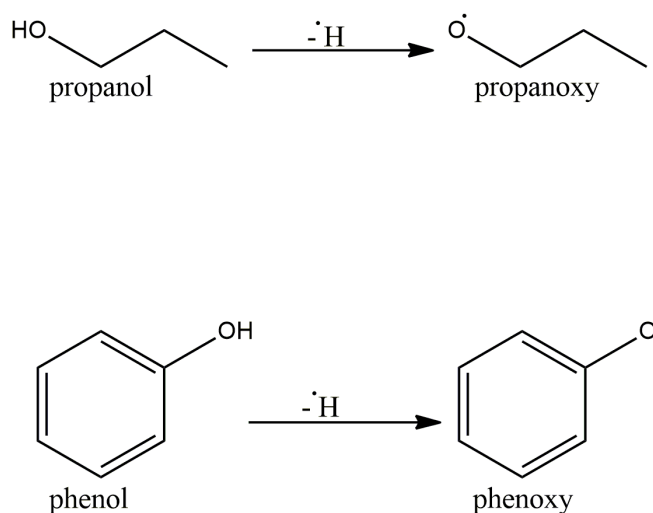
Figure 4.2: Propanol and Phenol yields from the combustion of SM1 cigarette brand.

It is evident from Figure 4.2 above that propanol and phenol are formed in low yields between 200 and 300 °C. Similarly, the yields of these two molecular products (propanol and phenol) decreased considerably at temperatures of 600 and 700 °C. This could suggest that at high temperature zones, most cigarette smoke products are being converted to more lethal polycyclic aromatic hydrocarbons (PAHs) such as benzo (a) pyrene and possibly cyclopentafused PAHs (Wang *et al.*, 2004). These compounds are well established cancer causing compounds (Wang *et al.*, 2004). The fact that propanol and phenol and probably other toxic molecular by-products from combustion of tobacco are released in low yields at low temperatures is an indication that designing cigarettes that maybe smoked at low temperatures can minimize

consumption of high doses of tobacco toxins. Optimum temperatures are therefore critical in tobacco and cigarette development (Kibet *et al.*, 2014).

4.1.1 Formation of Free Radicals

Reactive free radicals are formed once a hydrogen atom gets abstracted from the molecules (propanol and Phenol) at high temperatures as shown in scheme 4.1 below. These free radicals play a role in reactions which result to creation of new combustion by-products such as aldehydes, olefins and PAHs (Kibet *et al.*, 2014) with dibenzofuran as the most probable PAH to form in cigarette smoke.



Scheme 4.1: Formation of Propanoxy and Phenoxy Radicals from Propanol and Phenol respectively

The thermo-chemical properties of these formed radicals constitute paramount importance in this study. Different studies conducted elsewhere on free radicals have shown that common neural diseases such as Alzheimer's disease, Parkinson's disease and amyotrophic lateral sclerosis and other complications including diabetes, cardiovascular disease, prematurity in babies and cancer are associated with oxidative stress (Majima & Toyokuni, 2012).

4.1.2 Computational Details

4.1.2.1 Calculation of Enthalpy Changes (ΔH)

The energy change for the formation of a compound or a radical from the mother molecules were calculated using the thermodynamic equation 3.1(Ochterski, 2000). The sum of electronic and thermal 1enthalpies were calculated using DFT and the polarized basis set, B3LYP/ 6-31 ++ (d,p) level of theory and tabulated in Table 4.1 which reports the enthalpies and enthalpy changes for propanol, phenol and their corresponding free radicals calculated at the density functional level theory. The general trend was that there was significant variation in thermal energy with temperature for both propanol and phenol towards the formation of their respective free radicals under DFT level theory. It was also observed that the free radicals (propanoxy and phenoxy) had more positive enthalpy values hence lower stability compared to their parent compounds (propanol and phenol) respectively.

Table 4.1: DFT Thermochemical Data for Molecular Compounds and Subsequent Radicals

Temp. (K)	Propanol (Hartree/particle)	Propanoxy (Hartree/particle)	Phenol (Hartree/particle)	Phenoxy (Hartree/particle)
373	-194.30	-193.65	-307.45	-306.81
423	-194.30	-193.64	-307.44	-306.81
473	-194.30	-193.64	-307.44	-306.81
523	-194.30	-193.64	-307.44	-306.81
573	-194.29	-193.64	-307.43	-306.80
623	-194.29	-193.63	-307.43	-306.80
673	-194.29	-193.63	-307.43	-306.80
723	-194.28	-193.63	-307.42	-306.79
773	-194.28	-193.63	-307.42	-306.79
823	-194.28	-193.62	-307.41	-306.78
873	-194.27	-193.62	-307.41	-306.78
923	-194.27	-193.62	-307.41	-306.78
973	-194.27	-193.61	-307.40	-306.77
1023	-194.26	-193.61	-307.40	-306.77
1073	-194.26	-193.60	-307.39	-306.76
1123	-194.25	-193.60	-307.39	-306.76
1173	-194.25	-193.60	-307.38	-306.76
1223	-194.25	-193.59	-307.38	-306.75

Figure 4.3 and Figure 4.4 below displays results on the thermo-chemical behavior of propanol and phenol towards the formation of their respective free radicals as predicted by the DFT level theory.

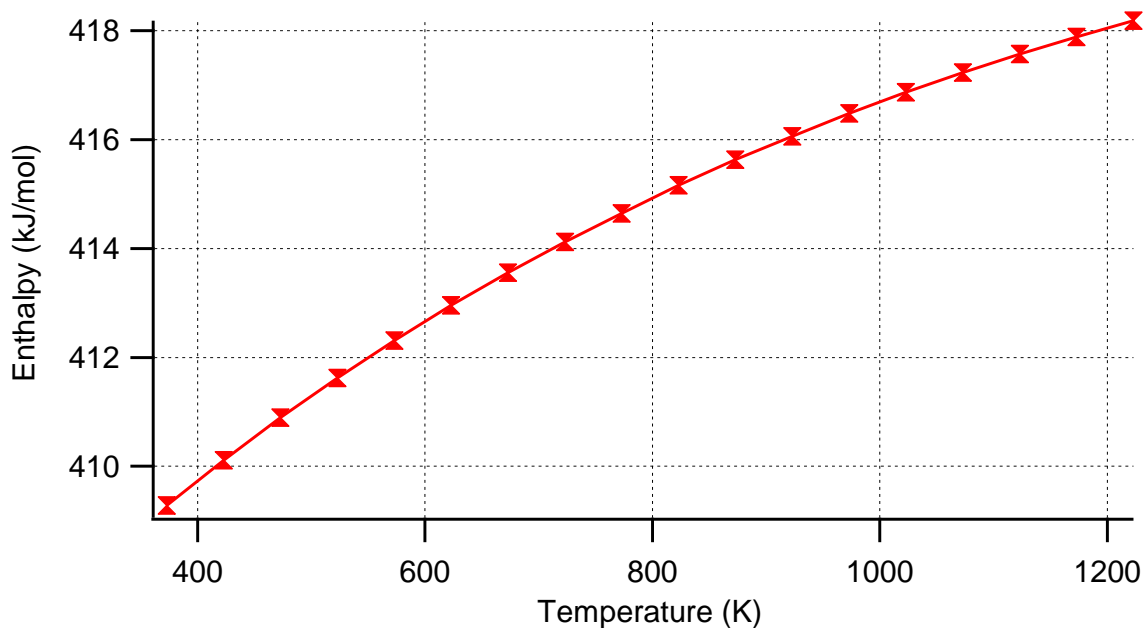


Figure 4.3: Enthalpy Change for the Formation of Propanoxy Radical by DFT level Theory

Figure 4.3 illustrates the enthalpy change for the formation of propanoxy radical from propanol as predicted by the DFT level theory. It is evident that an increase in temperature is accompanied by increase in absorption of energy from the surrounding (endothermicity). Likewise, in the formation of phenoxy radical the same trend is exhibited as illustrated in Figure 4.4 below.

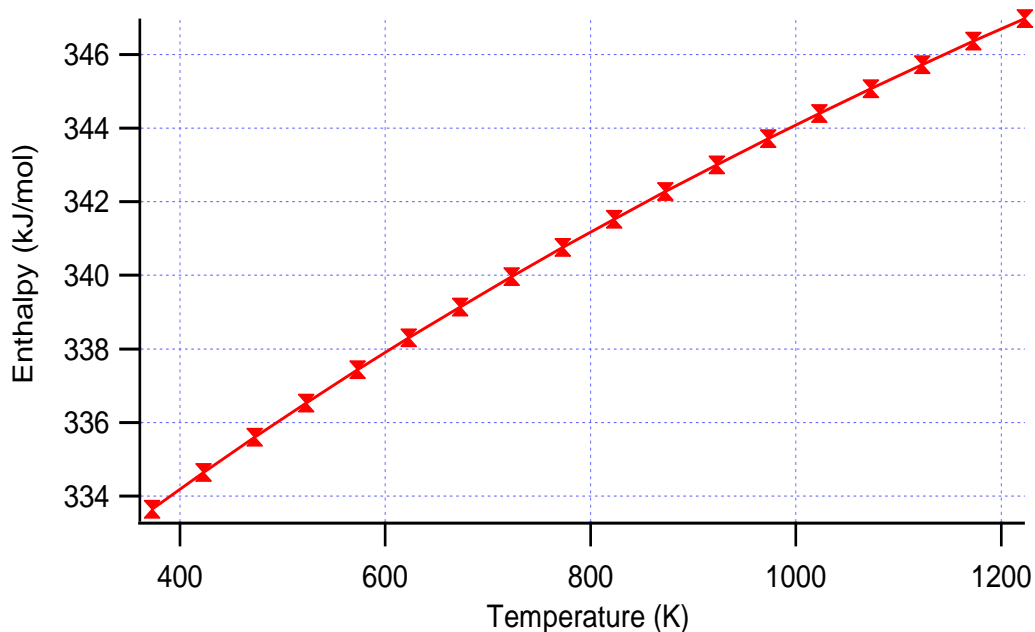
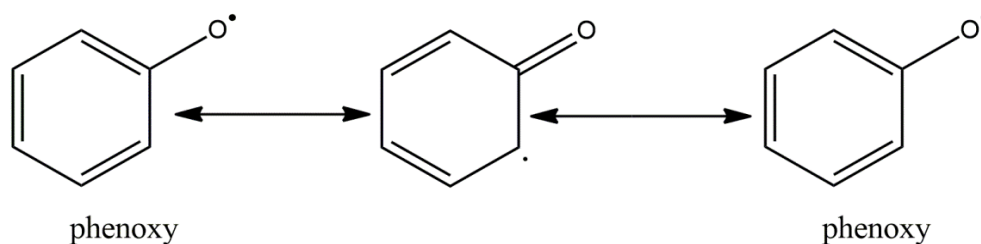


Figure 4.4: Enthalpy Change for the Formation of Phenoxy Radical prediction by DFT Theory

The formation of phenoxy radical from phenol is accompanied by heat energy being absorbed into the system hence high positive enthalpy change values. This implies that in the formation of propanoxy and phenoxy radicals, enthalpies of reaction are larger in the reaction leading to the formation of propanoxy than in Phenoxy. Heat energy must be absorbed by the mother molecules to get the oxygen-hydrogen bonds broken for the hydrogen atom to be abstracted. This suggests that the formation of propanoxy radical from propanol is not readily favored. This is characteristic of the structures of propanol and phenol molecules. Phenol molecule is more stable than the propanol molecule, hence, the phenoxy radical is viewed as most stable compared to the propanoxy radical because it exhibits various resonance structures as shown in scheme 4.2.



Scheme 4.2: Resonance Structures of Phenoxy Radical

Propanoxy radical has only one structure and thus cannot exhibit resonance behavior. However, propanoxy radical being unstable has a short life-time and therefore very reactive. This makes it biologically hazardous because of its ability to react more readily with DNA, lipids; other biological compounds such as microsomes, and RNA. However, phenoxy radical is a well-established biological pollutant(Dellinger *et al.*, 2007). It is classified as a persistent free radical that has long life-times and can react with biological molecules in the body to cause serious cellular damage and subsequent oxidative stress and cancer(Dellinger *et al.*, 2007).

4.1.2.2 Calculations of Change in Gibbs Energy (ΔG)

To calculate the change in Gibbs energy for reactions that lead to the formation of a compound or a radical from its constituents, the thermodynamic equation presented by (Ochterski, 2000) was employed.

$$\Delta G^0 = \sum(\varepsilon_0 - G_{corr})_{products} - \sum(\varepsilon_0 - G_{corr})_{reactants} \quad \text{Equation 4.2}$$

where, ΔG^0 is the change in Gibbs energy of reaction,

G_{corr} the thermal correction to Gibbs energy and

$\sum(\varepsilon_0 - G_{corr})$ the sum of electronic and thermal free energy.

The sum of electronic and thermal free energy were calculated using the DFT and the polarized basis set, B3LYP/6-311 + (d,p) level theory and results presented in Table 4.2. The energy present in propanol and phenol molecules at different temperatures is involved in initiating their conversion to their respective radicals as presented. At various temperatures, it can be seen that propanoxy radical has higher Gibbs energies compared to phenol. This implies that spontaneous reactions are more likely to occur in propanoxy without the need of any input of energy than in phenoxy radical. This findings support the idea of phenoxy being a more stable radical than propanoxy hence deeming propanoxy a more poisonous radical. Therefore, once the propanoxy radical has been formed, at presumably high temperatures, it is capable of starting spontaneous reactions in order to form a compound with a lower Gibbs energy. This transformation of propanoxy can lead to production of more toxic compounds.

Table 4.2: Gibbs Energy of Molecular Toxins and their respective Radicals

Temp. (K)	Propanol (Hartree/Particle)	Propanoxy (Hartree/Particle)	Phenol (Hartree/Particle)	Phenoxy (Hartree/Particle)
373	-194.35	-193.69	-307.49	-306.86
423	-194.35	-193.70	-307.49	-306.87
473	-194.36	-193.70	-307.50	-306.87
523	-194.37	-193.71	-307.51	-306.88
573	-194.37	-193.72	-307.52	-306.89
623	-194.38	-193.73	-307.52	-306.90
673	-194.39	-193.73	-307.53	-306.90
723	-194.40	-193.74	-307.54	-306.91
773	-194.41	-193.75	-307.55	-306.92
823	-194.41	-193.76	-307.56	-306.93
873	-194.42	-193.77	-307.57	-306.94
923	-194.43	-193.77	-307.57	-306.95
973	-194.44	-193.78	-307.58	-306.96
1023	-194.45	-193.79	-307.59	-306.97
1073	-194.46	-193.80	-307.60	-306.98
1123	-194.47	-193.81	-307.61	-306.99
1173	-194.48	-193.82	-307.62	-307.00
1223	-194.49	-193.83	-307.63	-307.00

Although the Gibbs energies of phenoxy are slightly lower than those of propanoxy, its ability of spontaneously getting converted to other compounds in order to minimize its Gibbs energy cannot be ignored.

The graphical representation of change in Gibbs energy is as shown in Figure 4.5 and Figure 4.6 below.

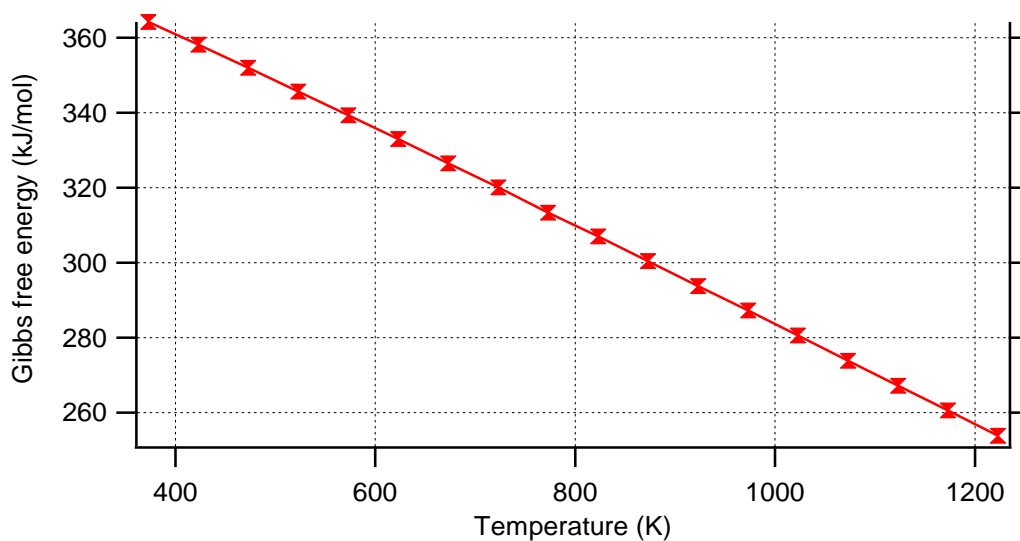


Figure 4.5: Change in Gibbs Energy for the Formation of Propanoxy Radical

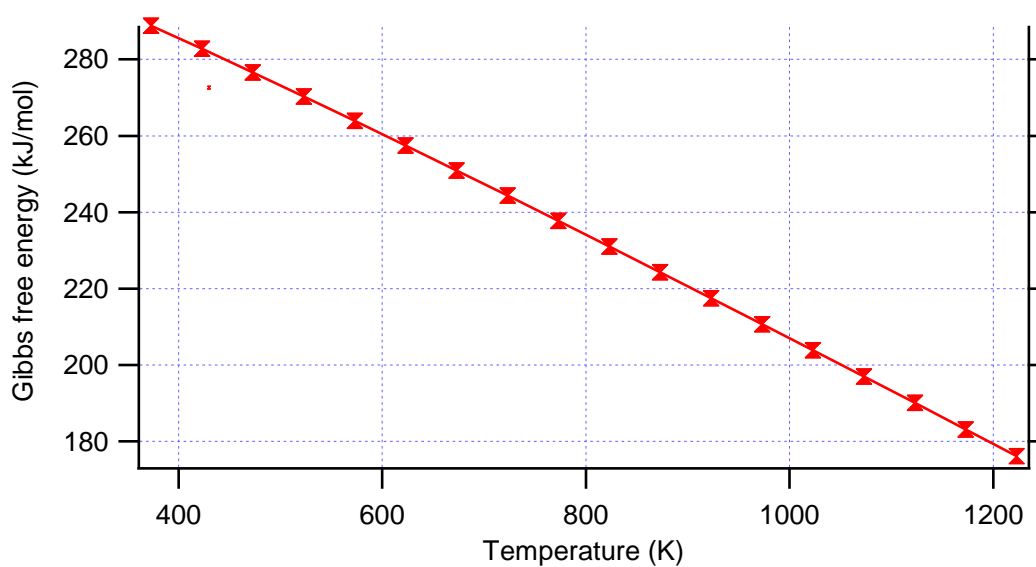


Figure 4.6: Change in Gibbs Energy for the Formation of Phenoxy Radical

Figure 4.5 and figure 4.6 above display a decreasing trend in the change in Gibbs energy for formation of both propanoxy and phenoxy radicals with increasing temperature. Also, it is noticeable that the formation of phenoxy radical from phenol is less endothermic when compared with the formation of propanoxy from propanol. To be precise, at the temperatures of 373, 573 and 773K, the changes in Gibbs energy for formation of propanoxy are 323.03, 298.55 and 273.18 kJmol⁻¹ respectively while that for phenoxy are 288.83, 270.28 and 237.71 kJmol⁻¹ respectively.

4.1.2.3 Calculation of Entropy Changes (ΔS)

The entropy change of a chemical reaction was calculated by getting the difference between the entropy values of the products and the reactants. The *Gaussian 03* system programs under DFT and the 6-311++G (d,p) diffuse-polarized basis set was manipulated in the calculation of entropies of the molecules under investigation and the thermodynamic equation 4.3 employed in calculating the entropy changes for formation of the propanoxy and phenoxy radicals from their parent compounds.

$$\Delta S_{\text{Reaction}} = \sum n_p S_{\text{products}} - \sum n_r S_{\text{reactants}} \quad \text{Equation 4.3}$$

where ΔS is change in entropy, n_p and n_r are the number of moles of the products and reactants respectively. Considering propanol and phenol as gaseous products resulting from incomplete combustion of tobacco, their entropy values will be higher. This gives the molecules more options of position than the same atoms in solid state. The change in entropy of reactions of propanol and phenol leading to the formation of their respective radicals showed an increasing trend with increase in temperature as shown in Figure 4.7 below.

This trend can be explained by the fact that an increase in temperature is associated with an absorption and redistribution of energy making more energy levels (rotational, vibrational and electronic) to be available.

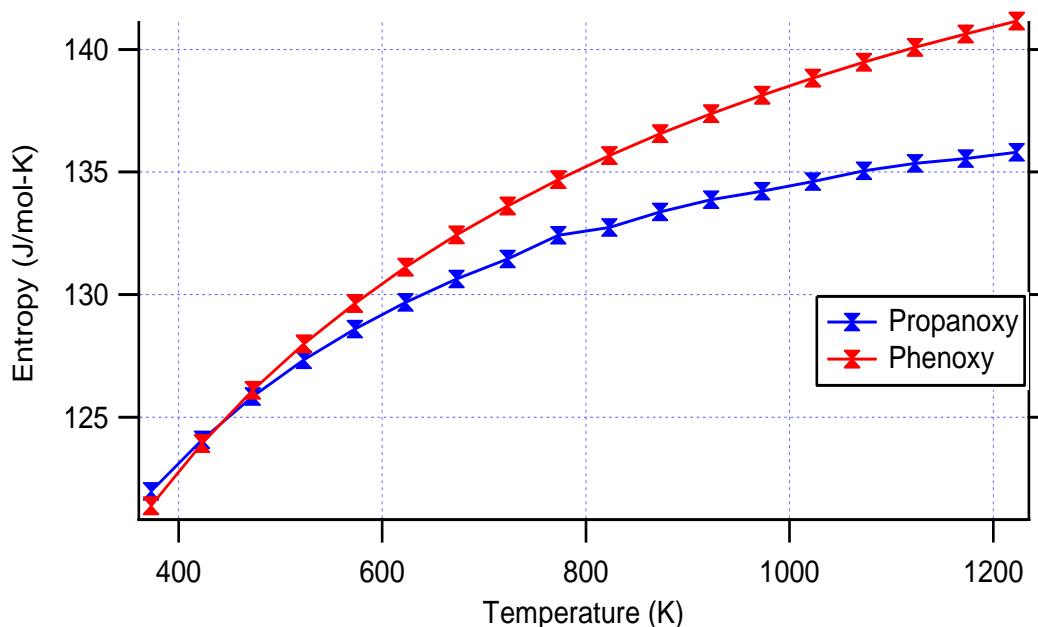


Figure 4.7: Change in Entropy for the Formation of Propanoxy and Phenoxy Radicals

It is evident from Figure 4.7 above that there is an increase in entropy change in the formation of propanoxy and phenoxy radicals with increase in temperature. At these theoretical temperature ranges, it can be observed that the entropy change in the formation of phenoxy is slightly higher than that of propanoxy radicals. This implies that in the conversion of phenol to its radicals, there are more options of position available for it than they are in propanoxy. This is majorly because phenoxy forms resonance structures in its radical state unlike propanoxy which does not exhibit any resonance structures as described in scheme 4.2. This observation supports the idea of propanoxy being unstable when compared to phenoxy radical.

4.1.3 Comparisons of MP2 and DFT Computational Results

This section gives a brief description of the results from MP2 explicitly carried out with *Gaussian 03* computational package using MP2 and the diffuse-polarized basis set, 6-311++G (d,p). The thermochemical equation 3.1 was used to calculate the energy change for formation of propanoxy and phenoxy from their mother molecules. Table 4.3 below gives a summary of the thermo-chemical data of propanol and phenol and their respective radicals under the MP2 level theory.

Table 4.3: MP2 Thermochemical Data for Molecular Compounds and their Subsequent radicals

Temp. (K)	Propanol (Hartree/particle)	Propanoxy(Hartree/ particle)	Phenol (Hartree/particle)	Phenoxy(Hartree/pa rticle)
373	-193.33	-192.69	-305.99	-305.34
423	-193.32	-192.69	-305.99	-305.34
473	-193.32	-192.68	-305.99	-305.33
523	-193.32	-192.68	-305.98	-305.33
573	-193.32	-192.68	-305.98	-305.33
623	-193.31	-192.68	-305.98	-305.32
673	-193.31	-192.67	-305.97	-305.32
723	-193.31	-192.67	-305.97	-305.32
773	-193.31	-192.67	-305.97	-305.31
823	-193.30	-192.67	-305.96	-305.31
873	-193.30	-192.66	-305.96	-305.31
923	-193.29	-192.66	-305.95	-305.30
973	-193.29	-192.66	-305.95	-305.30
1023	-193.29	-192.65	-305.95	-305.29
1073	-193.28	-192.65	-305.94	-305.29
1123	-193.28	-192.64	-305.94	-305.28
1173	-193.28	-192.64	-305.93	-305.28
1223	-193.27	-192.64	-305.93	-305.28

From Table 4.3 above, it is evident that as the temperature increases, there is an increase in endothermicity. The same trend was observed when the DFT level theory was employed. Also noticeable from this data is that the density functional level theory gave thermal enthalpy values that were slightly more exothermic than those of

MP2 level of theory for both propanol and phenol. For instance under the MP2 level theory, at the temperatures of 473, 673 and 973, the thermal enthalpies for propanol are -193.32, -193.31 and -193.29 hartree/particle respectively while in the density functional theory (DFT), the thermal enthalpies for the same compound at these temperatures were -194.30, -194.29 and -194.27 hartree/particle respectively. These results are very crucial in predicting the theory that is likely to give the best results. The enthalpy change in the formation of propanoxy and phenoxy radicals from their constituent molecules gave the same trends in both MP2 and density functional level theories as illustrated in Figure 4.8 and Figure 4.9 below.

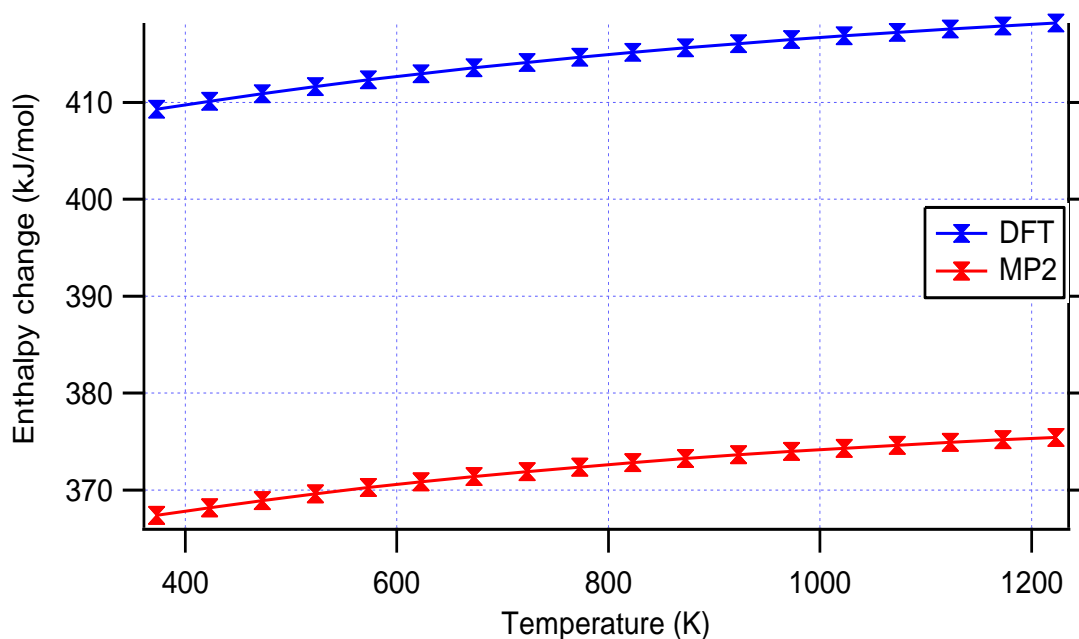


Figure 4.8: Enthalpy Change for the Formation of Propanoxy under DFT and MP2 Theories.

From figure 4.8 above, it is evident that in the formation of propanoxy radical from propanol, the density functional level theory predicts that more energy is absorbed from the surrounding than in MP2 level theory. On the other hand, the MP2 level theory predicts that more amount of energy is absorbed from the surrounding in the formation of phenoxy radical from phenol as shown in Figure 4.9 below. These

differences are brought about by the fact that results from DFT with the B3LYP hybrid function always provide a superior description of the geometries and vibrational frequencies unlike the Møller Plesset perturbation theory (MP2) (Beni & Monfared, 2013).

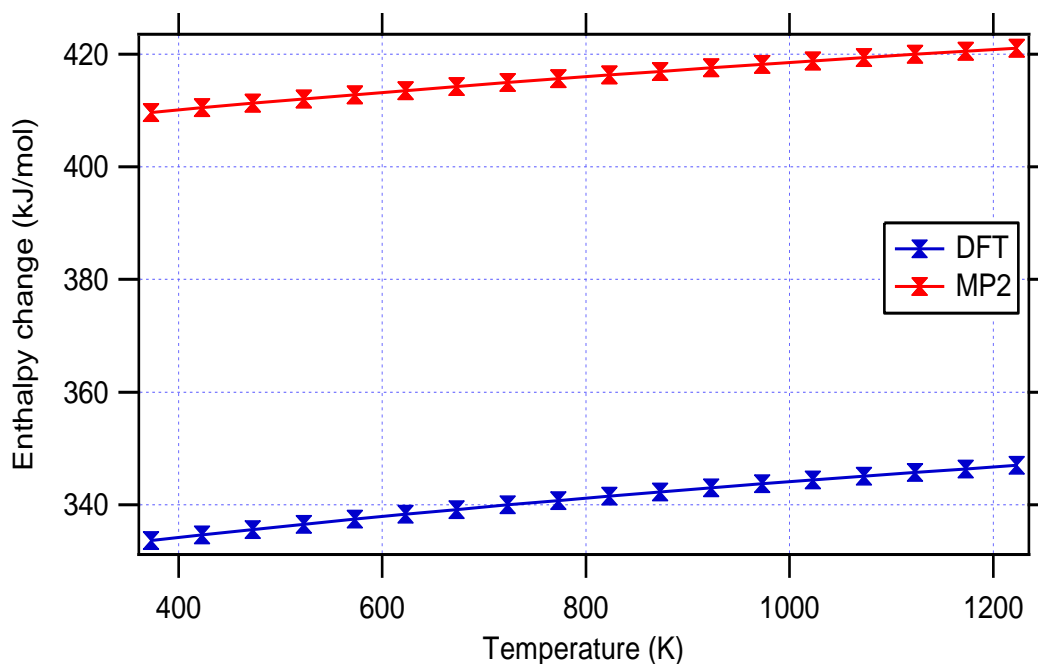


Figure 4.9: Enthalpy Change for the Formation of Phenoxy under DFT and MP2 Theories.

Owing to the fact that the phenoxy radical exhibits resonance structures unlike propanoxy, the density functional theory (DFT) takes into account the various geometries of these phenoxy structures thereby predicting lower enthalpy changes. According to Beni and Monfared (2013), density functional theory (DFT) is known to accurately predict the CO vibrational frequency shifts, thereby yielding better results than MP2 level theory. The Gibbs energies were calculated for both DFT and MP2 theories and the results showed the same trends in both. The general trend was that the change in Gibbs energy gave an inversely proportional relationship with respect to temperature variation. The temperature variations and associated Gibbs energy

changes for formation of propanoxy are illustrated in Figure 4.10 below. A very interesting observation from these results is that the DFT level predicted slightly higher values for Gibbs energy for formation of propanoxy radical compared to the MP2 values. However, in the formation of phenoxy radical, the MP2 level theory predicted slightly higher values of change in Gibbs free energy compared to the DFT level theory as illustrated in Figure 4.11 below.

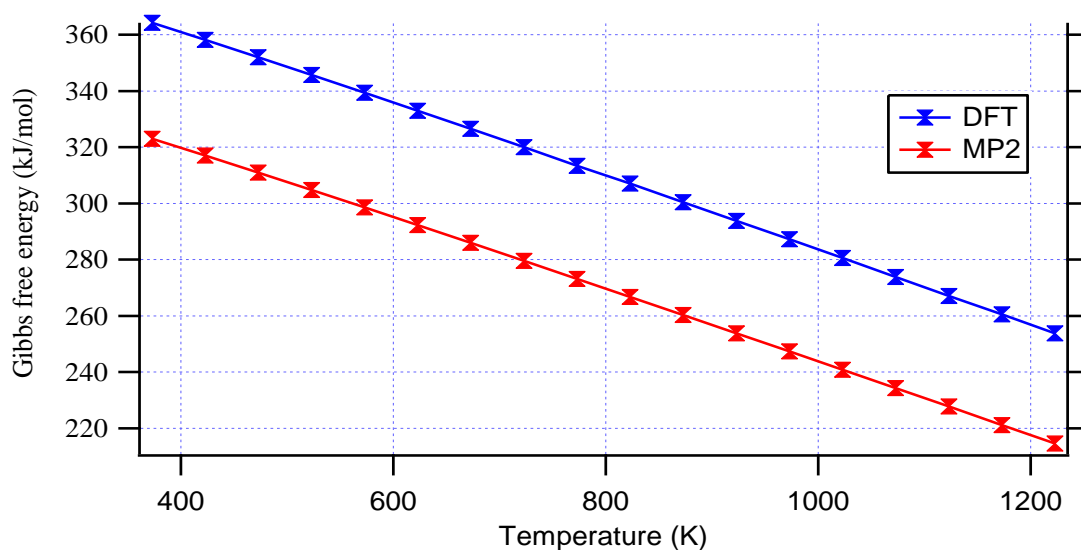


Figure 4.10: Change in Gibbs Free Energy for Formation of Propanoxy DFT and MP2

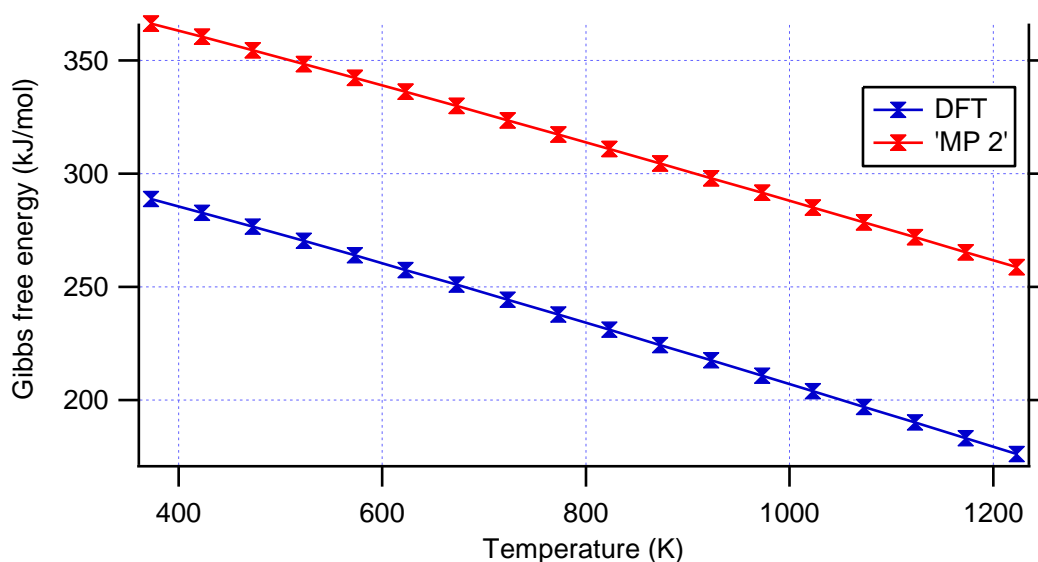


Figure 4.11: Change in Gibbs Energy for the Formation of Phenoxy in DFT and MP2 theories.

4.1.4 Calculation of IR Data

This section covers the IR spectrum of the organic molecules under study generated by the Gaussian 03 computational package. The organic molecules absorb at specific frequencies which are defined by their structures. These absorptions describe the resonance frequencies which can well be interpreted as the frequency which equates to the transition energy of the vibrating bonds. The mass of the atoms, the potential energy surfaces and the associated interactions between electronic vibrations and nuclear vibrations contribute a lot to the transitional energy of the molecules. The IR spectrum for propanol was as shown in Figure 4.12 below.

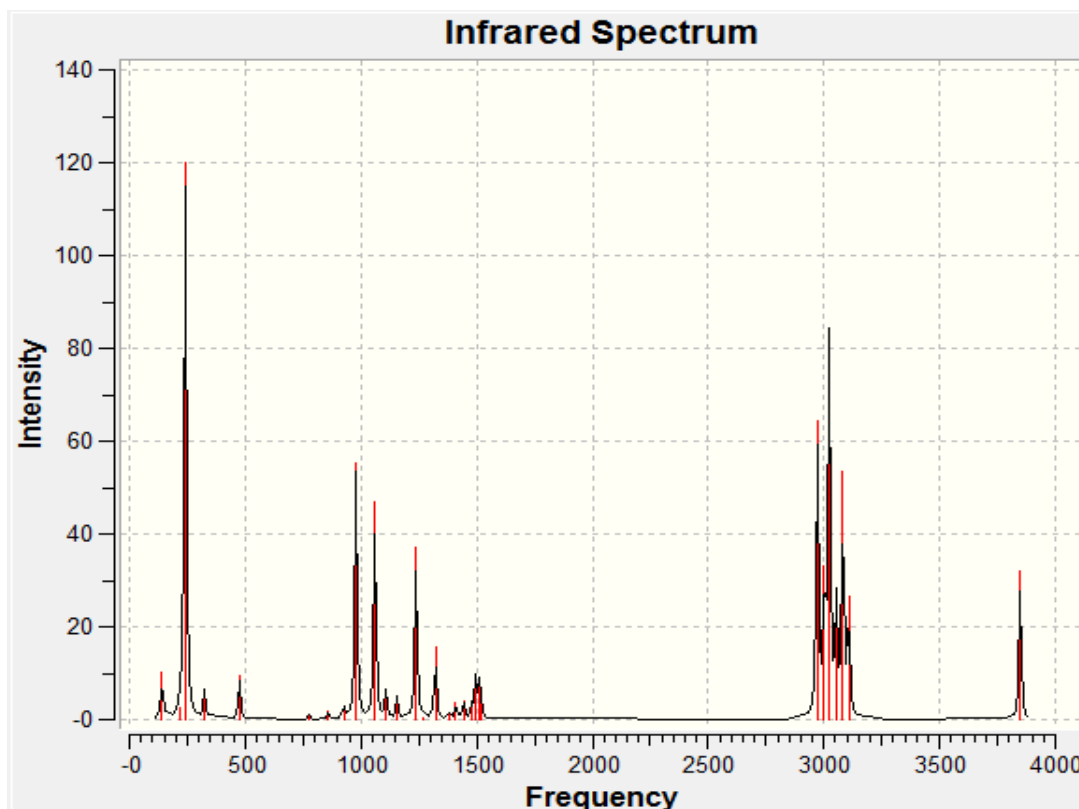


Figure 4.12:IR Spectrum for Propanol

This spectrum is as a result of the different vibrational modes in the molecule. Table 4.4 below gives a summary of the vibrational modes in the propanol molecule.

Table 4.4: Vibrational Modes Displayed By Propanol

Wave Number (cm ⁻¹)	Bond type	Vibrational mode	Wave number (cm ⁻¹)	Bond type	Vibrational mode
141.36	C-C	Twisting	1380.18	C1-H6, C1-H5, C2-H4	Wagging
220.29	H-C	Rocking	1409.98	C9-H11, C9-H12, C9-H10	Wagging
241.36	H-O	Rocking	1443.62	H4-C2, H3-C2, H10-C9, H11-C9, H12-C9	Wagging
				C2-O7, H8-O7	Scissoring
	C-O	Twisting	1478.07	C1-H5, C1-H6	Scissoring
323.99	H-C	rocking	1494.91	C9-H10, C9-H12	Twisting
				C9-H12, C9-H11	Scissoring
	H-O	rocking	1509.24	C9-H10, C9-H12	Scissoring
				C9-H11, C9-H12	Twisting
	C1-C9	twisting	1517.74	C2-H3, C2-H4	Scissoring
475.21	C1-C2, C2-O7	Scissoring	2971.98	C2-H3, C2-H4	symmetrical stretching
				C2-H3, C2-H4	Antisymmetrical stretching
773.57	C1-H5, C1-H6	rocking	3001.74	C1-H6, C1-H5	Symmetrical stretching
			3022.98	C9-H10, C9-H11, C9-H12	Symmetrical stretching
926.30	C2-H3, C2-H4	rocking	3024.24	C1-H5, C1-H6, C9-H12, C9-H10	Symmetrical stretching
978.69	C9-H10, C9-H11	twisting	3053.75	C1-H5, C1-H6	Antisymmetrical stretching
				C9-H10, C9-H11	Symmetrical stretching
1060.71	O7-H8, O7-C2	rocking	3082.41	C9-H11, C9-H12	Antisymmetrical stretching
1108.97	C2-H3, C2-H4	wagging	3107.17	C9-H10, C9-H11, C9-H12	Antisymmetrical stretching
				C9-H11, C9-H12	Symmetrical stretching
1156.19	C2-H4, C2-H3	rocking			
1238.41	O7-H8	scissoring			
1270.82	C2-H3, C2-H4	twisting	3848.39	O7-H8	Stretching
1322.06	C1-H5, C1-H6	twisting			

4.1.5 Effects of a given Basis Set on Internal Energy

The effects of basis sets on the internal energy for propanol, propanoxy, phenol and phenoxy have been explored in this work. The 3-21G, 3-21G+, 6-31G, 6-31G+(d,p) and STO-G basis sets at a temperature of 278K, were manipulated in the Gaussian 03 computational package in order to compare their effects on the organic toxins under investigation. The basis sets gave different amounts of internal energies for each single molecular product. A graph of internal energy as a function of the basis sets was generated as shown in Figure 4.13 below.

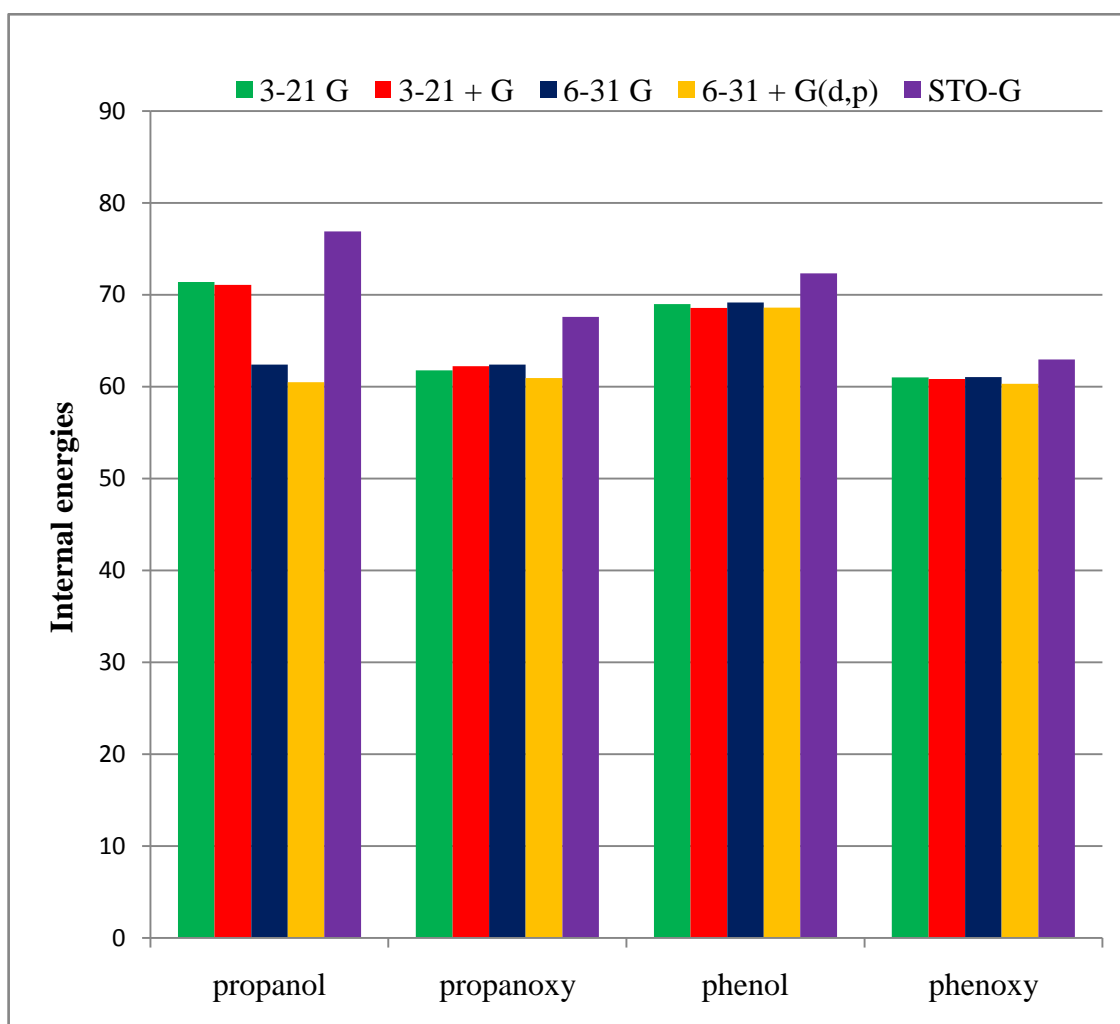


Figure 4.13: Variation in Internal Energy with Different Basis Sets

It is evident from Figure 4.13 above that the largest orbital (STO-G) had a higher internal energy than all the other basis sets investigated. For instance, in propanol, the internal energy was $76.901 \text{ kcalmol}^{-1}$ under the STO-G basis set while 6-31 + G (d,p) basis set recorded the minimum amount of internal energy of $60.491 \text{ kcalmol}^{-1}$. This suggests that the STO-G basis set is more likely to give exaggerated results unlike the 6-31 G+ (d,p) basis set. Also the internal energies of propanol and phenol were greater than the internal energies of their radicals for all the basis set used. These findings suggests that the polarized diffuse basis set 6-31G+(d,p) is expected to give accurate results for the organic compounds investigated given that it takes into consideration the existence of hydrogen bonding. For that matter, the polarized diffuse basis set 6-311 G + (d,p) in connection with the B3LYP function is found to be the best combination for these theoretical calculations (Glossman-Mitnik & Márquez-Lucero, 2001).

4.1.6 Toxicity Indices

The QSAR method incorporated in the HyperChem computational software program was used to explore the relative toxicities of the compounds under study (HyperChem®, 2002). The relative toxicity of a compound is determined using the logarithm of octanol-water partition coefficient (K_{ow}) parameters (Smith & Hansch, 2000). Log P predicts the lipophilicity and hydrophobicity of a pollutant. Lipophilicity correlates with many biological activities such as mutagenicity and carcinogenicity (Smith & Hansch, 2000; Young, 2001). QSAR modeling establishes an attractive approach to preliminary assessment of the impact on environmental health by a primary pollutant and the set of transformation products that may be persistent and toxic to the environment (Carlsen *et al.*, 2008).

It is clear from Table 4.5 below that although all the radicals of the molecular products reported higher toxicity indices than their respective mother molecules, propanoxy radical is about 204 times more soluble in water than in octanol and therefore highly hydrophilic. This supports the thermo-chemical data that propanoxy radical is indeed very reactive towards biological systems. This is because, biological systems are considered hydrophilic and advertently polar.

Table 4.5: QSAR Toxicity Indices for Organic Toxins and their Corresponding Free Radicals.

Compound/Radical	P	Log P
Propanol	3.55	0.55
Propanoxy radical	204.17	2.31
Phenol	3.72	0.57
Phenoxy radical	97.72	1.99
butyrolactone	1.02	0.01
Butyrolactone radical	1.07	0.03
Guaiacol	32.36	1.51
Guaiacol radical	123.02	2.09

High lipophilicity correlates more strongly with biological activity, which translates to more oxidative stress and extensive cellular injury (Smith & Hansch, 2000). Phenoxy radical on the other hand is about 98 times more soluble in water than in octanol and subsequently also very reactive when in contact with biological systems. Lipophilic compounds can cross biological barriers which contain lipids, for example, cell or microsomal membranes and skin stratum consequently causing cell aberrations and subsequent oxidative stress and cancer (Demarini, 2004; Smith & Hansch, 2000). The molecular products propanol, phenol and butyrolactone are less polar and less soluble in water. Their water-octanol partition coefficients were estimated to be 3.55, 3.72, and 1.02 respectively, (Table 4.5). This suggests that they are more soluble in octanol and therefore highly hydrophobic. Guaiacol had the highest partition coefficient estimated at 32.36 implying that it is highly hydrophilic. Low toxicity

index does not imply that a compound is less toxic but may react with non-polar biological components such as lipids and eventually cause cell alterations leading to cancer and gene mutation.

4.1.7 Molecular Geometries

The potential energy surfaces of the molecular products and their respective radicals have been calculated in detail using DFT with B3LYP/6-311G+ (d,P) level of theory. The geometry optimization determines the potential energy minimum that is nearest to the input structure on the potential energy surface(PES) (Osorio *et al.*, 2013). Geometry optimization therefore tends to find a minimum of functions of many variables. This search follows the potential energy surface such that it is continuously moving towards a lower energy (Osorio *et al.*, 2013).

The calculations converged once a minimum energy point on the PES was reached. Since the fundamental objective was to find the global minimum on the molecular structure, the input structures were well selected (Young, 2001). The minima on the potential energy surface the optimum geometries of a compound the way they naturally occur thereby making it possible for theoretical and experimental investigation of parameters such as chemical kinetics, spectroscopy and thermodynamics. The geometry optimization of the structures under investigation in this work (propanol, phenol, guaiacol and Butyrolactone) was quantum mechanically performed using the Gaussian 03 software under the DFT at B3LYP/ 6-31 ++ level of theory and the obtained results presented in Figure 4.14 below. The bond lengths are reported in Angstrom units (10^{-10} m) and the angles in degrees.

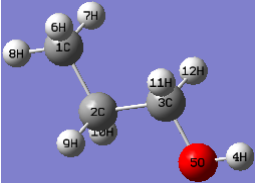
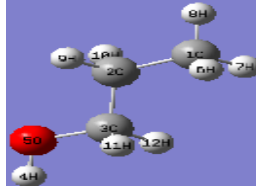
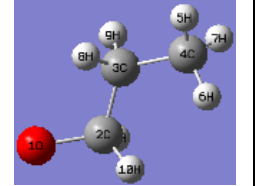
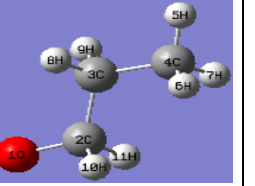
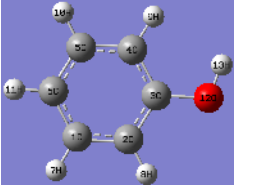
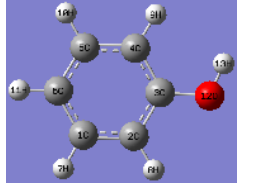

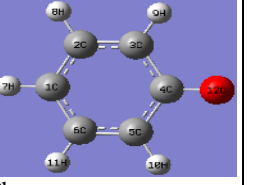
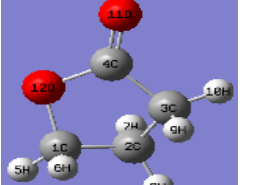

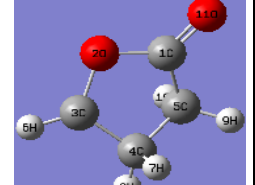

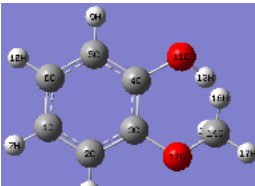
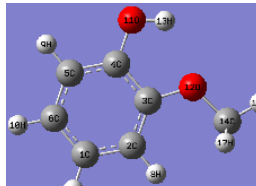
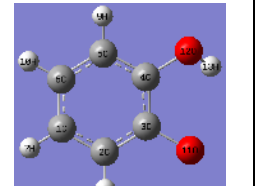
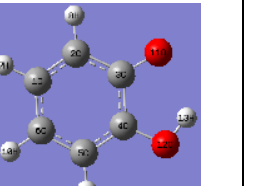
Input structure	Optimized structure	Radical input structure	Radical optimized structures
 <p>Propanol B= 0.96 (H4 O5) B= 1.43 (O5 C3) A= 109.47 (H4 O5 C3) A= 109.47 (H9 C2 C3) A=109.47 (C3 C2 C1)</p>	 <p>Propanol B=0.96 (H4 O5) B=1.43 (O5 C3) A=108.95 (H4 O5 C3) A=108.48 (H9 C2 C3) A=112.55 (C1 C2 C3)</p>	 <p>propanoxy B=1.43 (O1 C2) B=1.54 (C2 C3) A=109.47 (O1 C2 C3) A=120.00 (C2 C3 C4) A=107.19 (H8 C3 C2)</p>	 <p>Propanoxy B= 1.36 (O1 C2) B= 1.53 (C2 C3) A=116.32 (O1 C2 C3) A=112.55 (C2 C3 C4) A=108.39 (H8 C3 C2)</p>
 <p>Phenol B=1.40 (C3 C4) B=1.07 (H8 C2) A=109.47 (H13 O12 C3) A=120.00 (O12 C3 C4) A=120.01 (C1 C2 C3)</p>	 <p>Phenol B=1.40 (C3 C4) B=1.08 (H8 C2) A=109.76 (H13 O12 C3) A=120.19 (C2 C3 C4) A=119.55 (C1 C2 C3)</p>	 <p>Phenoxy B=1.43 (C4 O12) B=1.40 (C4 C5) A=120.00 (C3 C4 O12) A=120.00 (C2 C3 C4) A=120.00 (H9 C3 C4)</p>	 <p>Phenoxy B=1.25 (C4 O12) B=1.45 (C4 C5) A=121.46 (C3 C4 O12) A=120.83 (C2 C3 C4) A=117.06 (H9 C3 C4)</p>
 <p>B=1.26 (O11 C4) B=1.46 (C4 O12) B=1.07 (H8 C2) A=124.95 (O11 C4 C3) A=124.94 (O11 C4 O12) A=110.12 (O12 C4 C3)</p>	 <p>B=1.20 (O11 C4) B=1.36 (C4 O12) B=1.09 (H8 C2) A=128.50 (O11 C4 C3) A=122.41 (O11 C4 O12) A=109.09 (O12 C4 C3)</p>	 <p>B=1.26 (O11 C1) B=1.46 (C1 O2) B=1.07 (H7 C4) A=124.65 (O11 C1 C5) A=124.66 (O11 C1 O2) A=102.00 (C3 O2 C1)</p>	 <p>B=1.19 (O11 C1) B=1.38 (C1 O2) B=1.10 (H7 C4) A=129.70 (O11 C1 C5) A=121.89 (O11 C1 O2) A=110.57 (C3 O2 C1)</p>
 <p>B=1.43 (C4 O11) B=1.07 H17 C14) B=1.40 (C2 C3) A=109.47 (C14 O12 C3) A=120.00 (C4 C3 O12)</p>	 <p>B=1.36 (C4 O11) B=1.10 (H17 C14) B=1.39 (C2 C3) A=118.58 (C14 O12 C3) A=113.83 (C4 C3 O12)</p>	 <p>B=1.43 (C4 O12) B=1.07 (H8 C2) A=109.47 (H13 O12 C4) A=120.00 (C2 C3 C4) A=120.00 (C4 C3 O11)</p>	 <p>B=1.33 (C4 O12) B=1.08 (H8 C2) A=105.31 (H13 O12 C4) A=117.08 (C2 C3 C4) A=117.65 (C4 C3 O11)</p>

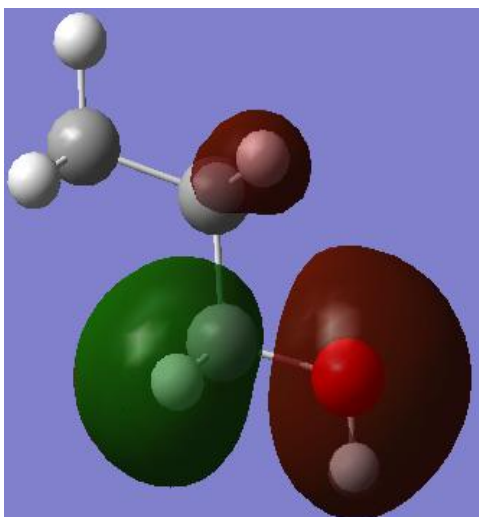
Figure 4.14: Optimized Geometries of Investigated Species

In Figure 4.14 above, both propanol and phenol have oxygen-carbon bond length of 0.96×10^{-10} m in the input and optimized structures. The oxygen-carbon bond slightly decreases after optimization during the formation of propanoxy radical from 1.43×10^{-10} m in propanol to 1.40×10^{-10} m in propanoxy. On the other hand, the hydrogen-carbon bond lengths of propanol converting to propanoxy increases from 1.07×10^{-10} m to 1.11×10^{-10} m. The oxygen-carbon-carbon and the carbon-carbon-carbon bond angles slightly increased while the hydrogen-carbon-carbon and the hydrogen-carbon-hydrogen bond angles slightly decreased in propanoxy radical when compared with the propanol molecule. These changes contribute a lot towards the physical and chemical properties of the molecule and its formed radical. The same trend was noted in the other species under study as presented in Figure 4.14. Geometrical parameters such as bond lengths and bond angles have a great influence on the strength of the bonds involved and consequently the potential energy surface. It follows that the stronger the molecular bond of a compound, the higher the vibrational frequency.

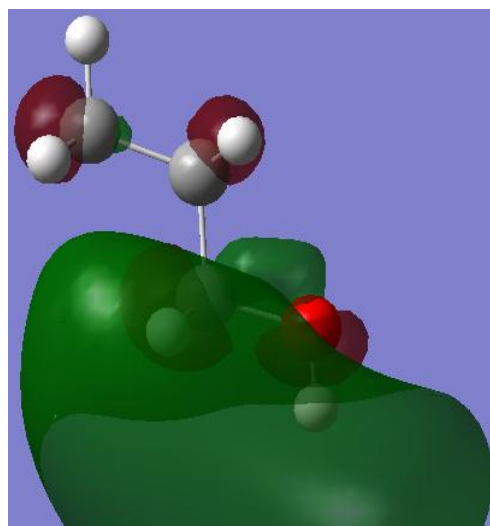
4.1.8 Molecular Orbitals

This section describes the tendency of electrons in the molecules under study to behave like waves, hence calculate the physical and chemical properties like the probability of finding these electrons occupying a given region. In order to construct molecular orbitals, atomic orbitals which calculate the location of an electron, are combined to produce interactions which if at symmetry results in a molecular orbital. These parameters give predictions of reaction mechanisms which a molecule can undergo given that they can show the site of attack during a chemical reaction making them significant in theoretical and experimental chemistry.

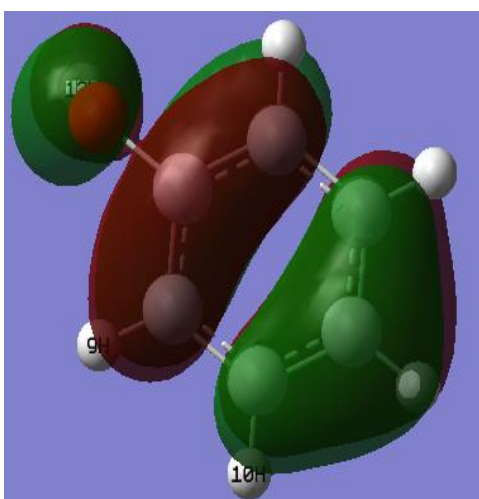
This study shows that in phenol, there is high electron density distribution around the region with double bonds along the benzene ring structure. This predicts the site of attack to be near the region where a proton is likely to leave. In the burning of phenol molecule, hydrogen atom is the most preferred leaving species during combustion leading to the formation of phenoxy radical. A summary of the molecular orbitals for the molecules under study in this work is given in Figure 4.15 below. The dark red lobes are representations of the bonding molecular orbitals while the green lobes represent the antibonding molecular orbitals.



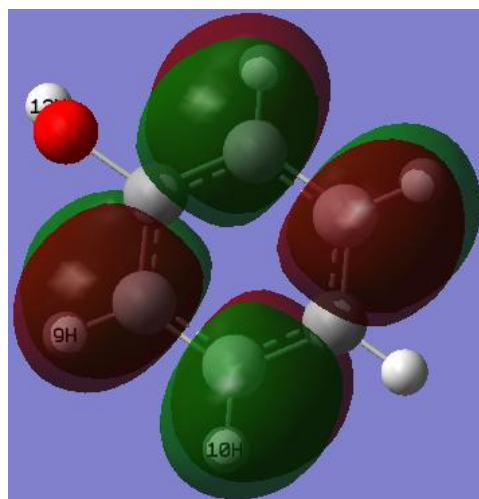
propanol HOMO



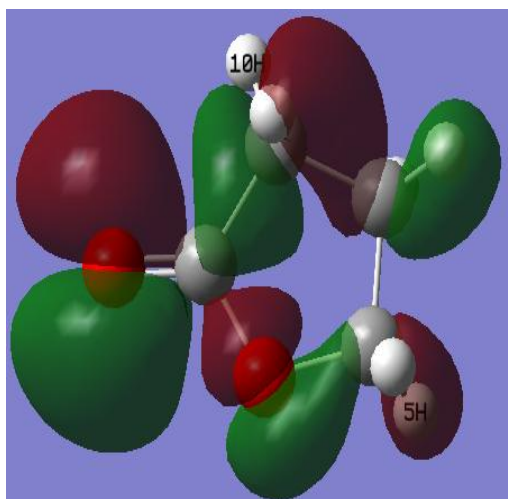
propanol LUMO



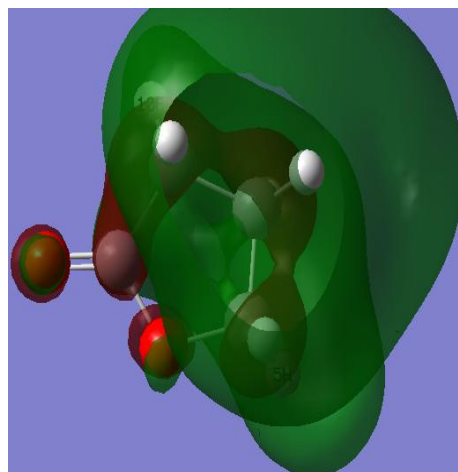
phenolHOMO



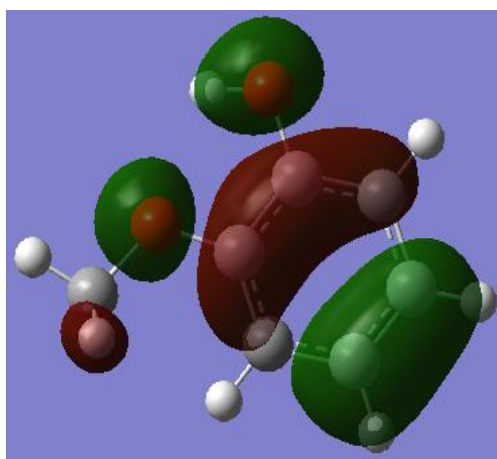
phenol LUMO



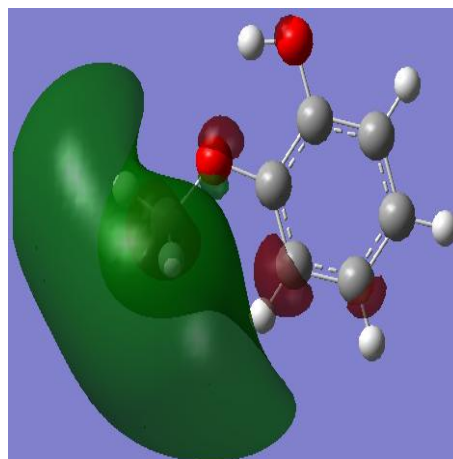
butyrolactone HOMO



butyrolactone LUMO



guaiacol HOMO



guaiacol LUMO

Figure 4.15: Molecular Orbitals for the Compounds under Study

4.2 Heavy Metals Analysis

4.2.1 Heavy Metal Concentrations Partitioned in the Gas-Phase Cigarette Smoke

The gas-phase matter of cigarette smoke is very dangerous because it is directly inhaled by cigarette smokers. As a result, this poses a direct effect on the health of tobacco users. The metals and their mean concentrations in replicate analysis of the samples using AAS technique are shown in Figure 4.16. The results which have been revealed in this study are very startling on the concentration of heavy metals present in the gas-phase of various cigarette brands sold in Kenya. Figure 4.16 shows that Pb constitutes the highest concentration of heavy metal as detected in all cigarettes investigated in this work. SM1, ES1 and Trd cigarettes contained $6.984 \pm 0.03 \mu\text{g.g}^{-1}$, $7.119 \pm 0.05 \mu\text{g.g}^{-1}$ and $6.776 \pm 0.02 \mu\text{g.g}^{-1}$ respectively. Chromium was less pronounced in ES1 cigarette brand thereby making ES1 one of the safest cigarettes with regard to the health effects caused by chromium. However, this advantage may be offset owing to the fact that ES1 was found to contain high lead concentrations. This tendency may well be attributed to processing, packaging and technological processes such as use of additives which may possibly increase the heavy metal contents in tobacco cigarette (Stephens *et al.*, 2005).

Figure 4.16 indicates that chromium and zinc concentration were also substantial in all the cigarette brands. Copper, manganese and cadmium on the other hand showed the minimum concentrations. Apart from the high lead concentrations noted in processed tobacco (ES1 and SM1), unprocessed cigarette indicated high levels of chromium and copper than the processed cigarettes. Interestingly, low levels of cadmium were detected in Trd cigarette ($0.003 \mu\text{g.g}^{-1}$) as compared to SM1 ($0.090 \mu\text{g.g}^{-1}$) and $0.084 \mu\text{g.g}^{-1}$ for ES1 cigarette. The Pb and Cr concentrations are largely

above the recommended levels of heavy metal content in cigarette smoke. On the other hand, the concentrations of Cd, Zn, Mn and Cu fell within the range given by International Energy Atomic Agency (IEAA-359). This trend observed in Figure 4.16 may be attributed to processing, packaging and technological processes such as use of additives which may increase the heavy metal content in tobacco cigarette (Stephens *et al.*, 2005). Growing conditions may also be responsible for the high levels of heavy metals observed in all the cigarette brands examined in this work (Feng *et al.*, 2004).

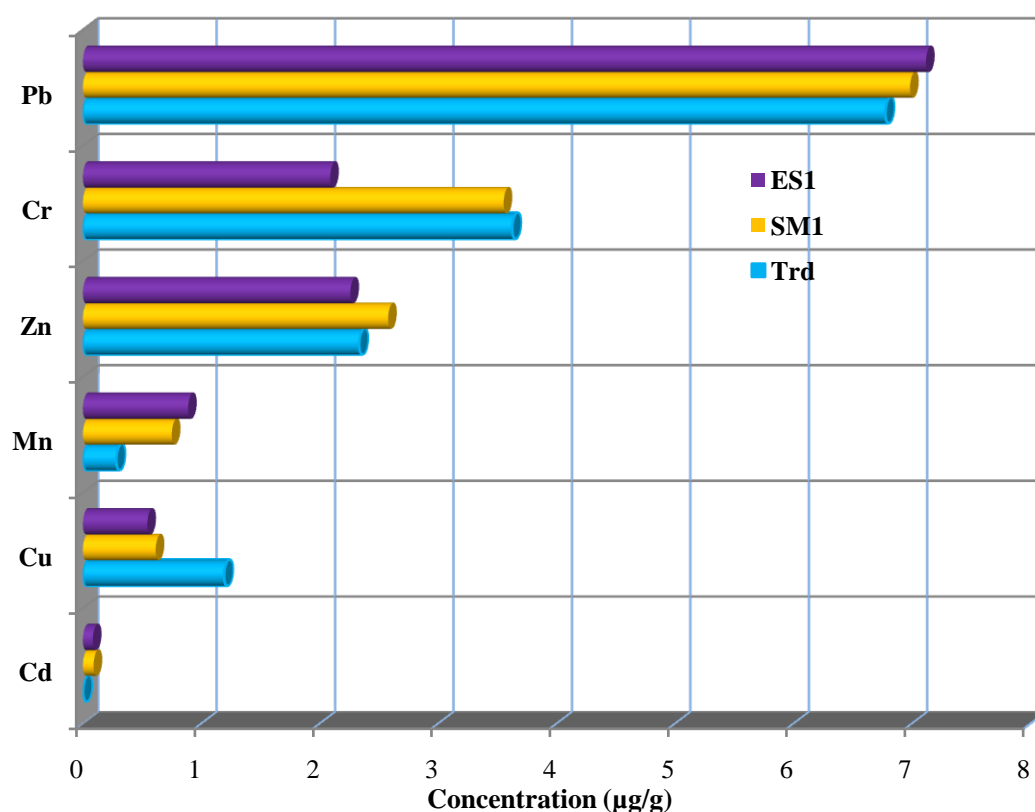


Figure 4.16: Concentration of Heavy Metals Partitioned in the Gas-Phase Cigarette Smoke

4.2.1.1 Mean Comparison for Heavy Metal Concentration in Cigarette Smoke

The mean concentration of heavy metals partitioned incigarette smoke was compared using the SPSS software and reported in Table 4.6 below.

Table 4.6: Mean Concentrations of Metals Partitioned in Cigarette Smoke

Metal (n=18)	Cigarette brand	Mean ($\mu\text{g}\cdot\text{g}^{-1}$)	Std. Dev. ($\mu\text{g}\cdot\text{g}^{-1}$)
Cr	Trd	3.6254 ^a	0.5916
	SM1	3.5527 ^a	0.1252
	ES1	2.0882 ^b	0.7282
Cu	Trd	1.1929 ^a	0.1157
	SM1	0.6148 ^b	0.2383
	ES1	0.5439 ^b	0.3037
Zn	Trd	2.3334 ^a	0.1434
	SM1	2.5772 ^a	0.2562
	ES1	2.2585 ^b	0.0336
Cd	Trd	0.1003 ^a	0.0111
	SM1	0.0901 ^a	0.0009
	ES1	0.0839 ^b	0.0112
Pb	Trd	6.7764 ^a	0.3993
	SM1	6.9842 ^a	0.1866
	ES1	7.1170 ^a	0.1157
Mn	Trd	0.2322 ^a	0.0553
	SM1	0.5904 ^b	0.1758
	ES1	0.7357 ^b	0.1669

Key: For every metal, means with similar superscript letters in column three are not significantly different from Tukey's HSD test.

One way Analysis of Variance (ANOVA) for the cigarette brands and the metal concentration was conducted and found to be significant for Cr, $F(2, 15) = 15.111$, $p < 0.0001$; Cu, $F(2, 15) = 14.046$, $P < 0.0001$; Zn, $F(2, 15) = 5.723$, $p = 0.014$; Cd, $F(2, 15) = 4.596$, $p = 0.028$ and Mn, $F(2, 15) = 19.557$, $p < 0.0001$. Post-hoc analysis was conducted by Tukey's Honestly Significant Difference test and the results are shown in table 4.6 above. Cr was found to be significantly higher in both Trd (mean, $3.6254\mu\text{g}\cdot\text{g}^{-1}$) and SM1 ($3.5527\mu\text{g}\cdot\text{g}^{-1}$) smoke compared to ES1 cigarette ($2.0882\mu\text{g}\cdot\text{g}^{-1}$) smoke. However, Pb concentration was found not to be significantly different in three cigarette brands, $F(2, 15) = 2.555$, $p = 0.111$.

4.2.2 Heavy Metal Concentration Partitioned in Cigarette Solid-Phase

Cigarette ash for the three samples displayed different concentration levels of the heavy metals as reported in Table 4.7 below.

Table 4.7: Levels of Heavy Metal Concentrations Partitioned in Cigarette Ash

Cigarette Brand	Concentration ($\mu\text{g}\cdot\text{g}^{-1}$)					
	Cd	Cu	Zn	Mn	Cr	Pb
Trd	0.093±0.02	2.818±0.02	1.143±0.04	0.390±0.02	3.605±0.02	6.712±0.12
SM1	0.063±0.01	2.668±0.03	0.219±0.03	0.694±0.01	3.293±0.05	6.637±0.07
ES1	0.073±0.01	1.914±0.01	0.329±0.03	0.795±0.01	1.590±0.03	7.066±0.04

The results in Table 4.7 above indicate that the concentration levels of lead and chromium metals constitutes more than 70% of all the metals present in the unprocessed and SM1 cigarettes and more than 80% in ES1 cigarette. However, these results are in contradiction with the observations made in the gas phase of cigarette smoke in that the concentration levels of Zn was detected in low levels in cigarette ash unlike in smoke where the concentrations were in high levels in all the cigarettes. On the other hand, the amount of Cu in the cigarette solid phase was found to be higher than that partitioned in the cigarette gas phase. These findings are important in elucidating the environmental impacts of cigarette ash as ‘fly ash’ even if not consumed by smokers. Cigarette ash contains fine particles in the micron region which can cause respiratory problems, act as irritants in the respiratory tract and may eventually cause asthma and emphysema. This makes cigarette ash as poisonous owing to the fact that it contains critical levels of heavy metals. Heavy metals in the

ash are precursors for mental retardation, nervous breakdown, and cancer related illnesses.

4.3 Rejection or Acceptance of Hypothesis

This study had formulated by two hypotheses; there are no heavy metals in the selected cigarette brands and that unprocessed cigarette is not toxic compared to sportsman and embassy cigarettes. The results from this study indicated the presence of heavy metals at different concentrations both in solid phase and gas phase leading to the rejection of the first hypothesis. Trd cigarette revealed high concentration levels of Cr ($3.6254\mu\text{g.g}^{-1}$), Cu ($1.1929\mu\text{g.g}^{-1}$) and Cd ($0.1003\mu\text{g.g}^{-1}$) with an average concentration level of heavy metal of $2.3768\mu\text{g.g}^{-1}$. ES1 displayed the highest concentration levels of Pb ($7.1170\mu\text{g.g}^{-1}$) and Mn ($0.7357\mu\text{g.g}^{-1}$) with mean heavy metal concentrations of $2.1379\mu\text{g.g}^{-1}$ while SM1 exhibited the highest concentration level of Zn ($2.5772\mu\text{g.g}^{-1}$) and heavy metal mean concentration of $2.4016\mu\text{g.g}^{-1}$. The results revealed that Trd cigarette had the highest number of heavy metals (Cr, Cu and Cd) present at high concentration levels followed by ES1 which exhibited highest concentration levels of Pb and Mn in gas phase. On the other hand, SM1 cigarette smoke had the least number of heavy metals (Zn) but the highest mean of heavy metal concentrations. Considering the toxicological effects caused by individual metals, Trd cigarette can be perceived as more toxic than SM1 and ES1 cigarettes. However, SM1 cigarette can be perceived as the most poisonous given that it had the highest heavy metal concentration mean. These results therefore rule out the idea that unprocessed cigarette is not toxic compared to SM1 and ES1 hence rejection of the hypothesis.

CHAPTER FIVE

5.0 CONCLUSION AND RECOMMENDATION

5.1 Conclusion

This study has successfully come up with findings showing that cigarettes in Kenya contain organic toxins and negligible concentrations of heavy metals whose clinical effects can be very devastating. This forms a basis towards understanding the composition of cigarette smoke.

Amongst the many toxic organic compounds present in tobacco, propanoxy radical was found to be very unstable and therefore capable of reacting with polar biological compounds thereby making it a major cause of oxidative stress, cancer and cardiovascular problems including emphysema and whizzing. Additionally, geometry optimization and the toxicity indices of the organic toxins were investigated using Gaussian 03 and HyperChem computational software respectively and propanoxy radical was found to be about 204 times more soluble in water than in octanol and therefore highly hydrophilic. Owing to the fact that little research has been carried out in investigating organic toxins and their radicals in cigarette smoke, this research has systematically explored the presence of propanol and phenol together with their radicals in mainstream cigarette smoke.

With the help of computational softwares, the thermodynamic parameters of propanol and phenol together with their respective radicals have been explored and the enthalpy data, entropy data and Gibbs energy data of these compounds reported. The findings show that there was an increase in endothermicity with increase in temperature in the formation of both propanoxy and phenoxy radicals from their mother molecules. The change in Gibbs energy on the other hand displayed a decreasing trend with increase

in temperature. The theoretical chemistry performed in investigating the properties of these organic contaminants relied on the fundamental Schrödinger wave equations from where the rigorous mathematical description of the chemical phenomenon was computationally solved. A large extent of approximation has been employed in this work, but the solutions obtained are more accurate than the empirical data. Although these results are not absolute, they are estimates which can be significant in giving interpretations to most experimental results thereby giving a leeway to trends and expected solutions before actual experiments can be performed.

Heavy metals present in the cigarette mainstream smoke were experimentally determined and analysed and the results revealed that lead was the major heavy metal component in the mainstream smoke of all the cigarette brands under investigation while cadmium had the least concentration levels detected. It is critical to note that the results from all cigarette brands analyzed showed high concentration levels of the heavy metals in both gas phase (cigarette smoke) and the solid phase (cigarette ash). Also important to note is the fact that in all the cigarette brands analyzed in this work, there was no substantial difference in the concentrations of all the heavy metals. The results on the heavy metals partitioned in cigarette ash are very startling given that these levels are deemed to be very dangerous to human health and equally dangerous as those metals present in cigarette smoke. The inhalation of these metals can cause severe respiratory problems given that most of these heavy metals are established carcinogens.

5.2 Recommendations

Most tobacco products in Kenya are largely unregulated especially in terms of the toxic content such as heavy metals and organic toxins. This calls for monitoring of the growing conditions of tobacco as well as manufacturing process to ensure minimal input of toxins in tobacco.

It is also evident from the experimental results that there is an increase in the yield of the organic toxins with increase in temperature from the smoking of cigarettes. These toxins are further converted to more lethal polycyclic aromatic hydrocarbons (PAHs) such as benzo(a)pyrene and possibly cyclopentafused PAHs. Therefore, cigarette manufacturers design cigarettes that can be smoked at lower temperatures.

The scope of analysis of the heavy metal content in mainstream cigarette smoke and cigarette ash should be widened to other cigarette brands in the Kenyan market in order to make elaborate findings so as informed decisions can be made with regard to the toxicological effects of cigarette smoking.

For further work, a more comprehensive study should be performed on computational modeling and the use of computational softwares in identification of more toxic organic products from the smoking of cigarettes and their potential effects to smokers.

REFERENCES

- Agency for Toxic Substances and Disease Registry, A. (2008). Chromium toxicity *Case studies in Environmental Medicine (CSEM)*.
- Al-Bader, A., Omu, A. E., & Dashti, H. (1999). Chronic cadmium toxicity to sperm of heavy cigarette smokers: immunomodulation by zinc. *Systems Biology in Reproductive Medicine*, 43(2), 135-140.
- Ashish, B., Neeti, K., & Himanshu, K. (2013). Copper toxicity: A comprehensive study. *Research Journal of Recent Sciences*, 2, 58-67.
- Ashraf, M. W. (2012). Levels of heavy metals in popular cigarette brands and exposure to these metals via smoking. *The Scientific World Journal*, 2012, 5. doi: 10.1100/2012/729430
- Aydin, M., Dede, Ö., & Akins, D. L. (2011). Density functional theory and Raman spectroscopy applied to structure and vibrational mode analysis of 1,1', 3,3'-tetraethyl-5,5', 6,6'-tetrachloro-benzimidazolocarboyanine iodide and its aggregate. *The Journal of chemical physics*, 134(6), 064325.
- Bargholz, A., Oswald, R., & Botschwina, P. (2013). Spectroscopic and thermochemical properties of the c-C₆H₇ radical: a high-level theoretical study. *The Journal of chemical physics*, 138(1), 014307. doi: 10.1063/1.4773015
- Beni, A. S., & Monfared, S. M. (2013). DFT and MP2 calculations on new series of hydroxythioxanones. *Journal of Molecular Structure*, 1039, 8-21. doi: <http://dx.doi.org/10.1016/j.molstruc.2013.01.060>
- Bernhard, D., Rossmann, A., & Wick, G. (2005). Metals in cigarette smoke. *Iubmb Life*, 57(12), 805-809.
- Binkley, J. S., Pople, J. A., & Hehre, W. J. (1980). Self-consistent orbital methods. 21. small split-valence basis sets for first-row elements. *Journal of the America Chemical Society*, 102(3), 939-947.
- Blakley, R. L., Henry, D. D., & Smith, C. J. (2001). Lack of correlation between cigarette mainstream smoke particulate phase radicals and hydroquinone yield. *Food and Chemical Toxicology*, 39(4), 401-406.
- Borgerding, M., & Klus, H. (2005). Analysis of complex mixtures—cigarette smoke. *Experimental and Toxicologic Pathology*, 57, 43-73.
- Burdock, G. A. (2009). *Fenaroli's Handbook of Flavor Ingredients* (CRC Ed. 6 ed.).
- Capelle, K. (2006). A bird's-eye view of density-functional theory. *Brazilian Journal of Physics*, 36(4A), 1318-1343.

- Carlsen, L., Kenessov, B. N., & Batyrbekova, S. Y. (2008). A QSAR/ QSTR study on the environmental health impact by the rocket fuel 1,1-dimethylhydrazine and its transformations products. *Environmental Health Insights*, 1, 11-20. doi: 10.1021/jf0107398
- Carmines, E. L. (2002). Evaluation of the potential effects of ingredients added to cigarettes. Part 1: Cigarette design, testing approach, and review of results. *Food and Chemical Toxicology*, 4(1), 77-91.
- Centers for Disease Control Prevention, C. (2002). Annual smoking-attributable mortality, years of potential life lost, and economic costs--United States, 1995-1999 *MMWR Morb Mortal Wkly Rep* (2002/05/11 ed., Vol. 51, pp. 300-303).
- Chalouhi, N., Ali, M. S., Starke, R. M., Jabbour, P. M., Tjoumakaris, S. I., Gonzalez, L. F., . . . Dumont, A. S. (2012). Cigarette smoke and inflammation: Role in cerebral aneurysm formation and rupture. *Mediators of Inflammation*, 2012, 12. doi: 10.1155/2012/271582
- Chiba, M., & Masironi, R. (1992). Toxic and trace elements in tobacco and tobacco smoke. *Bulletin of the World Health Organization*, 70(2), 269-275.
- Cho, K., Frijters, J. C., Zhang, H., Miller, L. L., & Gruen, J. R. (2013). Prenatal exposure to nicotine and impaired reading performance. *The Journal of pediatrics*, 162(4), 713-718. e712.
- Çifçi, H., & Ölcücu, A. (2007). Determination of Iron, Copper, Cadmium and Zinc in Some Cigarette Brands in Turkey. *International Journal of Science & Technology*, 2(1), 29-32.
- Crossgrove, J., & Zheng, W. (2004). Manganese toxicity upon overexposure. *NMR in biomedicine*, 17(8), 544-553. doi: 10.1002/nbm.931
- Czégény, Z., Blazsó, M., Várhegyi, G., Jakab, E., Liu, C., & Nappi, L. (2009). Formation of selected toxicants from tobacco under different pyrolysis conditions. *Journal of Analytical and Applied Pyrolysis*, 85(1), 47-53.
- De Silva, P., & Wesolowski, T. A. (2012). Pure-state noninteracting v-representability of electron densities from Kohn-Sham calculations with finite basis sets. *Physical Review A*, 85(3), 032518.
- Dellinger, B., Lomnicki, S., Khachatryan, L., Maskos, Z., Hall, R. W., Adoukpe, J., . . . Truong, H. (2007). Formation and stabilization of persistent free radicals. *Proceedings of the Combustion Institute*, 31(1), 521-528. doi: <http://dx.doi.org/10.1016/j.proci.2006.07.172>
- Demarini, D. M. (2004). The genotoxicity of tobacco smoke condensate: a review. *Mutation Research*, 567, 447-474.
- Dempsey, R., Coggins, C. R., & Roemer, E. (2011). Toxicological assessment of cigarette ingredients. *Regulatory Toxicology and Pharmacology*, 61(1), 119-128.

- Dreizler, R. M., & Gross, E. K. (2012). *Density functional theory: an approach to the quantum many-body problem*: Springer Science & Business Media.
- Dumatar, C., & Chauhan, J. (2011). A Study of the Effect of Cigarette Smoking On Cognitive Parameters In Human Volunteers. *NJIRM*, 2(3), 71-76.
- Duncan, J. R., Garland, M., Myers, M. M., Fifer, W. P., Yang, M., Kinney, H. C., & Stark, R. I. (2009). Prenatal nicotine-exposure alters fetal autonomic activity and medullary neurotransmitter receptors: implications for sudden infant death syndrome. *Journal of Applied Physiology*, 107(5), 1579-1590.
- Erzen, I., & Kragelj, L. (2006). Cadmium concentrations in blood in a group of male recruits in Slovenia related to smoking habits. *Bulletin of environmental contamination and toxicology*, 76(2), 278-284.
- Feng, J. W., Zheng, S. K., & Maciel, G. E. (2004). EPR investigations of charring and char/air interaction of cellulose, pectin, and tobacco. . *Energy & Fuels*, 18, 560-568. doi: 10.1021/ef0301497
- Fewtrell, L., Prüss-Üstün, A., Landrigan, P., & Ayuso-Mateos, J. (2004). Estimating the global burden of disease of mild mental retardation and cardiovascular diseases from environmental lead exposure. *Environmental Research*, 94(2), 120-133.
- Foresman, J. B., & Frisch, A. (1996). *Exploring Chemistry with Electronic Structure Methods* (2 ed.): Gaussian Inc.
- Fowles, J., & Dybing, E. (2003). Application of toxicological risk assessment principles to the chemical constituents of cigarette smoke. *Tobacco Control*, 12(4), 424-430.
- Furche, F., & Rappoport, D. (2005). *Density functional methods for excited States: Equilibrium structure and electronic spectra* (Olivucci Ed. Vol. 16).
- Fuster, V., Kelly, B., B., & Vedanthan, R. (2011). Promoting Global Cardiovascular Health Moving Forward. *Circulation*, 123(15), 1671-1678.
- Gairola, C. G., & Wagner, G. J. (1991). Cadmium accumulation in the lung, liver and kidney of mice and rats chronically exposed to cigarette smoke. *Journal of Applied Toxicology*, 11(5), 355-358.
- Galażyn-Sidorczuk, M., Brzóska, M. M., & Moniuszko-Jakoniuk, J. (2008). Estimation of Polish cigarettes contamination with cadmium and lead, and exposure to these metals via smoking. *Environmental monitoring and assessment*, 137(1-3), 481-493.
- Gianturco, F. A., & Huo, W. M. (2013). *Computational Methods for Electron—Molecule Collisions*: Springer Science & Business Media.

- Glossman-Mitnik, D., & Márquez-Lucero, A. (2001). Influence of the basis set and correlation method on the calculation of molecular structures: thiadiazoles revisited. *Journal of Molecular Structure: THEOCHEM*, 548(1–3), 153-163. doi: [http://dx.doi.org/10.1016/S0166-1280\(01\)00509-7](http://dx.doi.org/10.1016/S0166-1280(01)00509-7)
- Hammond, P. B., & Dietrich, K. N. (1990). Lead exposure in early life and consequences. In G. W. Ware (Ed.), *Reviews of Environmental Contamination and Toxicology* (Vol. 115, pp. 91-124). New York: Springer-Verlag.
- Harrison. (2003) An introduction to density functional theory. *Computer And Systems Sciences. NATO Science Series* (pp. 45-70.).
- Harrison, R., & Laxen, D. (1981). *Lead pollution. Causes and control*. New York, London.
- Hecht, S. S. (2012). Lung carcinogenesis by tobacco smoke. *International Journal of Cancer*, 131(12), 2724-2732.
- Hehre, W. J. (2003). *A Guide to Molecular Mechanics and Quantum Chemical Calculations*. California: Irvine.
- Hoffmann, D., Hoffmann, I., & El-Bayoumy, K. (2001). The less harmful cigarette: a controversial issue. *Journal of Chemical Research Toxicology*, 14(7), 767-790.
- HyperChem®. (2002). HyperChem Release 7. HyperChem
- Inoue, N., & Makita, Y. (Eds.). (1996). *Neurological aspects in human exposures to manganese*. : Boca Raton.
- International Agency for Research on Cancer, I. (2004). Chromium (VI) Compounds *IARC monographs on the evaluation of carcinogenic risks to humans* (Vol. 90, pp. 147-167).
- International Agency for Research on Cancer, I. (2012). Inorganic and organic lead compounds *IARC monographs on the evaluation of carcinogenic risks to humans* (Vol. 100, pp. 121-145).
- ISO. (1999:3402). Tobacco and Tobacco products *Atmosphere for Conditioning and Testing*: International Organization for Standardization.
- Jung, M. C., Thornton, I., & Chon, H. T. (1998). Arsenic, cadmium, copper, lead, and zinc Concentrations in cigarettes produced in Korea and the United Kingdom. *Environmental Technology*, 19(2), 237-241. doi: 10.1080/09593331908616676
- Karelson, M., Maran, U., Wang, Y., & Katritzky, A. R. (1999). QSPR and QSAR models derived with CODESSA multipurpose statistical analysis software *AAAI Technical Report* (pp. 12).
- Kibet, J. K., Khachatryan, L., & Dellinger, B. (2013). Molecular products from the pyrolysis and oxidative pyrolysis of tyrosine. *Chemosphere*, 91(7), 1026-1034.

- Kibet, J. K., Mathenge, A. B., Limo, S. C., & Omare, M. O. (2014). Theoretical modeling and experimental investigation of propanol and phenol in mainstream cigarette smoking. *The African Review of Physics*, 9(32), 251-258.
- Kjellström, T. (1979). Exposure and accumulation of cadmium in populations from Japan, the United States, and Sweden. *Environmental health perspectives*, 28, 169-197.
- Kong, J., White, C. A., Krylov, A. I., Sherrill, D., Adamson, R. D., Furlani, T. R., . . . Adams, T. R. (2000). Q-Chem 2.0: a high-performance ab initio electronic structure program package. *Journal of Computational Chemistry*, 21(16), 1532-1548.
- Kulshreshtha, N. P., & Moldoveanu, S. C. (2003). A nalysis of pyridines in mainstream cigarette smoke. *Journal of Chromatography A*, 985, 303-312.
- Langhoff, S. R., & Kern, C. W. (1977). *Molecular fine structure In Applications of Electronic Structure Theory* (Vol. 4): Springer Science & Business Media.
- Leach, A. R. (2001). *Molecular Modelling, Principles, Applications and Education*: Pearson education.
- Lee, J.-W. (2000). Manganese intoxication. *Archives of neurology*, 57(4), 597-599.
- Leffingwell, J. (1999). *Chemical constituents of tobacco leaves and differences among tobacco types*. Blackwell.
- Leffingwell, J., & Alford, E. (2005). Volatile constituents of perique tobacco. *Electronic Journal of Environmental, Agricultural and Food Chemistry*, 4(2), 899-915.
- Lessigiarska, I., Worth, A. P., & Netzeva, T. I. (2005). Comparative review of QSARs for acute toxicity *Scientific and Technical Research Report*. European Communities.
- Lisko, J. G., Stanfill, S. B., Duncan, B. W., & Watson, C. H. (2013). Application of GC-MS/MS for the analysis of tobacco alkaloids in cigarette filler and various tobacco species. *Analytical Chemistry*, 85(6), 3380-3384. doi: 10.1021/ac400077e
- Lobo, V., Patil, A., Phatak, A., & Chandra, N. (2010). Free radicals, antioxidants and functional foods: Impact on human health. *Pharmacognosy reviews*, 4(8), 118.
- Lou, R., Wu, S., Gao-jin, L., & Guo, D. (2010). Pyrolytic products from rice straw and enzymatic/ mild acidolysis lignin (EMAL). *BioResources*, 5(4), 2184-2194.
- Majima, H. J., & Toyokuni, S. (2012). Mitochondria and free radical studies on health, disease and pollution. *Free radical research*, 46(8), 925-926.

- Massadeh, A., Alali, F., & Jaradat, Q. (2003). Determination of copper and zinc in different brands of cigarettes in Jordan. *Acta Chimica Slovenica*, 50(2), 375-381.
- Miller, R. (2013). *Chemicals in cigarette smoke That Cause Cancer*. Disease and Conditions.
- Nadendla, R. R. (2004). Molecular modeling: A powerful tool for drug design and molecular docking. *Resonance*, 9(5), 51-60.
- Nevin, R. (2000). How lead exposure relates to temporal changes in IQ, violent crime, and unwed pregnancy. *Environmental Research*, 83(1), 1-22.
- Nnorom, I., Osibanjo, O., & Oji-Nnorom, C. (2005). Cadmium determination in cigarettes available in Nigeria. *African Journal of Biotechnology*, 4(10), 1128-1132.
- Nriagu, J. (2007). *Zinc Toxicity in Humans*. School of Public health: university of Michigan.
- Ochterski, J. W. (2000). Thermochemistry in gaussian. *Gaussian Inc, Pittsburgh, PA*, 1-17.
- Osorio, E., Vasquez, A., Florez, E., Mondragon, F., Donald, K. J., & Tiznado, W. (2013). Theoretical design of stable aluminium-magnesium binary clusters. *Physical Chemistry and Chemical Physics*, 15(6), 2222-2229. doi: 10.1039/c2cp42015e
- Pappas, R. S., Polzin, G. M., Watson, C. H., & Ashley, D. L. (2007). Cadmium, lead, and thallium in smoke particulate from counterfeit cigarettes compared to authentic US brands. *Food and Chemical Toxicology*, 45(2), 202-209.
- Pesch, H. J., Bloß, S., Schubert, J., & Seibold, H. (1992). The mercury, cadmium and lead content of cigarette tobacco: Comparative analytical-statistical studies in 1987 and 1991 employing Zeeman-AAS. *Fresenius' Journal of Analytical Chemistry*, 343(1), 152-153. doi: 10.1007/BF00332087
- Petersson, G. A., Bennett, A., Tensfeldt, T. G., Al-Laham, M. A., Shirley, W. J., & Mantzaris, J. (1988). A complete basis set model chemistry. I. the total energies of a closed-shell atoms and hydrides of the first row elements. *Journal of Chemical Physics*, 89, 2193-2218.
- Petruzielo, F. R., Toulouse, J., & Umrigar, C. (2011). Basis set construction for molecular electronic structure theory: Natural orbital and Gauss–Slater basis for smooth pseudopotentials. *The Journal of chemical physics*, 134(6), 064104.
- Plum, L. M., Rink, L., & Haase, H. (2010). The essential Toxin: impact of zinc on human health. *International journal of environmental research and public health*, 7(4), 1342-1365. doi: 10.3390/ijerph7041342

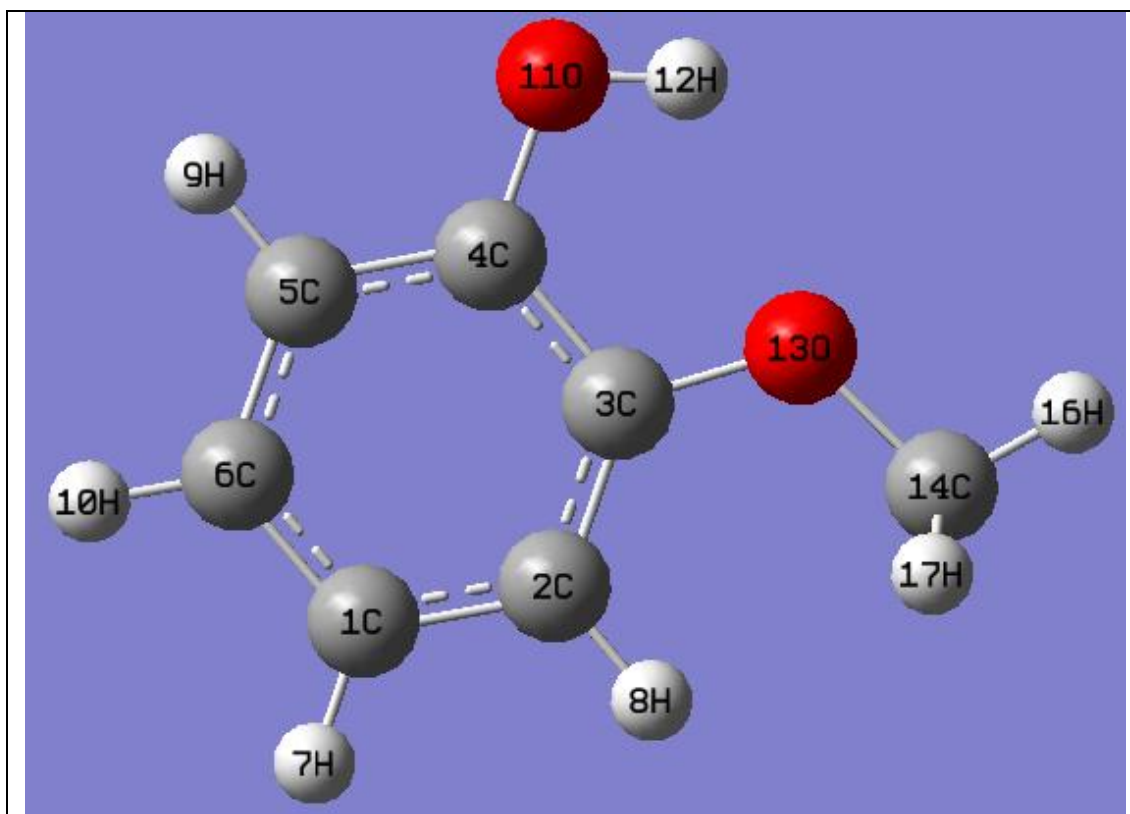
- Pourhabbaz, A., & Pourhabbaz, H. (2012). Investigation of toxic metals in the tobacco of different Iranian cigarette brands and related Health issues. *Iranian Journal of Basic Medical Sciences*, 15(1), 636-644.
- Prüss-Üstün, A., Fewtrell, L., Landrigan, P., & Ayuso-Mateos, J. (2004). *Lead exposure in Comparative Quantification of Health Risks*. Geneva: World Health Organization.
- Ramachandran, K., Deepa, G., & Namboori, K. (2008). *Computational chemistry and Molecular modelling*. Springer-Verlag: Springer Berlin Heidelberg.
- Rauhamaa, M., Salmela, S. S., Leppänen, A., & Pyysalo, H. (1986). Cigarettes as a source of some trace and heavy metals and pesticides in man. *Archives of Environmental Health: An International Journal*, 41(1), 49-55.
- Ryan, J., & Clark, M. (2010). Trace metal determination in tobacco and cigarette ash by inductively coupled plasma-atomic emission spectroscopy. *concordia College Journal of Analytical Chemistry*, 1, 34-41.
- Schlegel, H. B. (2011). Geometry optimization. *Wiley Interdisciplinary Reviews: Computational Molecular Science*, 1(5), 790-809.
- Schlotzhauer, W. S., Martin, R. M., Snook, M. E., & Williamson, R. E. (1982). Pyrolytic studies on the contribution of tobacco leaf constituents to the formation of smoke catechols. *Journal of Agricultural and Food Chemistry*, 30(2), 372-374.
- Senneca, O., Ciaravolo, S., & Nunziata, A. (2007). Composition of the gaseous products of pyrolysis of tobacco under inert and oxidative conditions. *Journal of Analytical and Applied Pyrolysis*, 79(1), 234-243.
- Shaper, A., Pocock, S., Walker, M., Wale, C., Clayton, B., Delves, H., & Hinks, L. (1982). Effects of alcohol and smoking on blood lead in middle-aged British men. *British Medical Journal*, 299-302(6312), 299.
- Sivilotti, M. L. A., Burns, M. J., Aaron, C. K., & Greenberg, M. J. (2001). Pentobarbital for severe gamma-butyrolactone withdrawal. *Annals of Emergency Medicine*, 38(6), 660-665. doi: <http://dx.doi.org/10.1067/mem.2001.119454>
- Smith, Perfetti, T. A., Morton, M. J., Rodgman, A., Garg, R., Selassie, C. D., & Hansch, C. (2002). The relative toxicity of substituted phenols reported in cigarette mainstream smoke. *Toxicological Sciences*, 69(1), 265-278.
- Smith, C. J., & Hansch, C. (2000). The relative toxicity of compounds in mainstream cigarette smoke condensate. *Journal of Food and Toxicology*, 38(7), 637-646 doi: 10.1016/s0278-6915(00)00051-x
- Stephens, W. E., Calder, A., & Newton, J. (2005). Source and health implications of high toxic metal concentrations in illicit tobacco products. *Environmental science & technology*, 39(2), 479-488.

- Stewart, J. J. (1989). Optimization of parameters for semiempirical methods I. Method. *Journal of Computational Chemistry*, 10(2), 209-220.
- Talhout, R., Schulz, T., Florek, E., Van Benthem, J., Wester, P., & Opperhuizen, A. (2011). Hazardous compounds in tobacco smoke. *International journal of environmental research and public health*, 8(2), 613-628.
- Tangahu, B. V., Abdullah, S. R., Basri, H., Idris, M., Anuar, N., & Mukhlisin, M. (2011). A review on heavy metals (As, Pb, and Hg) uptake by plants through phytoremediation. *International Journal of Chemical Engineering*, 2011. doi: 10.1155/2011/939161
- Taylor, P. R. (2011). *Accurate Calculations and Calibration*. Victorian Life Sciences Computation Initiative.
- Truhlar, D. G., Cramer, C. J., Lewis, A., & Bumpus, J. A. (2004). Molecular modeling of environmentally important processes: Reduction potentials. *Journal of chemical education*, 81(4), 596-604.
- Wang, S. F., Liu, B. Z., Sun, K. J., & Su, Q. D. (2004). Gas chromatographic–mass spectrometric determination of polycyclic aromatic hydrocarbons formed during the pyrolysis of phenylalanine. *Journal of Chromatography A*, 1025(2), 255-261.
- Weigend, F., Furche, F., & Ahlrichs, R. (2003). Gaussian basis sets of quadruple zeta valence quality for atoms H–Kr. *The Journal of chemical physics*, 119(24), 12753-12762.
- WHO. (2006). Tobacco: deadly in any form or disguise.
- Young, D. C. (2001). *Computational Chemistry: A Practical Guide for Applying Techniques to Real-World Problems*: John Wiley & Sons Inc.
- Zhang, C., Miura, J. i., & Nagaosa, Y. (2005). Determination of cadmium, zinc, nickel and cobalt in tobacco by reversed-phase high-performance liquid chromatography with 2-(8-quinolylazo)-4,5-diphenylimidazole as a chelating reagent. *Analytical sciences*, 21(9), 1105-1110.
- Zhou, S., Wang, C., Xu, Y., & Hu, Y. (2011). The pyrolysis of cigarette paper under the conditions that simulate cigarette smouldering and puffing. *J. Thermal Analysis and Calorimetry*, 104(3), 1097-1106. doi: 10.1007/s10973-011-1354-7

APPENDICES

APPENDIX A1. Table of Geometrical Parameters

Compound/ Radical	Bond angle ($^{\circ}$)	Bond length (\AA)
Propanol	O5 C3 C2=108.30	H4 O5= 0.96
	H4 O5 C3 = 108.95	O5 C3= 1.43
	H9 C2 C3 = 108.48	C3 H12=1.11
	H12 C3 H11 =107.76	C2 C3 =1.52
	C1 C2 C3 =112.55	
Propanoxy	O1 C2 C3=116.32	C2 C3= 1.53
	C2 C3 C4=112.55	H10 C2= 1.11
	H8 C3 C2=108.39	O1 C2= 1.36
	H5 C4 H6=107.51	
Phenol	H13 O12 C3=109.759	H13 O12=0.96279
	O12 C3 C4=122.544	C3 O12=1.3699
	C2 C3 C4=120.178	C3 C4=1.39619
	C1 C2 C3=119.547	H8 C2=1.08328
Phenoxy	C3 C4 O12=121.457	C4 O12=1.25267
	C2 C3 C4=120.834	C4 C5 =1.45227
	H9 C3 C4=117.061	H9 C3=1.08395
	H9 C3 C2=122.105	
Butyrolactone	O11 C4 C3=128.495	O11 C4=1.19717
	O11 C4 O12=122.412	C4 O12=1.36401
	O12 C4 C3=109.092	H8 C2=1.09064
	C1 O12 C4=110.948	C1 O12=1.44523
	C2 C3 C4=103.680	
	O12 C1 C2=105.522	
Butyrolactone radical	O11 C1 C5=129.701	O11 C1=1.193
	O11 C1 O2=121.886	C1 O2=1.3834
	O2 C1 C5=108.405	C3 O2=1.381
	C4 C5 C1=104.431	H7 C4=1.100
	C3 O2 C1=110.565	
Guaiacol	H13 O12 C4=109.471	C4 O12=1.43
	C2 C3 C4=120.0	C3 O11=1.43
	C4 C3 O11=120.0	C2 C3=1.401
	H9 C5 C6=120.0	H8 C2=1.07
Guaiacol radical	H13 O12 C4=105.306	C4 O12=1.33
	C2 C3 C4=117.075	H8 C2=1.08
	C4 C3 O11= 117.654	

Appendix A2: Optimized Structure for Guaiacol and Geometrical Parameters


B= 0.96667 (H12-O11)

A= 109.456 (H17 C14 H16)

B= 1.09483 (C14-H17)

A= 118.578 (C14 O13 C3)

B= 1.42222 (O13-C14)

A= 113.829 (O13 C3 C4)

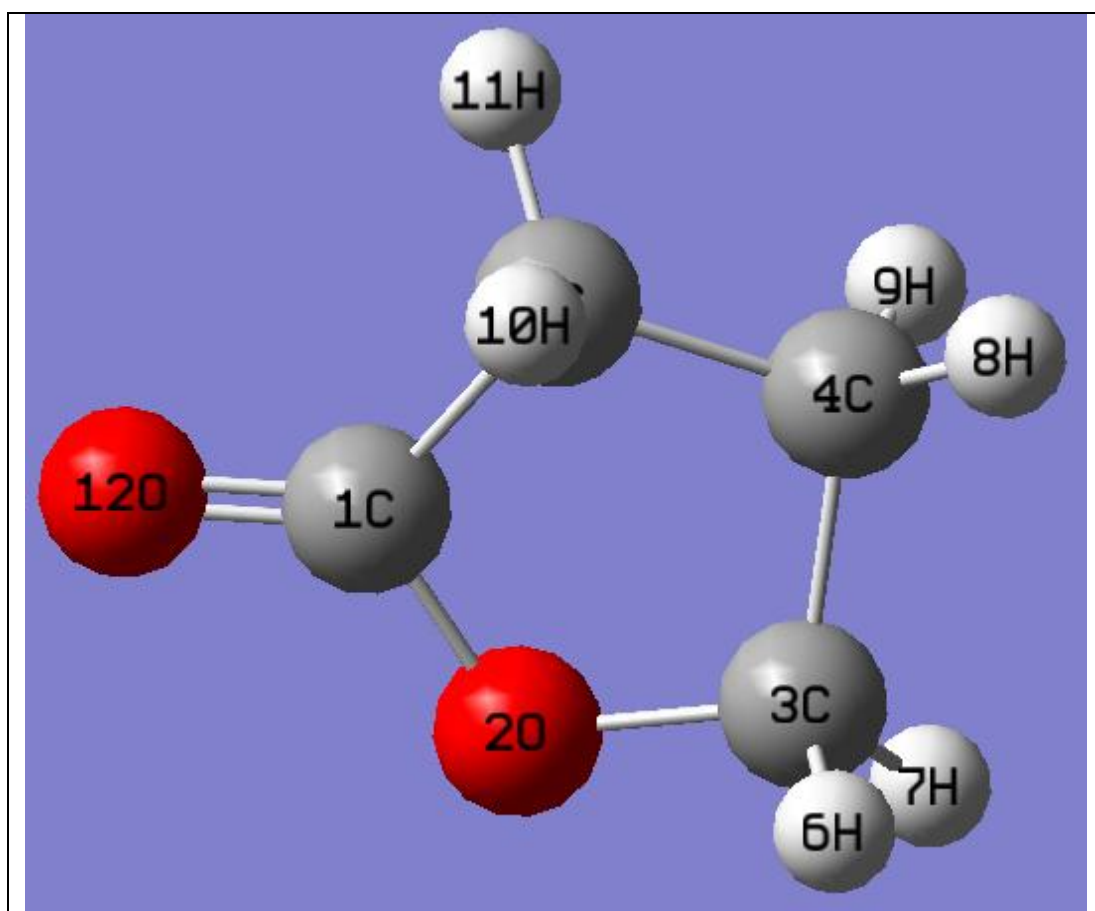
B= 1.37450 (C3-O13)

A=107.77 (H12 O11 C4)

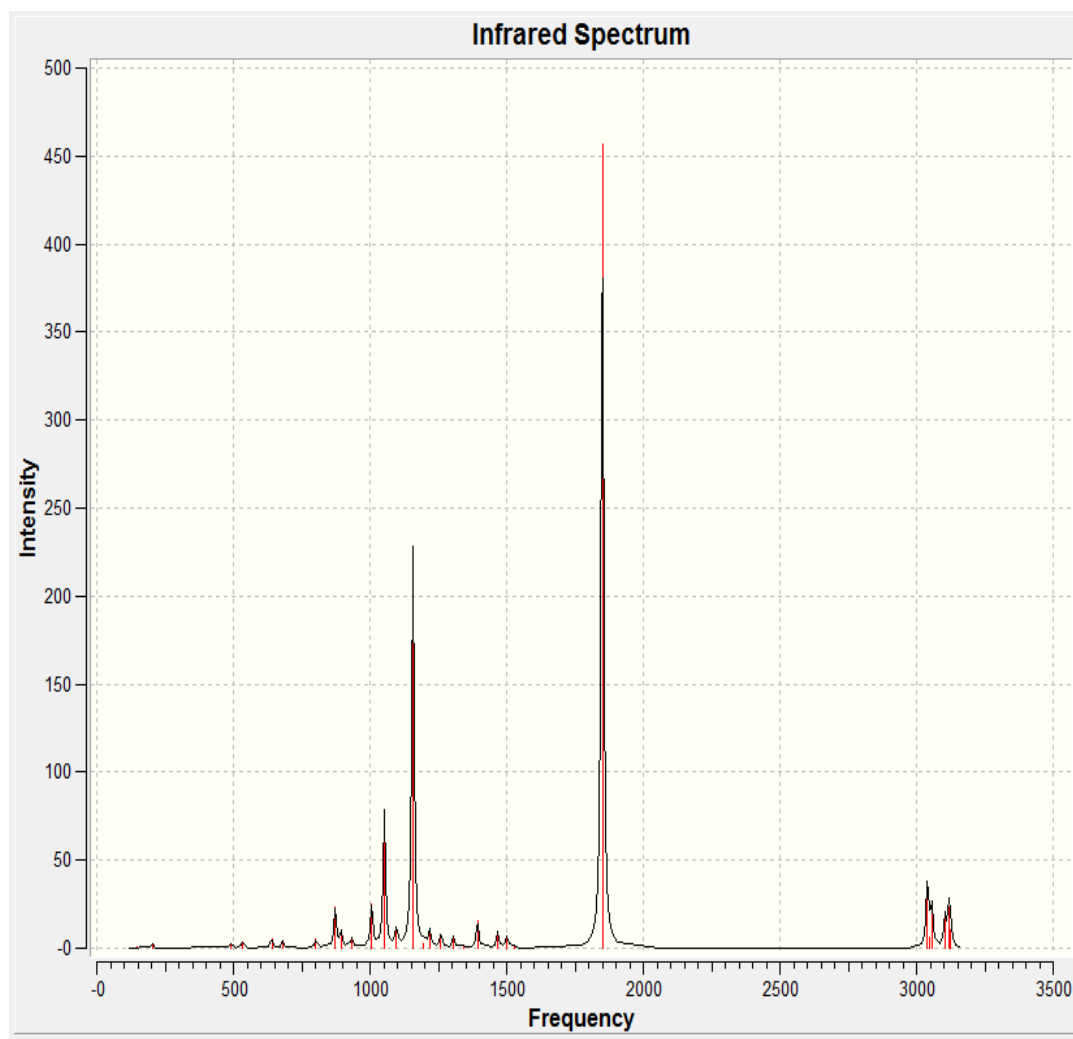
B=1.08342 (H7-C1)

A=119.986 (C4 C5 C6)

Appendix A3: Optimized Structure for Butyrolactone and Geometrical Parameters

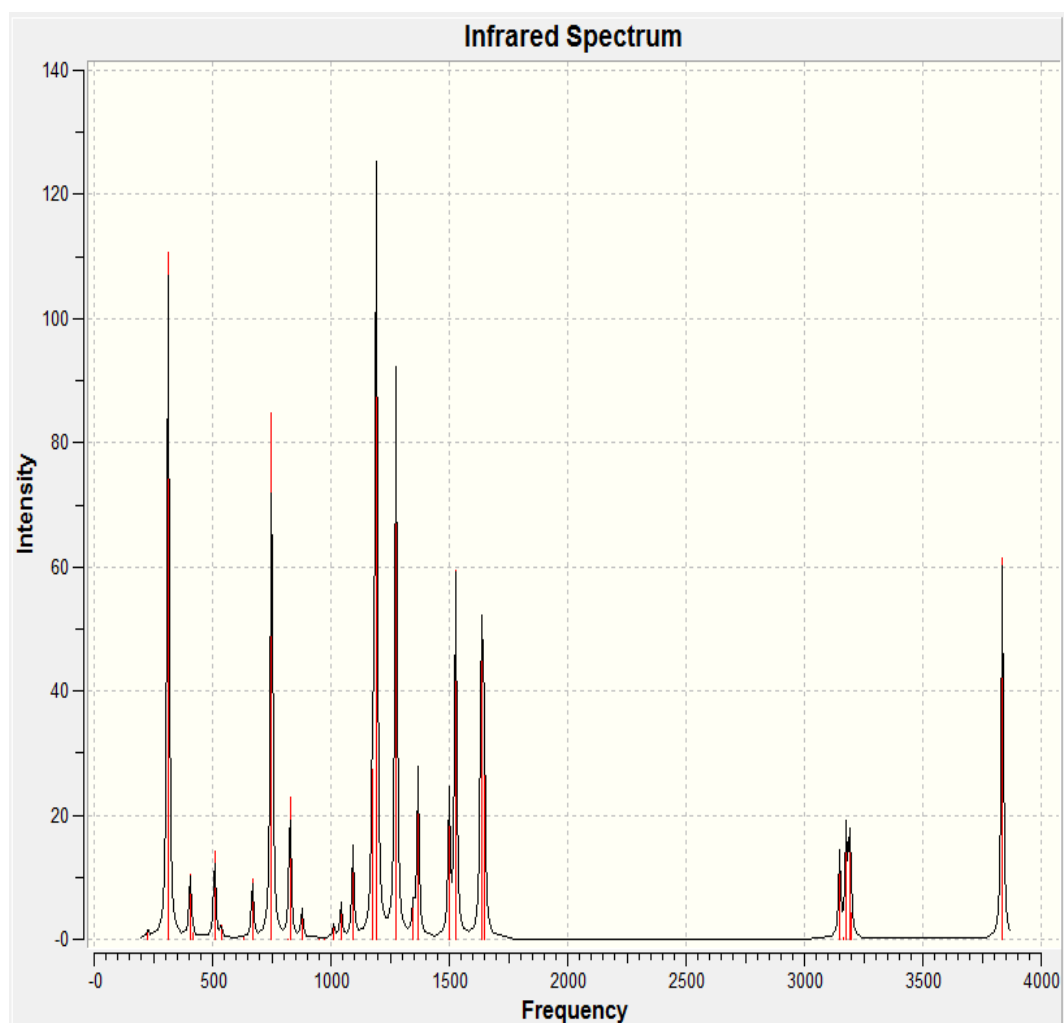


B= 1.19717 (O1 C1)	A= 122.412 (O12 C1 O2)
B= 1.36401 (O2 C1)	A= 110.948 (C1 O2 C3)
B= 1.52453 (C1 C5)	A= 109.044 (H6 C3 H7)
B= 1.09064 (H8 C4)	A=101.925 (C3 C4 C5)
B=1.53104 (C5 C4)	A=128.495 (O12 C1 C5)

Appendices B1: Display for Butyrolactone IR spectrum

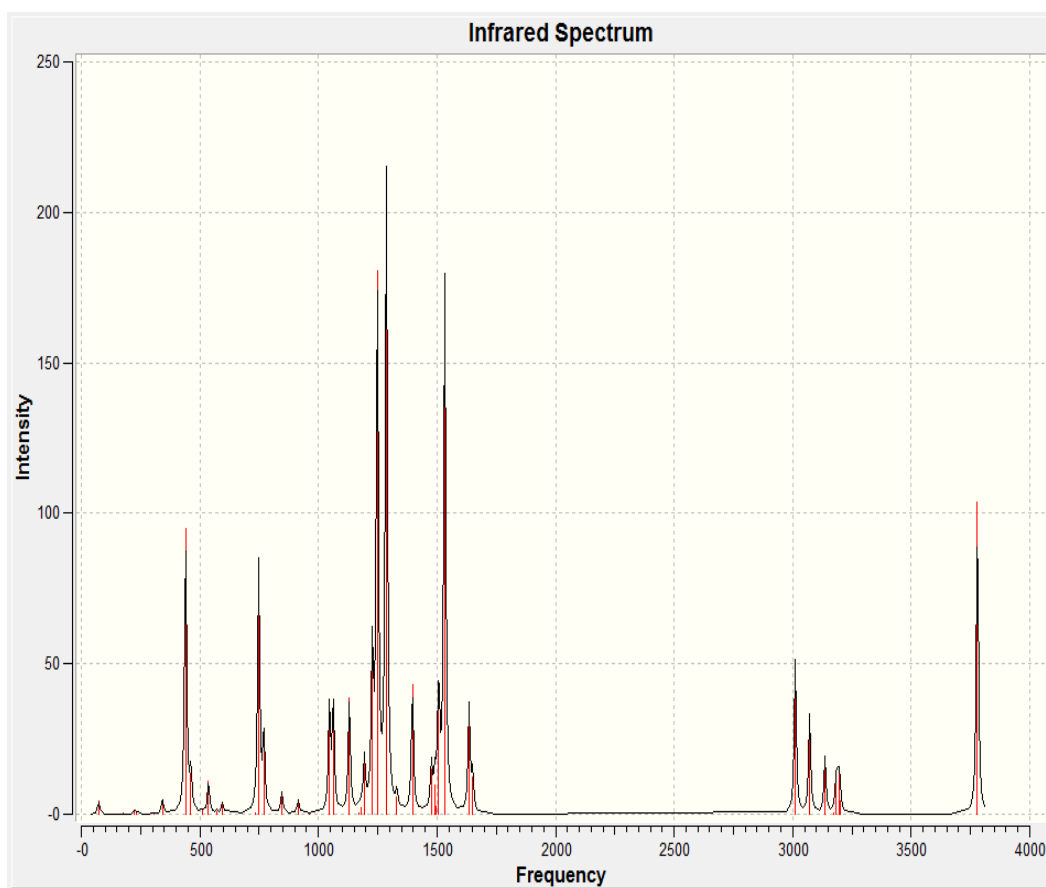
PEAKS		
F=881.89, I= 23.8764	F=3038.39, I=37.9213	
F=1061.02, I=77.2472		
F=1157.48, I=227.528		
F=1853.35, I=455.056		

Appendix B2: Display for Phenol IR Spectrum



PEAKS		
F=318.681, I=110.409	F=831.947, I=32.8774	F=1530.78, I=59.4316
F=412.646, I=10.6927	F=1091.51, I=14.4227	F=1643.93, I=52.7176
F=512.479, I=13.9254	F=1198.17, I=130.053	F=3174.71, I=17.6554
F=672.213, I=9.44938	F=1277.87, I=91.5098	F=3833.61, I=61.421
F=758.735, I=84.5471	F=1371.05, I=27.1048	

Appendix B3: Display for Guaiacol IR spectrum



PEAKS		
F=451.243, I=94.9454	F=1292.54, I=213.115	F=3082.22, I=33.4699
F=757.17, I=84.0164	F=1407.27, I=43.0328	F=3143.4, I=18.4426
F=1063.1, I=39.6175	F=1537.28, I=178.962	F=3204.59, I=14.4509
F=1139.58, I=37.5683	F=1644.36, I=35.5191	F=3785.85, I=103.324
F=1254.3, I=180.328	F=3021.03, I=51.2295	

Appendix C 1: Propanol Gaussian thermochemical data output

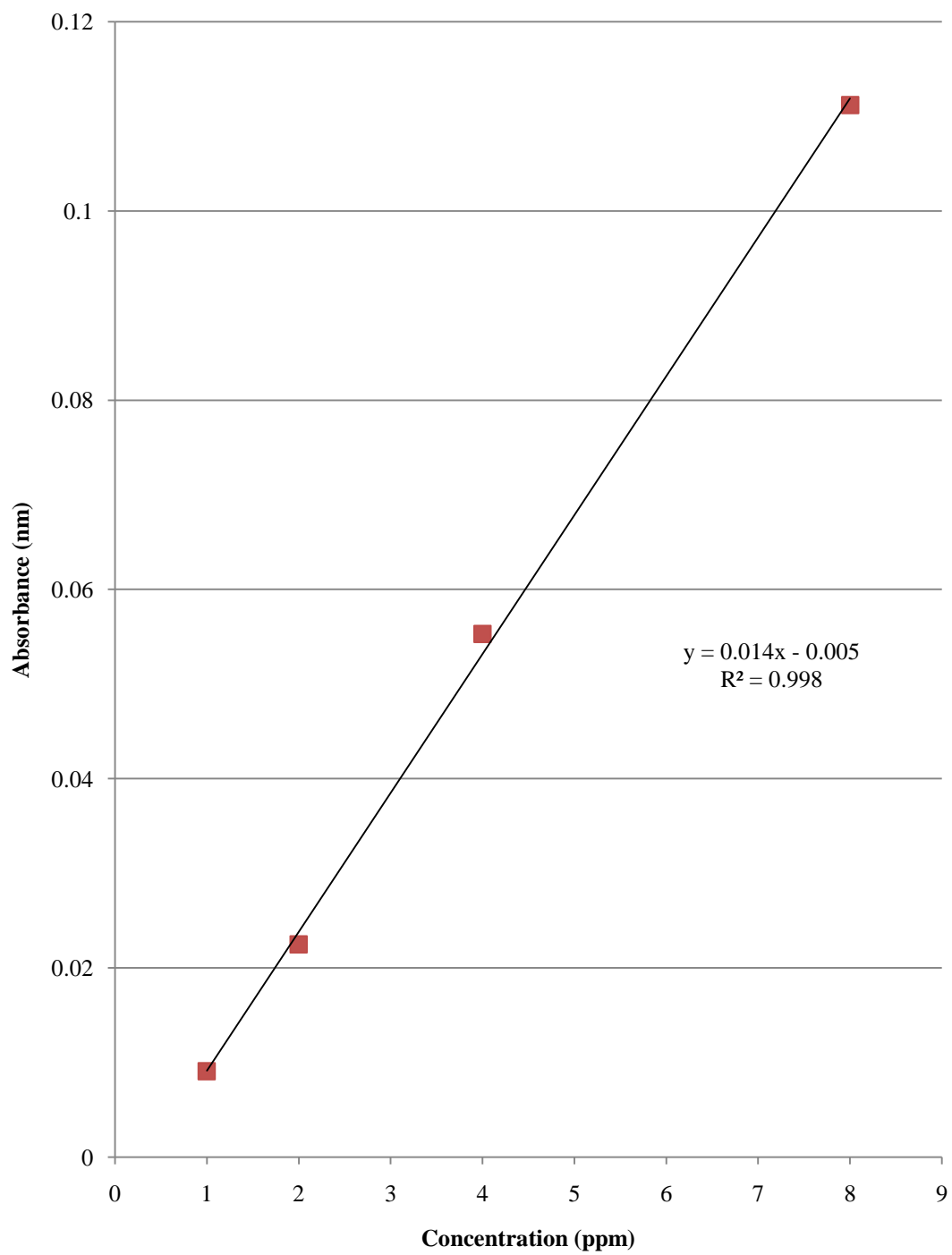
Zero-point correction=	0.108086
(Hartree/Particle)	
Thermal correction to Energy=	0.133217
Thermal correction to Enthalpy=	0.135506
Thermal correction to Gibbs free energy=	0.022259
Sum of electronic and zero-point Energies=	-194.311313
Sum of electronic and thermal Energies=	-194.286182
Sum of electronic and thermal Enthalpies=	-194.283892
Sum of electronic and thermal Free Energies=	-194.397139

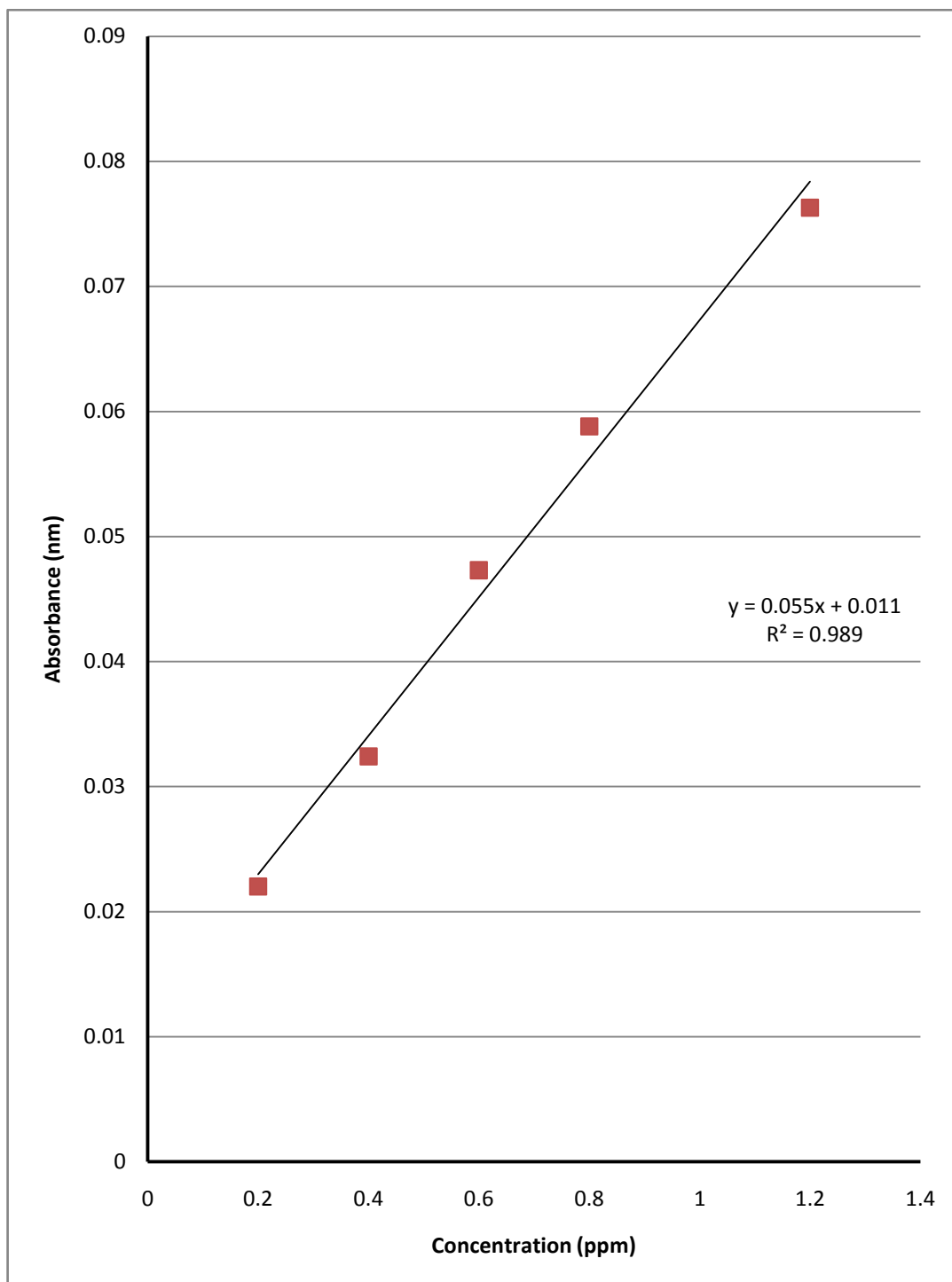
	E (Thermal)	CV	S
	KCal/Mol	Cal/Mol-Kelvin	Cal/Mol-Kelvin
Total	83.595	37.837	98.290
Electronic	0.000	0.000	0.000
Translational	2.155	2.981	42.599
Rotational	2.155	2.981	27.088
Vibrational	79.285	31.876	28.603
Vibration 1	1.446	1.974	4.514
Vibration 2	1.460	1.956	3.642
Vibration 3	1.464	1.949	3.463
Vibration 4	1.486	1.920	2.893

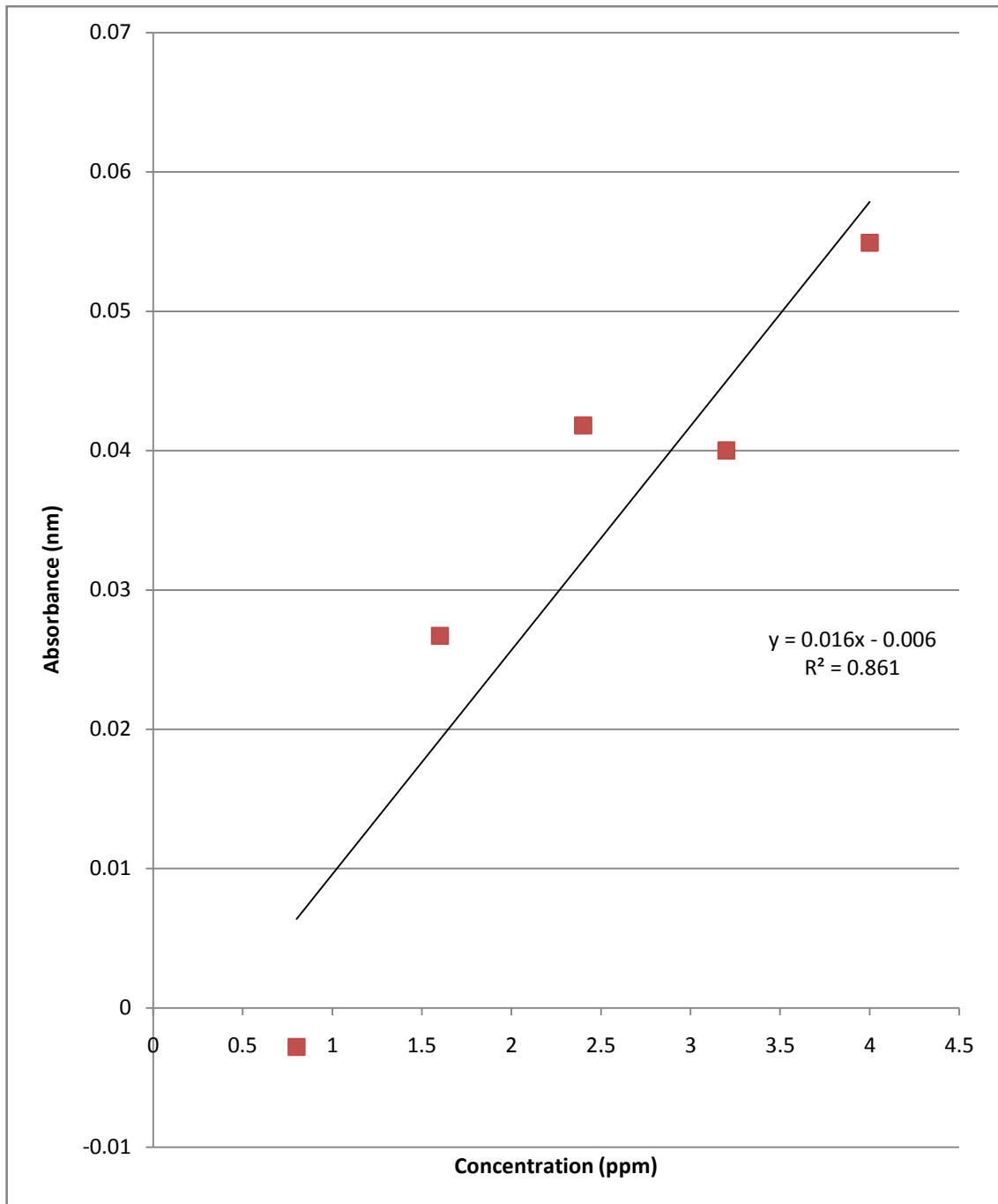
Appendix C2: phenol Gaussian thermochemical data output

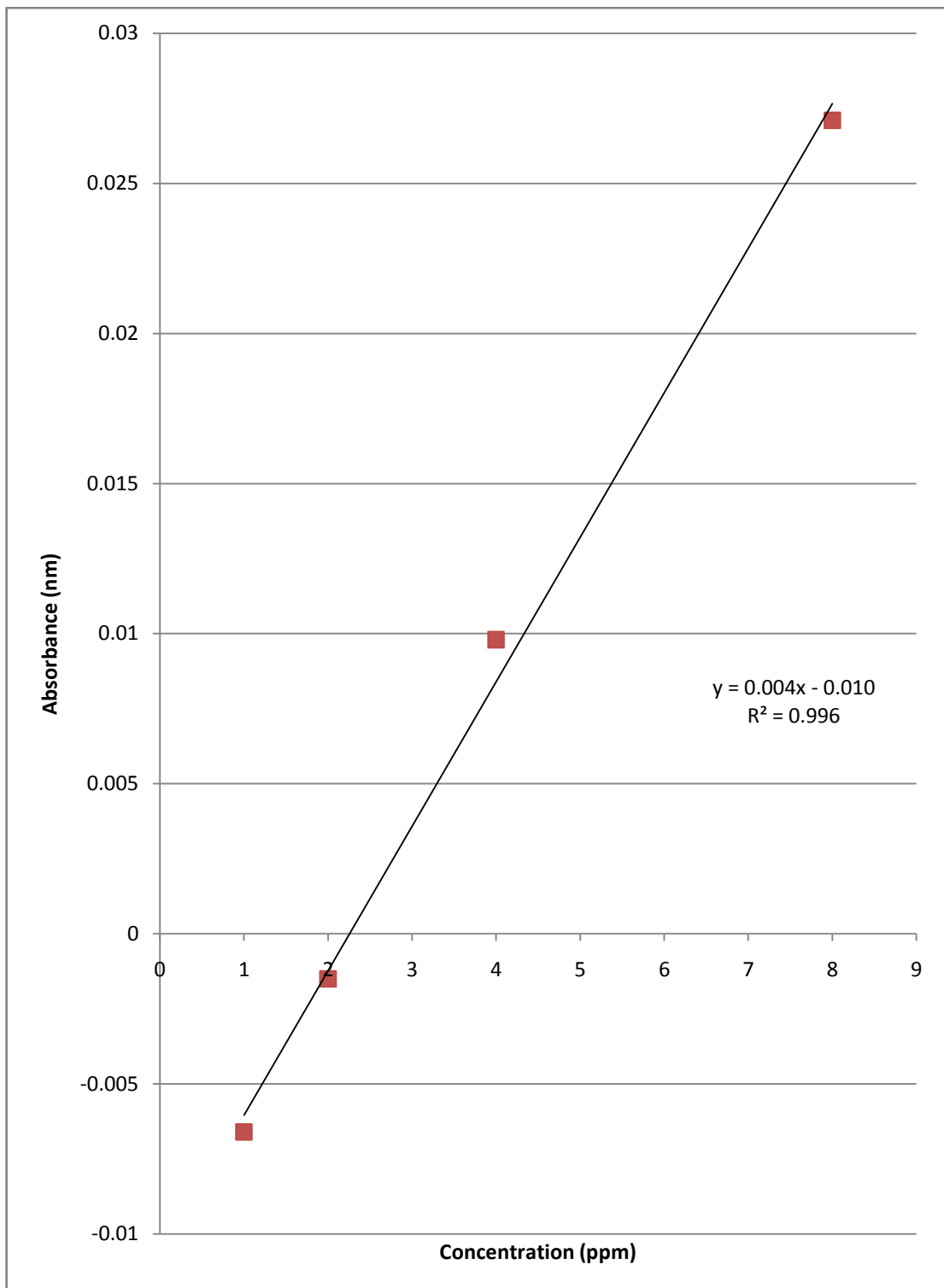
Zero-point correction=	0.103158 (Hartree/Particle)
Thermal correction to Energy=	0.134921
Thermal correction to Enthalpy=	0.137369
Thermal correction to Gibbs free energy=	0.005573
Sum of electronic and zero-point Energies=	-307.449971
Sum of electronic and thermal Energies=	-307.418208
Sum of electronic and thermal Enthalpies=	-307.415760
Sum of electronic and thermal Free Energies=	-307.547556

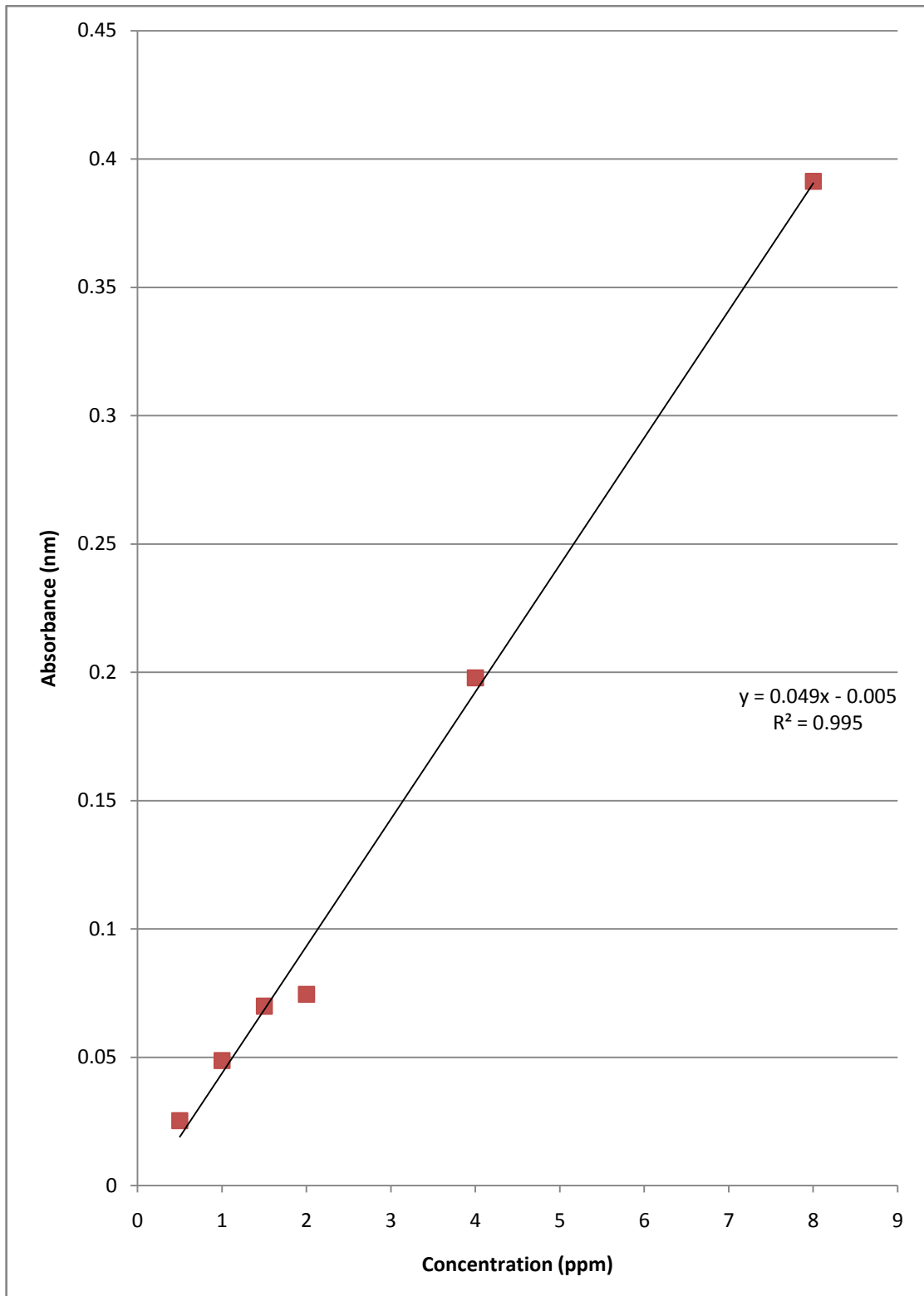
	E (Thermal)	CV	S
	KCal/Mol	Cal/Mol-Kelvin	Cal/Mol-Kelvin
Total	84.664	45.737	106.990
Electronic	0.000	0.000	0.000
Translational	2.304	2.981	44.268
Rotational	2.304	2.981	29.748
Vibrational	80.056	39.775	32.975
Vibration 1	1.559	1.958	3.708
Vibration 2	1.610	1.894	2.576
Vibration 3	1.614	1.889	2.522
Vibration 4	1.643	1.852	2.218

Appendix D1: Standard calibration curve for Pb

Appendix D2: Standard calibration curve for Zn

Appendix D3: Standard calibration curve for Cu

Appendix D4: Standard calibration curve for Cr

Appendix D5: Standard calibration curve for Mn

Appendix E1: Mean concentrations of heavy metals partitioned in cigarette smoke

		Descriptives							
				95% Confidence Interval for					
				Mean					
		N	Mean	Std. Deviation	Std. Error	Lower Bound	Upper Bound	Minimum	Maximum
Cr	Trd	6	3.625400	0.5916499	0.2415401	3.004502	4.246298	3.0853	4.1655
	SM1	6	3.552650	0.1251546	0.0510942	3.421308	3.683992	3.4384	3.6669
	ES1	6	2.088150	0.7281971	0.2972852	1.323954	2.852346	1.4234	2.7529
	Total	18	3.088733	0.8913408	0.2100910	2.645480	3.531987	1.4234	4.1655
Cu	Trd	6	1.192850	0.1157338	0.0472481	1.071395	1.314305	1.0872	1.2985
	SM1	6	0.614750	0.2383141	0.0972913	0.364655	0.864845	0.3972	0.8323
	ES1	6	0.543900	0.3036574	0.1239676	0.225231	0.862569	0.2667	0.8211
	Total	18	0.783833	0.3704282	0.0873108	0.599624	0.968043	0.2667	1.2985
Zn	Trd	6	2.333400	0.1433938	0.0585403	2.182917	2.483883	2.2025	2.4643
	SM1	6	2.577150	0.2561698	0.1045809	2.308316	2.845984	2.3433	2.8110
	ES1	6	2.258500	0.0336302	0.0137295	2.223207	2.293793	2.2278	2.2892
	Total	18	2.389683	0.2127830	0.0501534	2.283869	2.495498	2.2025	2.8110
Cd	Trd	6	0.100250	0.0111188	0.0045392	0.088582	0.111918	0.0901	0.1104
	SM1	6	0.090100	0.0008764	0.0003578	0.089180	0.091020	0.0893	0.0909
	ES1	6	0.083850	0.0119951	0.0048970	0.071262	0.096438	0.0729	0.0948
	Total	18	0.091400	0.0112811	0.0026590	0.085790	0.097010	0.0729	0.1104
Pb	Trd	6	6.776400	0.3992897	0.1630094	6.357371	7.195429	6.4119	7.1409
	SM1	6	6.984200	0.1865543	0.0761605	6.788423	7.179977	6.8139	7.1545
	ES1	6	7.117000	0.1156790	0.0472258	6.995602	7.238398	7.0114	7.2226
	Total	18	6.959200	0.2861234	0.0674399	6.816914	7.101486	6.4119	7.2226
Mn	Trd	6	0.232150	0.0552652	0.0225619	0.174153	0.290147	0.1817	0.2826
	SM1	6	0.590350	0.1757642	0.0717554	0.405897	0.774803	0.4299	0.7508
	ES1	6	0.735700	0.1669458	0.0681554	0.560501	0.910899	0.5833	0.8881
	Total	18	0.519400	0.2561116	0.0603661	0.392039	0.646761	0.1817	0.8881

Appendix E2: One Way Analysis of Variance for metals partitioned in smoke

ANOVA						
		Sum of Squares	df	Mean Square	F	Sig.
Cr	Between Groups	9.026	2	4.513	15.111	0.000
	Within Groups	4.480	15	0.299		
	Total	13.506	17			
Cu	Between Groups	1.521	2	0.760	14.046	0.000
	Within Groups	0.812	15	0.054		
	Total	2.333	17			
Zn	Between Groups	0.333	2	0.167	5.723	0.014
	Within Groups	0.437	15	0.029		
	Total	0.770	17			
Cd	Between Groups	0.001	2	0.000	4.596	0.028
	Within Groups	0.001	15	0.000		
	Total	0.002	17			
Pb	Between Groups	0.354	2	0.177	2.555	0.111
	Within Groups	1.038	15	0.069		
	Total	1.392	17			
Mn	Between Groups	0.806	2	0.403	19.557	0.000
	Within Groups	0.309	15	0.021		
	Total	1.115	17			

Appendix E3: Heavy metals concentration mean differences in Trd, SM1 and ES1 smoke

Multiple Comparisons								
Dependent Variable	(I) Brand	(J) Brand	Mean Difference			95% Confidence Interval		
			(I-J)	Std. Error	Sig.	Lower Bound	Upper Bound	
Cr	Tukey HSD	Trd	SM1	0.0727500	0.3155215	0.971	-0.746808	0.892308
			ES1	1.5372500*	0.3155215	0.001	0.717692	2.356808
		SM1	Trd	-0.0727500	0.3155215	0.971	-0.892308	0.746808
			ES1	1.4645000*	0.3155215	0.001	0.644942	2.284058
		ES1	Trd	-1.5372500*	0.3155215	0.001	-2.356808	-0.717692
	SM1		-1.4645000*	0.3155215	0.001	-2.284058	-0.644942	
	Games-Howell	Trd	SM1	0.0727500	0.2468850	0.954	-0.707555	0.853055
			ES1	1.5372500*	0.3830406	0.007	0.479960	2.594540
		SM1	Trd	-0.0727500	0.2468850	0.954	-0.853055	0.707555
			ES1	1.4645000*	0.3016440	0.009	0.502239	2.426761
ES1		Trd	-1.5372500*	0.3830406	0.007	-2.594540	-0.479960	
	SM1	-1.4645000*	0.3016440	0.009	-2.426761	-0.502239		
Cu	Tukey HSD	Trd	SM1	0.5781000*	0.1343278	0.002	0.229187	0.927013
			ES1	0.6489500*	0.1343278	0.001	0.300037	0.997863
		SM1	Trd	-0.5781000*	0.1343278	0.002	-0.927013	-0.229187
			ES1	0.0708500	0.1343278	0.859	-0.278063	0.419763
		ES1	Trd	-0.6489500*	0.1343278	0.001	-0.997863	-0.300037
	SM1		-0.0708500	0.1343278	0.859	-0.419763	0.278063	
	Games-Howell	Trd	SM1	0.5781000*	0.1081572	0.002	0.262066	0.894134
			ES1	0.6489500*	0.1326663	0.005	0.249546	1.048354
		SM1	Trd	-0.5781000*	0.1081572	0.002	-0.894134	-0.262066
			ES1	0.0708500	0.1575867	0.896	-0.365176	0.506876
ES1		Trd	-0.6489500*	0.1326663	0.005	-1.048354	-0.249546	
	SM1	-0.0708500	0.1575867	0.896	-0.506876	0.365176		
Zn	Tukey HSD	Trd	SM1	-0.2437500	0.0984975	0.063	-0.499594	0.012094
			ES1	0.0749000	0.0984975	0.732	-0.180944	0.330744
		SM1	Trd	0.2437500	0.0984975	0.063	-0.012094	0.499594
			ES1	0.3186500*	0.0984975	0.014	0.062806	0.574494
		ES1	Trd	-0.0749000	0.0984975	0.732	-0.330744	0.180944
	SM1		-.3186500*	0.0984975	0.014	-0.574494	-0.062806	
	Games-Howell	Trd	SM1	-.2437500	0.1198504	0.167	-0.587563	0.100063
			ES1	0.0749000	0.0601287	0.475	-0.114019	0.263819
		SM1	Trd	0.2437500	0.1198504	0.167	-0.100063	0.587563
			ES1	0.3186500	0.1054783	0.062	-0.020518	0.657818
ES1		Trd	-0.0749000	0.0601287	0.475	-0.263819	0.114019	
	SM1	-0.3186500	0.1054783	0.062	-0.657818	0.020518		
Cd	Tukey HSD	Trd	SM1s	0.0101500	0.0054597	0.185	-0.004031	0.024331
			ES1	0.0164000*	0.0054597	0.023	0.002219	0.030581

		SM1	Trd	-0.0101500	0.0054597	0.185	-0.024331	0.004031
			ES1	0.0062500	0.0054597	0.503	-0.007931	0.020431
		ES1	Trd	-0.0164000*	0.0054597	0.023	-0.030581	-0.002219
			SM1	-0.0062500	0.0054597	0.503	-0.020431	0.007931
	Games-Howell	Trd	SM1	0.0101500	0.0045533	0.158	-0.004601	0.024901
			ES1	0.0164000	0.0066772	0.080	-0.001921	0.034721
		SM1	Trd	-0.0101500	0.0045533	0.158	-0.024901	0.004601
			ES1	0.0062500	0.0049100	0.466	-0.009667	0.022167
		ES1	Trd	-0.0164000	0.0066772	0.080	-0.034721	0.001921
			SM1	-0.0062500	0.0049100	0.466	-0.022167	0.009667
Pb	Tukey HSD	Trd	SM1	-0.2078000	0.1518832	0.382	-0.602312	0.186712
			ES1	-0.3406000	0.1518832	0.096	-0.735112	0.053912
		SM1	Trd	0.2078000	0.1518832	0.382	-0.186712	0.602312
			ES1	-0.1328000	0.1518832	0.664	-0.527312	0.261712
		ES1	Trd	0.3406000	0.1518832	0.096	-0.053912	0.735112
			SM1	0.1328000	0.1518832	0.664	-0.261712	0.527312
	Games-Howell	Trd	SM1	-0.2078000	0.1799235	0.514	-0.736166	0.320566
			ES1	-0.3406000	0.1697125	0.193	-0.865659	0.184459
		SM1	Trd	0.2078000	0.1799235	0.514	-0.320566	0.736166
			ES1	-0.1328000	0.0896141	0.347	-0.386632	0.121032
		ES1	Trd	0.3406000	0.1697125	0.193	-0.184459	0.865659
			SM1	0.1328000	0.0896141	0.347	-0.121032	0.386632
Mn	Tukey HSD	Trd	SM1	-0.3582000*	0.0828776	0.002	-0.573472	-0.142928
			ES1	-0.5035500*	0.0828776	0.000	-0.718822	-0.288278
		SM1	Trd	0.3582000*	0.0828776	0.002	0.142928	0.573472
			ES1	-0.1453500	0.0828776	0.219	-0.360622	0.069922
		ES1	Trd	0.5035500*	0.0828776	0.000	0.288278	0.718822
			SM1	0.1453500	0.0828776	0.219	-0.069922	0.360622
	Games-Howell	Trd	SM1	-0.3582000*	0.0752189	0.008	-0.589226	-0.127174
			ES1	-0.5035500*	0.0717927	0.001	-0.722963	-0.284137
		SM1	Trd	0.3582000*	0.0752189	0.008	0.127174	0.589226
			ES1	-0.1453500	0.0989646	0.346	-0.416759	0.126059
		ES1	Trd	0.5035500*	0.0717927	0.001	0.284137	0.722963
			SM1	0.1453500	0.0989646	0.346	-0.126059	0.416759

*. The mean difference is significant at the 0.05 level.

Appendix E4: Mean concentrations of heavy metals partitioned in cigarette ash

		Descriptives							
		N	Mean	Std. Deviation	Std. Error	95% Confidence Interval for Mean			
						Lower Bound	Upper Bound	Minimum	Maximum
Cr	Trd	6	3.552300	0.0572918	0.0233893	3.492176	3.612424	3.5000	3.6046
	SM1	6	3.196500	0.1057105	0.0431561	3.085564	3.307436	3.1000	3.2930
	ES1	6	1.594800	0.0056963	0.0023255	1.588822	1.600778	1.5896	1.6000
	Total	18	2.781200	0.8785059	0.2070658	2.344329	3.218071	1.5896	3.6046
Cu	Trd	6	1.071550	0.0783791	0.0319981	0.989296	1.153804	1.0000	1.1431
	SM1	6	0.259650	0.0442012	0.0180451	0.213264	0.306036	0.2193	0.3000
	ES1	6	0.364400	0.0389978	0.0159208	0.323474	0.405326	0.3288	0.4000
	Total	18	0.565200	0.3748349	0.0883494	0.378799	0.751601	0.2193	1.1431
Zn	Trd	6	2.859100	0.0448037	0.0182910	2.812081	2.906119	2.8182	2.9000
	SM1	6	2.684150	0.0173628	0.0070883	2.665929	2.702371	2.6683	2.7000
	ES1	6	1.856800	0.0622213	0.0254017	1.791503	1.922097	1.8000	1.9136
	Total	18	2.466683	0.4518162	0.1064941	2.242000	2.691366	1.8000	2.9000
Cd	Trd	6	0.086600	0.0072299	0.0029516	0.079013	0.094187	0.0800	0.0932
	SM1	6	0.281400	0.2394643	0.0977609	0.030098	0.532702	0.0628	0.5000
	ES1	6	0.336450	0.2887046	0.1178631	0.033473	0.639427	0.0729	0.6000
	Total	18	0.234817	0.2314321	0.0545491	0.119728	0.349905	0.0628	0.6000
Pb	Trd	6	6.655850	0.0611806	0.0249769	6.591645	6.720055	6.6000	6.7117
	SM1	6	6.818400	0.1989328	0.0812140	6.609633	7.027167	6.6368	7.0000
	ES1	6	6.832950	0.2551839	0.1041784	6.565151	7.100749	6.6000	7.0659
	Total	18	6.769067	0.1967647	0.0463779	6.671218	6.866915	6.6000	7.0659
Mn	Trd	6	0.394800	0.0056963	0.0023255	0.388822	0.400778	0.3896	0.4000
	SM1	6	0.647150	0.0516502	0.0210861	0.592946	0.701354	0.6000	0.6943
	ES1	6	0.747600	0.0521432	0.0212874	0.692879	0.802321	0.7000	0.7952
	Total	18	0.596517	0.1578482	0.0372052	0.518021	0.675013	0.3896	0.7952

Appendix E5: One Way Analysis of Variance for metals partitioned in cigarette ash

ANOVA						
		Sum of Squares	df	Mean Square	F	Sig.
Cr	Between Groups	13.048	2	6.524	1350.739	0.000
	Within Groups	0.072	15	0.005		
	Total	13.120	17			
Cu	Between Groups	2.340	2	1.170	365.013	0.000
	Within Groups	0.048	15	0.003		
	Total	2.389	17			
Zn	Between Groups	3.439	2	1.720	834.772	0.000
	Within Groups	0.031	15	0.002		
	Total	3.470	17			
Cd	Between Groups	0.207	2	0.103	2.204	0.145
	Within Groups	0.704	15	0.047		
	Total	0.911	17			
Pb	Between Groups	0.116	2	0.058	1.605	0.234
	Within Groups	0.542	15	0.036		
	Total	0.658	17			
Mn	Between Groups	0.396	2	0.198	109.744	0.000
	Within Groups	0.027	15	0.002		
	Total	0.424	17			

Appendix E6: Metal concentration mean differences in Trd, SM1 and ES1 cigarette smoke

Tukey HSD							
Dependent Variable	(I) Brand	(J) Brand	Multiple Comparisons			95% Confidence Interval	
			Mean Difference (I-J)	Std. Error	Sig.	Lower Bound	Upper Bound
Cr	Trd	SM1	0.3558000*	0.0401241	0.000	0.251579	0.460021
		ES1	1.9575000*	0.0401241	0.000	1.853279	2.061721
	SM1	Trd	-0.3558000*	0.0401241	0.000	-0.460021	-0.251579
		ES1	1.6017000*	0.0401241	0.000	1.497479	1.705921
	ES1	Trd	-1.9575000*	0.0401241	0.000	-2.061721	-1.853279
		SM1	-1.6017000*	0.0401241	0.000	-1.705921	-1.497479
Cu	Trd	SM1	0.8119000*	0.0326902	0.000	0.726988	0.896812
		ES1	0.7071500*	0.0326902	0.000	0.622238	0.792062
	SM1	Trd	-0.8119000*	0.0326902	0.000	-0.896812	-0.726988
		ES1	-0.1047500*	0.0326902	0.015	-0.189662	-0.019838
	ES1	Trd	-0.7071500*	0.0326902	0.000	-0.792062	-0.622238
		SM1	0.1047500*	0.0326902	0.015	0.019838	0.189662
Zn	Trd	ES1	0.1749500*	0.0262050	0.000	0.106883	0.243017
		ES1	1.0023000*	0.0262050	0.000	0.934233	1.070367
	SM1	Trd	-0.1749500*	0.0262050	0.000	-0.243017	-0.106883
		ES1	0.8273500*	0.0262050	0.000	0.759283	0.895417
	ES1	Trd	-1.0023000*	0.0262050	0.000	-1.070367	-0.934233
		SM1	-0.8273500*	0.0262050	0.000	-0.895417	-0.759283
Cd	Trd	SM1	-0.1948000	0.1250537	0.294	-0.519623	0.130023
		ES1	-0.2498500	0.1250537	0.147	-0.574673	0.074973
	SM1	Trd	0.1948000	0.1250537	0.294	-0.130023	0.519623
		ES1	-0.0550500	0.1250537	0.899	-0.379873	0.269773
	ES1	Trd	0.2498500	0.1250537	0.147	-0.074973	0.574673
		SM1	0.0550500	0.1250537	0.899	-0.269773	0.379873
Pb	Trd	SM1	-0.1625500	0.1097655	0.327	-0.447663	0.122563
		ES1	-0.1771000	0.1097655	0.271	-0.462213	0.108013
	SM1	Trd	0.1625500	0.1097655	0.327	-0.122563	0.447663
		ES1	-0.0145500	0.1097655	0.990	-0.299663	0.270563
	ES1	Trd	0.1771000	0.1097655	0.271	-0.108013	0.462213
		SM1	0.0145500	0.1097655	0.990	-0.270563	0.299663
Mn	Trd	SM1	-0.2523500*	0.0245382	0.000	-0.316087	-0.188613
		ES1	-0.3528000*	0.0245382	0.000	-0.416537	-0.289063
	SM1	Trd	0.2523500*	0.0245382	0.000	0.188613	0.316087
		ES1	-0.1004500*	0.0245382	0.003	-0.164187	-0.036713
	ES1	Trd	0.3528000*	0.0245382	0.000	0.289063	0.416537
		SM1	0.1004500*	0.0245382	0.003	0.036713	0.164187

*. The mean difference is significant at the 0.05 level.

Appendix F1: Grant letter



**NATIONAL COMMISSION FOR SCIENCE,
TECHNOLOGY AND INNOVATION**

Telephone: +254-20-2213471,
2241349, 310571, 2219420
Fax: +254-20-318245, 318249
Email: secretary@nacosti.go.ke
Website: www.nacosti.go.ke
When replying please quote

9th Floor, Utalii House
Uhuru Highway
P.O. Box 30623-00100
NAIROBI-KENYA

Ref. No. **NACOSTI/RCD/ST&I 6th CALL MSc/274**

Date: **10th March, 2015**

Micah Omari Omare
Moi University
P.O. Box 3900-30100
ELDORET, KENYA.

RE: SCIENCE, TECHNOLOGY AND INNOVATION RESEARCH GRANT (MSc)

I'm pleased to inform you that, you have been awarded the Science, Technology and Innovation (ST&I) grant for your **MSc research proposal**.

National Commission for Science, Technology and Innovation (NACOSTI) has approved an amount of Kenya shillings (**Ksh 163,825/=**) towards your MSc research proposal titled "**Computational Modelling of Toxic Molecular Products and Determination of Heavy Metals from Combustion of Sportsman Embassy, and Traditional Cigarettes**". Your awarded grant will be disbursed in yearly instalment basis.

Find the enclosed **Research Grant Contract Form (NCST/ST&I/CONTRACT/FORM 1C)** that should be duly completed. You should attach a certified copy of your *national identity card, detailed work plan, breakdown of the yearly budget and a letter accepting the grant offered. Your recent passport size photograph and an abstract of your proposal, not exceeding 500 words should be submitted in soft copy (Ms Word format) to the email:- postgraduates@nacosti.go.ke*

Your duly signed contract form, acceptance letter and the abstract should be sent back to reach us not later than **31st March 2015** for our further actions.

DR. MOSES K. RUGUTT, PhD, HSC.
DIRECTOR GENERAL

cc: Vice Chancellor,
Moi University